

GuideTech

Precision Time & Frequency
Test & Measurement Instruments, ATE

GT668SLR Event-Timer

Multi-Channel, 2.7GHz, 0.9pS, 4M m/s



GT9000PSLR-USB3

APPLICATIONS

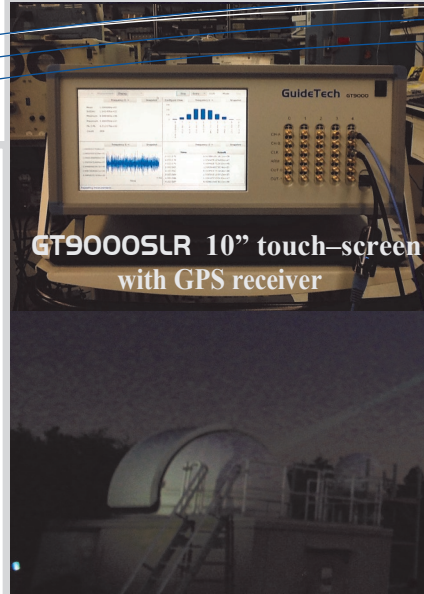
- Event Timing, UTC Synchronized
- Laser Ranging Timing Subsystem
- Real Time, Time stamping
- Long Distance Time Transfer
- Radar & Ultrasonic timing
- 1 PPS Monitoring
- Fast Time Measurements & Analysis
- Variation in Pulse Timing
- Frequency Modulation
- Allan Variance
- Measure jitter and skew

SOFTWARE SUPPORT

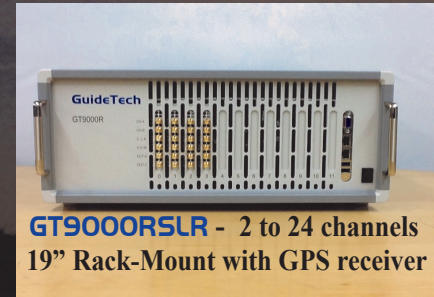
- Software package & APIs for SLR
- SLR GUI
- Windows 32bit, 64 bit
- Linux 32bit, 64 bit
- NI LabVIEW
- Python
- Java
- Custom software Development/
Support

KEY FEATURES

- UTC synchronizable with 1 PPS
- Programmable gates controlling
Source & receiver subsystems
- Easy cross-platform integration
- Very high throughput & accuracy
- Built-in NIST traceable time-base
- Expandable test systems 2 to 34 syn-
chronized channels
- Available in PCI , PCIe, PXI, PXIe
BUS & Test-System with SLR GUI



GT9000SLR 10" touch-screen
with GPS receiver



GT9000RSLR - 2 to 24 channels
19" Rack-Mount with GPS receiver

With a 50% smaller foot-print and much more powerful performance than its previous generation **GT658** Event-Timers, **GuideTech's GT668SLR** computer-based **Event-Timer** was co-designed with the ILRS community to provide a one-box Multi-Channel system-solution for SLR.

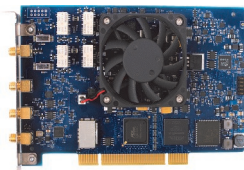
The **GT668SLR** Event-Timer has the following additional functions & software support:

- ◆ 1PPS input
- ◆ Integrated Two Programmable triggering outputs relative to beginning of measurement or to the Arming signal or at a user specified Real-Time to operate/control the Detector & other sub systems.
- ◆ Ability to synchronize with UTC time reference
- ◆ Software package, APIs for SLR & SLR GUI
- ◆ Integrated GPS receiver with OCXO, Rubidium or Cesium

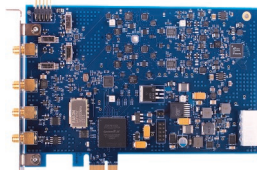
With easy expansion (up to 34 Channels) and modular capabilities, the **GT668SLR** is offered as follows:

- * **GT9000SLR** Scalable system, 2 to 24 channels, Touch-Display
- * **GT9000RSLR** Rack-Mount scalable system, 2 to 24 channels
- * **GT9000PSLR-USB3** Portable 2 channel system
- * **GT8000SLR PXI/PXIe** scalable, 2 to 34 channels
- * **GT668SLR** 2 channels **PCI, PCIe, PXI & PXIe** plug-in boards

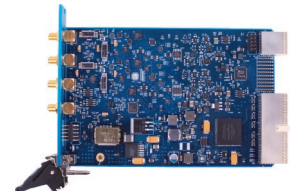
All of **GuideTech's** SLR systems & board products come with **NIST** traceable calibration, **SLR** APIs and customizable **SLR GUI**. The **GT9000SLR** & **GT9000RSLR** come with an optional integrated GPS receiver, providing a one-box, multi-channel solution for optimal test at lower cost.



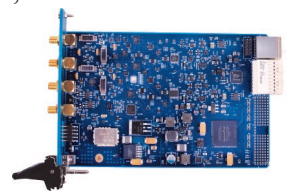
GT668SLRPCI



GT668SLRPCIe



GT668SLRPXI



GT668SLRPXIe



7 Slot Hybrid
GT8000SLR - PXI/PXIe

GuideTech

(408) 733-6555

(408) 988-9998

sales@guidetech.com

www.guidetech.com

GuideTech

Precision Time & Frequency
Test & Measurement Instruments, ATE

GT668SLR Event-Timer

Multi-Channel, 2.7GHz, 0.9pS, 4M m/s



GT9000PSLR-USB3

SPECIFICATIONS



GT8000SLR - PXI / PXIe
Scalable from 2 to 34 channels

GT668SLR MODELS

PCI

- ◆ GT668SLRPCI-1
- ◆ GT668SLRPCI-2
- ◆ GT668SLRPCI-15
- ◆ GT668SLRPCI-40

PCIe

- ◆ GT668SLRPCIe-1
- ◆ GT668SLRPCIe-2
- ◆ GT668SLRPCIe-15
- ◆ GT668SLRPCIe-40

PXI

- ◆ GT668SLRPXI-1
- ◆ GT668SLRPXI-2
- ◆ GT668SLRPXI-15
- ◆ GT668SLRPXI-40

PXIe

- ◆ GT668SLRPXIe-1
- ◆ GT668SLRPXIe-2
- ◆ GT668SLRPXIe-15
- ◆ GT668SLRPXIe-40

- * -1 = 0.9pS resolution
- * -2 = 1.8pS resolution
- * -15 = 15pS resolution
- * -40 = 40pS resolution

- Time Res. single-shot - 0.9ps
- Freq. Res. (Digits/S) - up to 12
- Max. Meas. rate - 4M m/s

MAIN INPUT CHANNELS:

TIMEBASE:

EXTERNAL CLOCK & ARM INPUTS:

EXTERNAL CONNECTIONS

- No. of channels: 2 per site, A & B
- Frequency range: DC - 2.7 GHz
- Sensitivity:
 - * 50 mV rms (DC - 2.7 GHz)
- Input impedance: 1K Ω / 10 pF, or 50 Ω software programmable
- Coupling: DC or AC
- Threshold setting (each channel):
 - * Range: -5V to +5V
 - * Resolution: 153 μ V
 - * Absolute accuracy: 0.1% of setting
 - * Automatic threshold setting option
- Frequency 100MHz locked to:
 - * Internal 10MHz OCXO
 - * External clock: 5 or 10 MHz (\pm 3KHz)
- Minimum pulse width: 6nS
- Oven Oscillator:
 - * Temp: 0 - 45 $^{\circ}$ C \pm 25ppb
 - * Aging: \pm 1 ppm first year, \pm 3 ppm over 20 years
- Sensitivity: 50mV rms
- Input impedance: 1K Ω
- Threshold setting
 - * Range: - 5V to + 5V
 - * Resolution: 153 μ V
 - * Absolute accuracy: 0.1% of setting
- Automatic threshold setting available
- Main channels: 2, SMA per site
- External clock: 1, SMA
- External arm: 1, SMA
- Digital input: 1 SMA (for 1PPS UTC synch)
- Digital output: 2, SMA (software programmable, to control user subsystems)

GuideTech

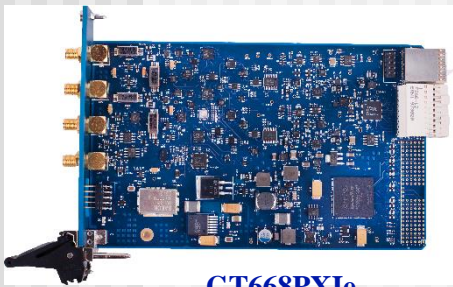
(408) 733-6555

(408) 988-9998

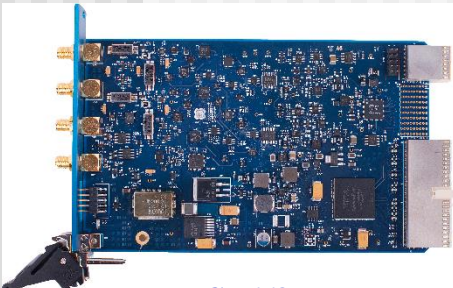
sales@guidetech.com

www.guidetech.com

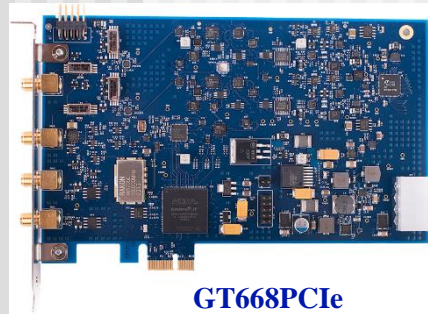
www.jitter.com



GT668PXIe



GT668PXI



GT668PCIe



GT668PCI



GT9000R PXIe

19" Rack-Mount, 2 to 24 channels



GT9000 with 10" touch-screen



GT9000R 2 to 24 Channels



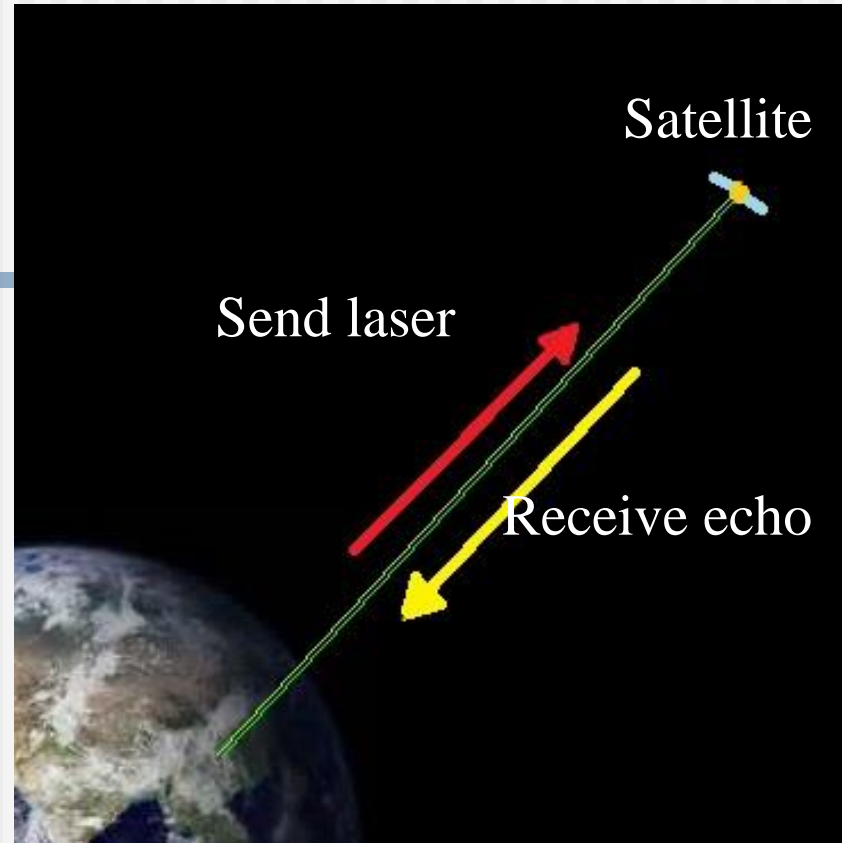
GT9000P-USB3 Portable

Some Basics

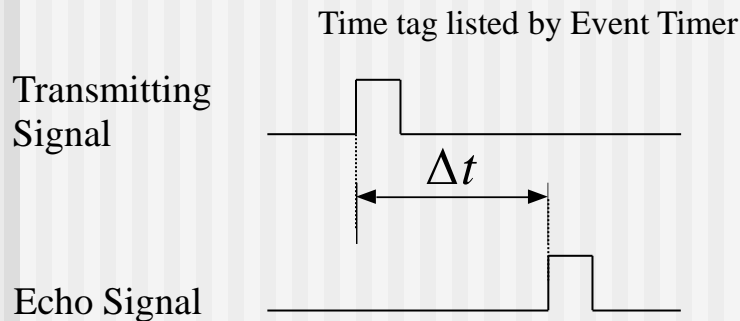
- Principle of Laser Ranging

- Send laser pulse toward the Satellite and record the transmitting time point
- Receive the echo and record the returning time point
- Calculate the distance (Ideal):

$$DISTANCE = (t_{receive} - t_{transmit}) * C$$



- Event Timer: Epoch Measurement



Time data view of An Event Timer

Events	Time/second
t0	1234.0012345678
t1	1234.0022345678
...	...

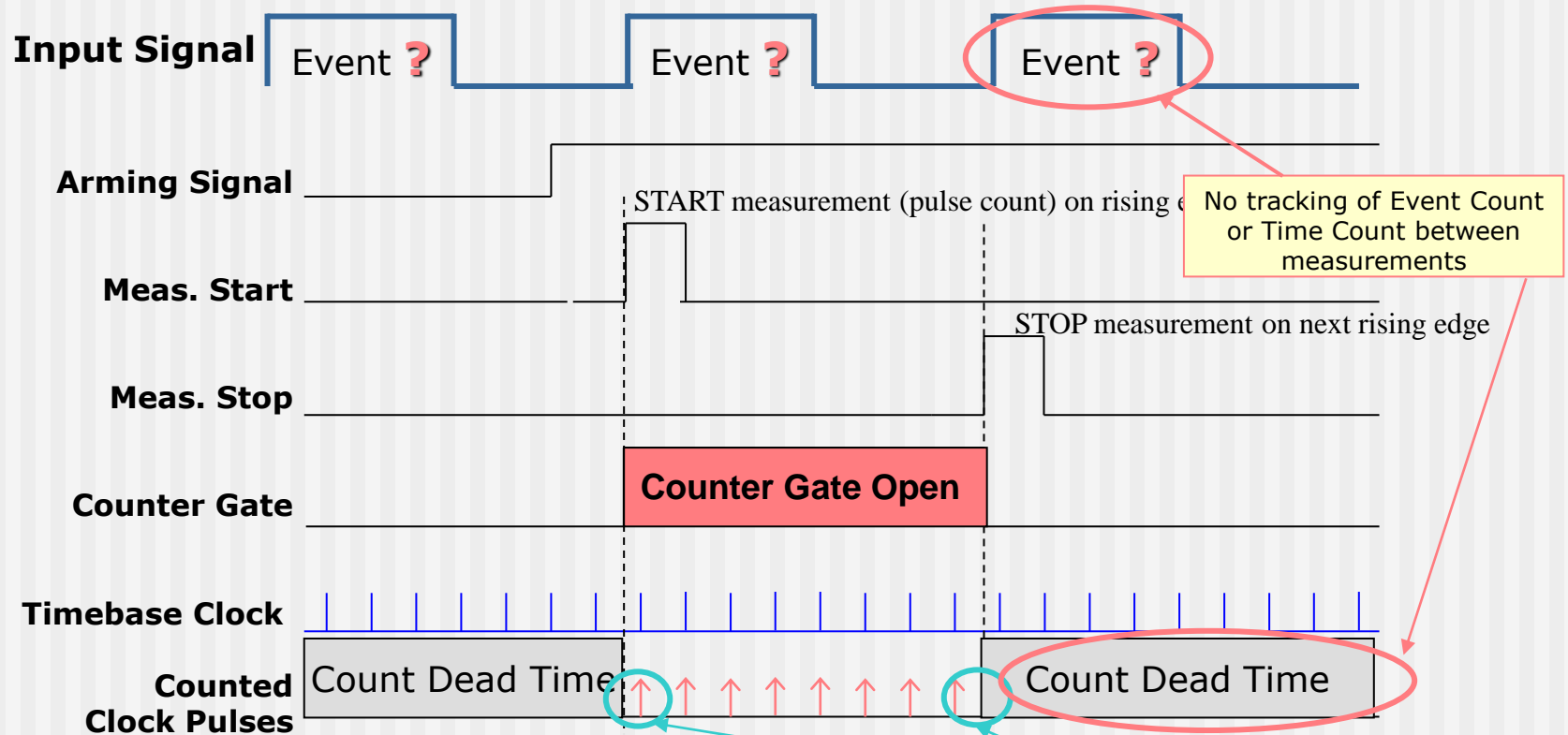
Overview

Time Interval Measurement Options

Time Counter (TC)	Measures the <i>delta time interval</i> between two electrical events.
Time Interval Analyzer (TIA)	Measures and records a “ <i>time stamp</i> ” (Time Tag) for multiple events <i>measured continuously</i> (no dead-time) on one or more electrical signals <i>with correlation to a common time reference</i> , T0.
Digital Sampling Oscilloscope (DSO)	Samples and reconstructs electrical waveforms (repetitive only) and <i>interpolates between measurement points to determine the delta time interval</i> between two electrical events.
High-Speed Digitizer	Digitizes electrical waveforms in one-shot and <i>interpolates between measurement points to determine the delta time interval</i> between two electrical events.
Digital Edge Search	<i>Calculates intervals of time</i> between rising and falling edges of electrical signals (repetitive signals only) by <i>sweeping a digital pattern capture strobe</i> through a signal to search for the zero/one crossover points then multiplying by digital capture strobe period.

Overview

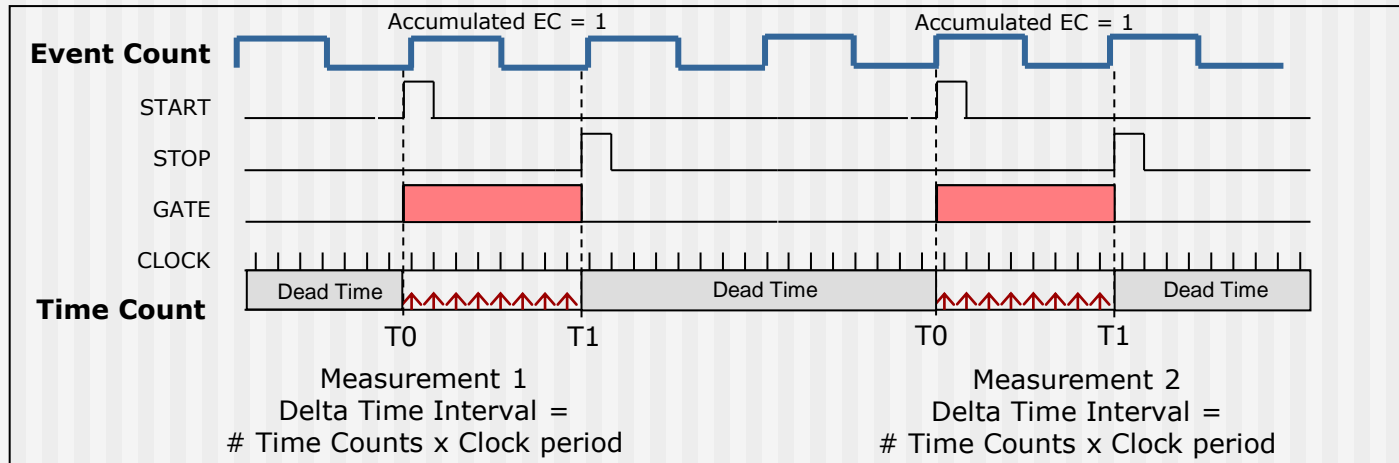
Time Interval Measurement Theory *Time Counter (TC) Method*



$$\text{Time Interval} = (\# \text{ Pulses counted} \times \text{Timebase period}) + \text{Interpolation values (optional)}$$

Overview

Time Interval Measurement Theory *Time Counter (TC) Method*



TC architecture obtains:

Delta # of Time Counts

- Number of Timebase Clock Pulses between two events

Delta # of Event Counts

- Number of Events between two events

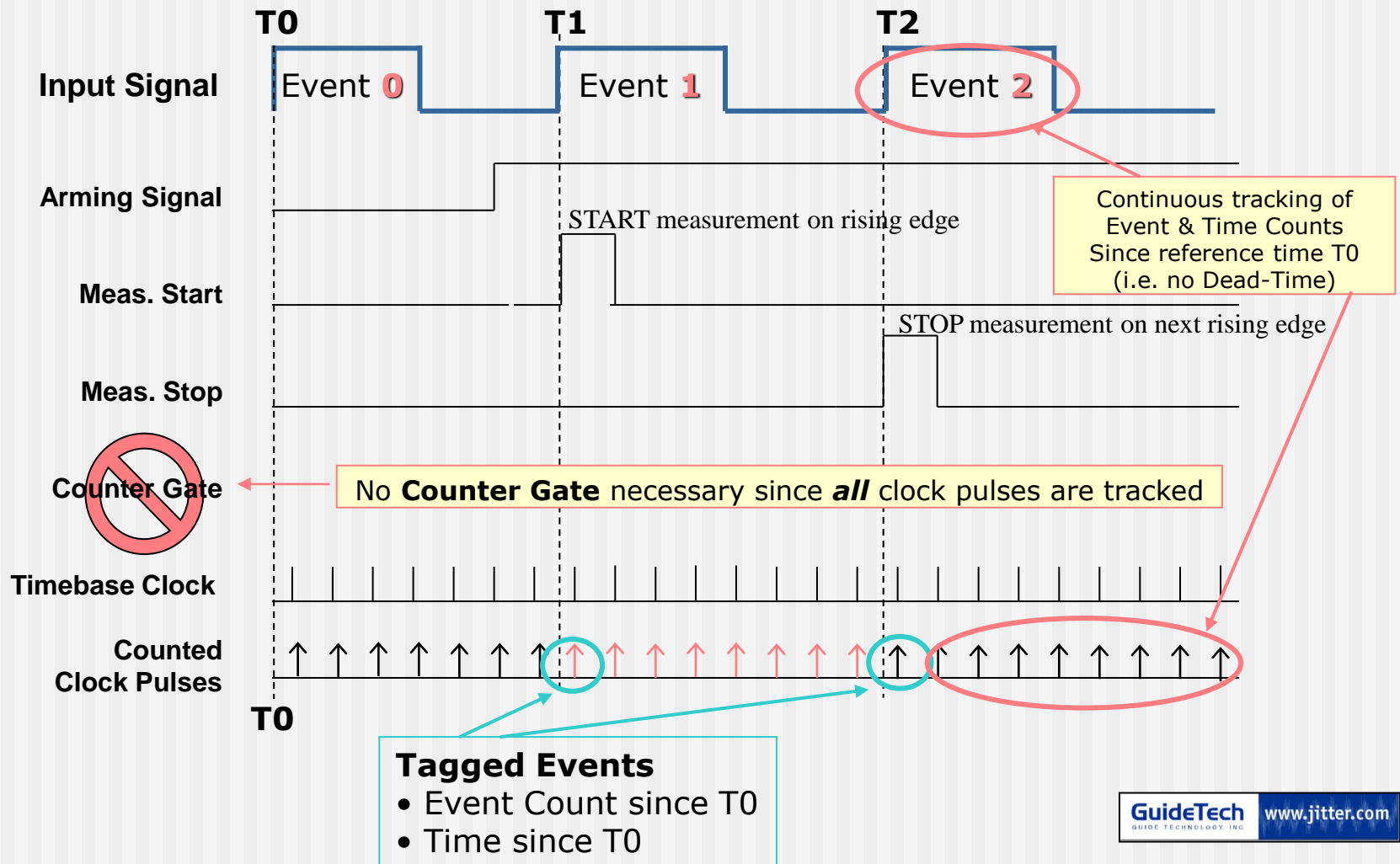
To provide user with:

Delta Time Interval (non-continuous and non-correlated with other measurements)

Overview

Time Interval Measurement Theory

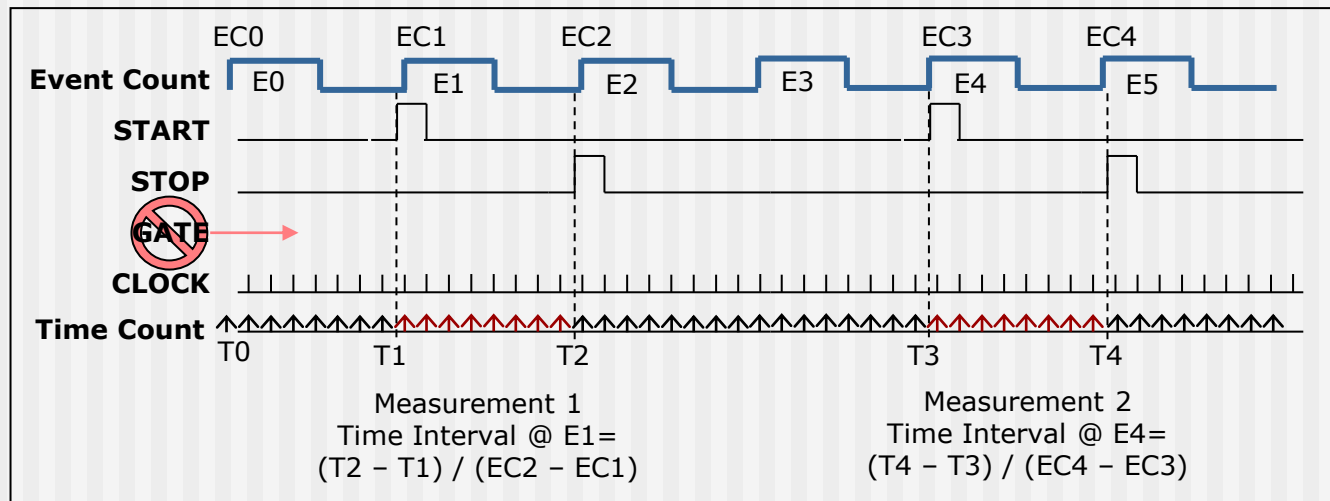
Time Interval Analyzer (TIA) Method



Overview

Time Interval Measurement Theory

Time Interval Analyzer (TIA) Method



TIA architecture obtains:

Continuous, Correlated Event Count (Tag)

- Number of Events since "time zero", T0, for each measurement

Continuous, Correlated Time Count (Tag)

- Number of Clock Pulses since "time zero", T0, for each measurement

To provide user with:

Correlated Time Interval (all measurements referenced to same T0)

Overview

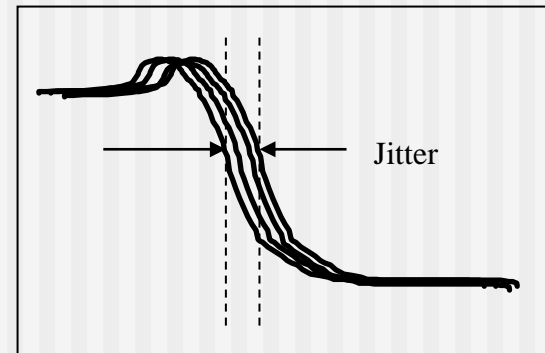
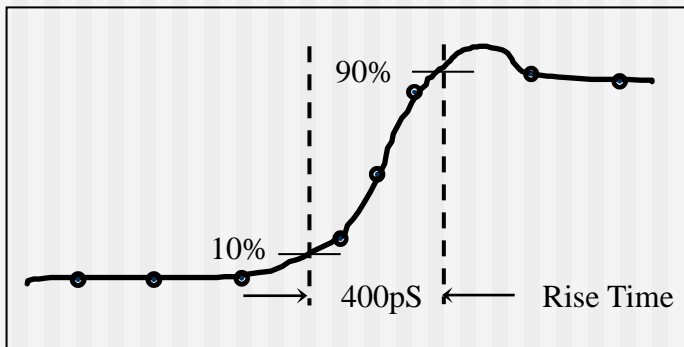
Time Interval Measurement Theory

Digital Sampling Oscilloscope (DSO) Method



Step 1: Under-sample at a coherent time interval $T = Nt + \delta t$

where T is the time between measurement samples; $N = \text{integer}$;
 $t = \text{Input signal period}$; $\delta t = \text{effective sampling period}$



Step 2: Reconstruct the waveform & interpolate between sample points

Step 3: Calculate time interval between two measured (or interpolated) points

Overview

Time Interval Measurement Techniques *Comparison Summary*

	T ime I nterval A nalyzer	T ime C ounter	D igital S ampling O scilloscope	High-Freq Digitizer	Digital Edge Search
Frequency & Time Interval Measurement	Y	Y	Y	Y	Y
Time-Correlation between measurement points	Y	N	Y	Y	?
Speed of Time Measurements	VERY FAST	SLOW	SLOW	VERY SLOW	SLOW
PLL Loop BW Analysis	Y	N	Y	Y	N
Jitter Measurement < 100ps	Y	Y	N	N	N
Jitter Modulation Analysis	Y	N	N	N	?
> 2 channels measured simultaneously	Y	N	N	N	Y

GT 9000 at Paris Observatory

F. FRANK, P.-E. POTTIE

Systèmes de Référence Temps-Espace

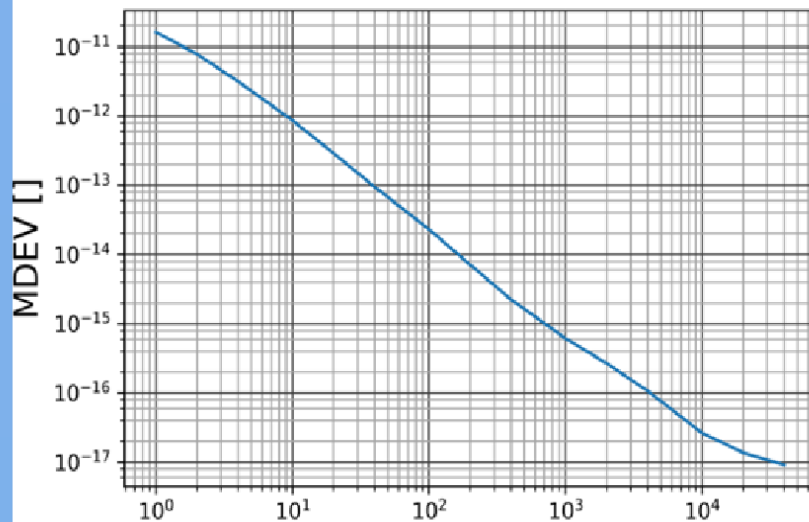
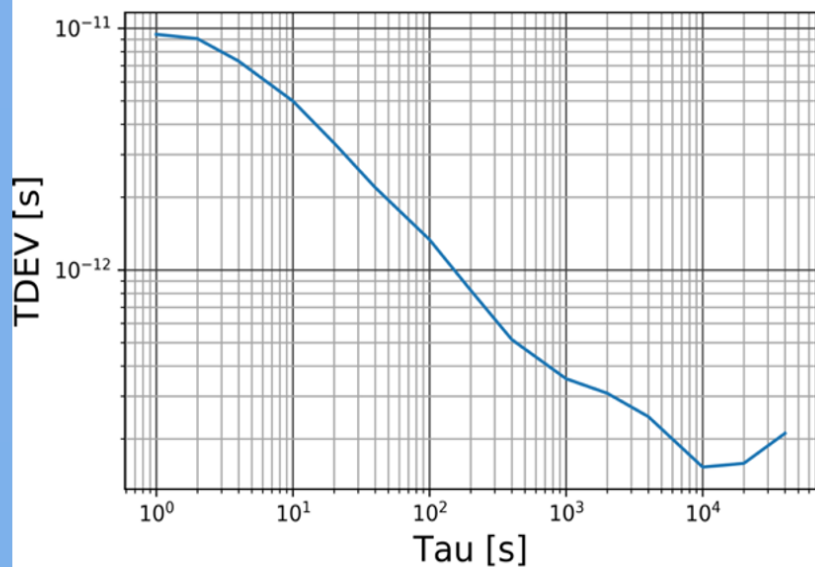
GT 9000 is in use at Paris Observatory for :

- measuring phase noise at high rate,
- frequency and time interval counter

For remote operation and integration into a LAN, GuideTech released for us an **integrated solution with Ubuntu as OS.**

We are presenting here the measurement of time interval between two PPS signals. The PPS are from TimeTech PPS distribution unit. The average delay between the two PPS is 2 ns. The clock signals are derived from an ultra-stable 1 GHz microwave signal generated and distributed over fiber link at SYRTE.

The data set is 200kpts long, acquired in one shot, at 1 Hz rate. The short term deviation is limited by the rising time of the PPS signal. The deviation averages out as $\sqrt{\tau}$ as expected and reach the very low 10^{-13} s level. Regarded as Modified Allan deviation, the resolution of the measurement reaches 10^{-17} within one day of measurement.



GT668SLR Solutions

- **1PPS input**
- **Integrated Two Programmable triggering outputs relative to beginning of measurement or to the Arming signal or at a user specified Real-Time to operate/control the Detector & other sub systems.**
- **Ability to synchronize with UTC time reference**
- **Software package, APIs for SLR & SLR GUI**
- **Integrated GPS receiver with OCXO, Rubidium or Cesium**

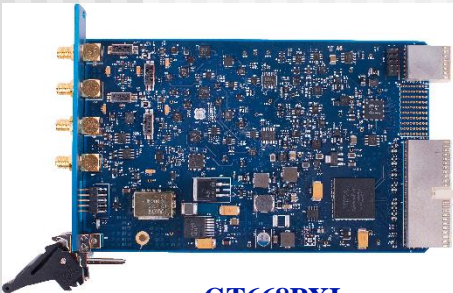
GT668SLR Solutions

With easy expansion (up to 34 Channels) and modular capabilities, the GT668SLR is offered as follows:

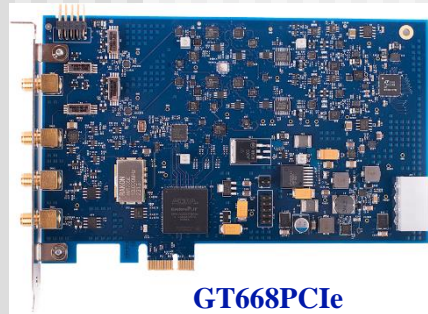
- GT9000SLR Scalable system, 2 to 24 channels, Touch-Display
- GT9000RSLR Rack-Mount scalable system, 2 to 24 channels
- GT9000PSLR-USB3 Portable 2 channel system
- GT8000SLR PXI/PXIe scalable, 2 to 34 channels
- GT668SLR 2 channels PCI, PCIe, PXI & PXIe plug-in boards



GT668PXIe



GT668PXI



GT668PCIe

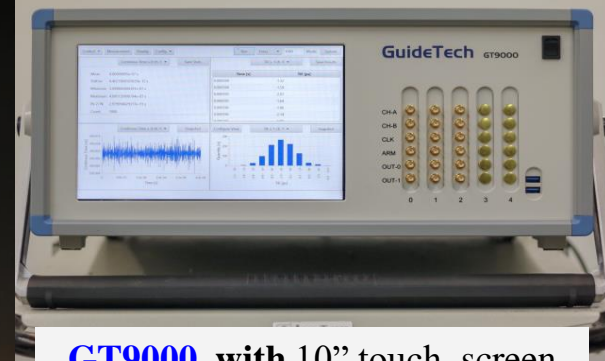


GT668PCI



GT9000R PXIe

19" Rack-Mount, 2 to 24 channels



GT9000 with 10" touch-screen



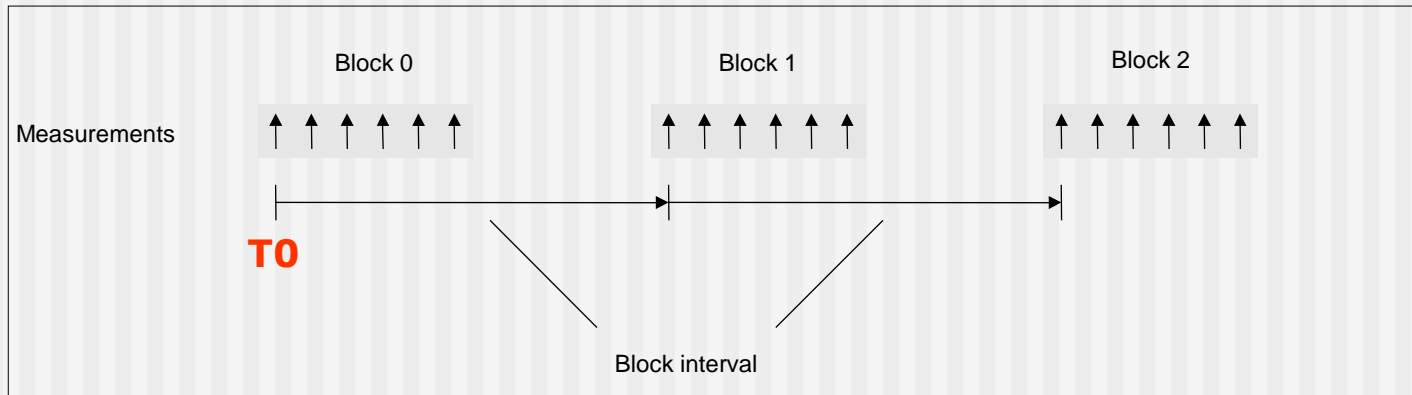
GT9000R 2 to 24 Channels



GT9000P-USB3 Portable

Measurement Terminology

Measurement Blocks



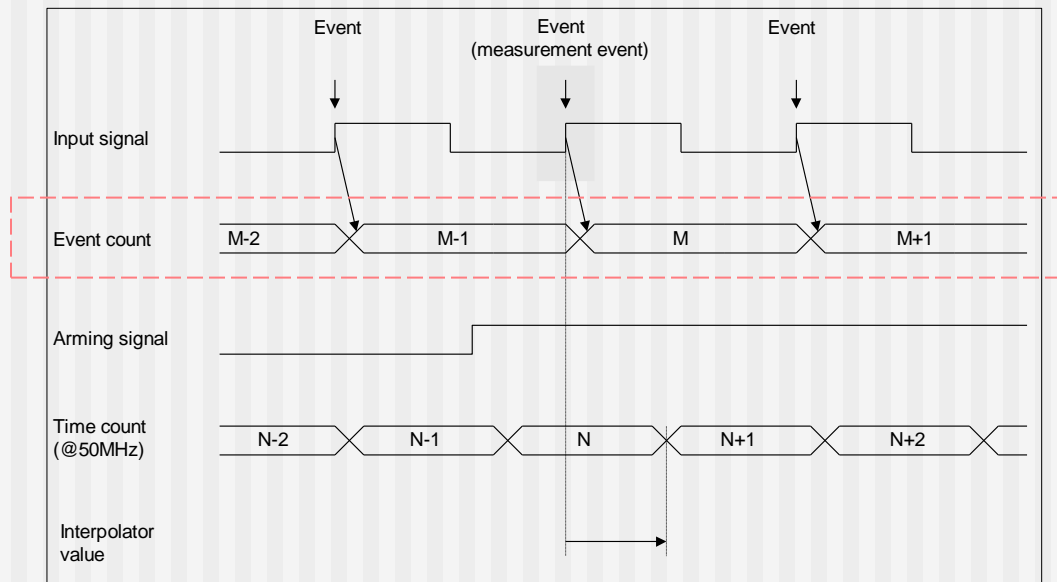
The Femto 2000 supports collection of multiple sets, or **blocks**, of measurements. For measurements requiring multiple sets of blocks, all measurements in each block maintains its time reference to **T0** for the entire measurement period.

The user can specify:

- Number of measurements per block
- Number of blocks
- Block arming

Measurement Terminology

Event Counter



Every measurement channel has an **Event Counter** that is incremented on every input event (input pulse) from beginning of each set of measurement blocks

Tracking all event counts enables the ability to "tag" each measurement on every channel with its corresponding Event ID# with respect to T0 for each set of measurement blocks.

Example:

Period

Event Count

1us

0

1.1us

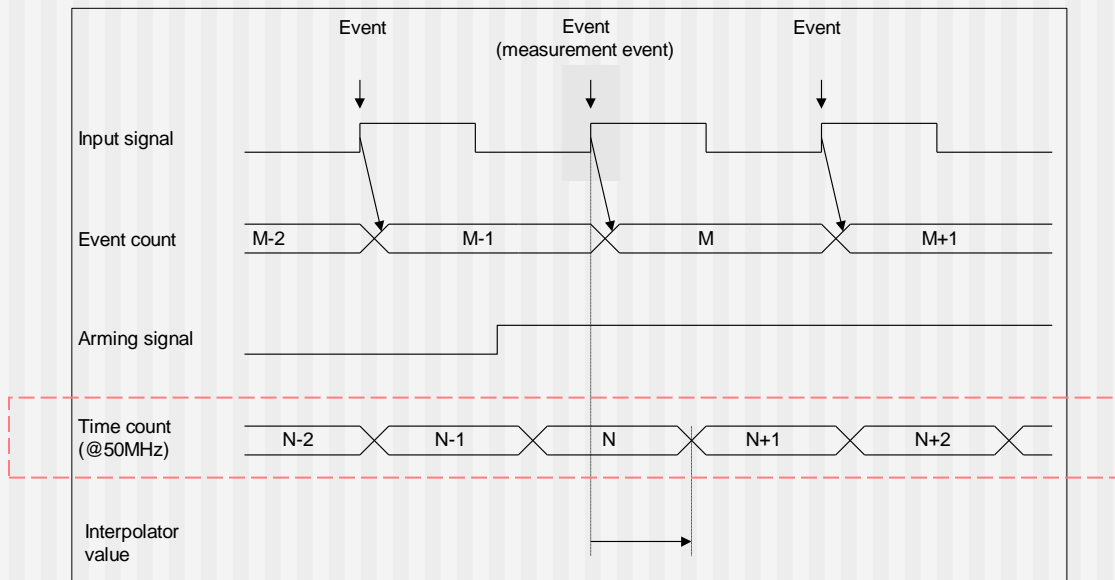
100

0.9us

200

Measurement Terminology

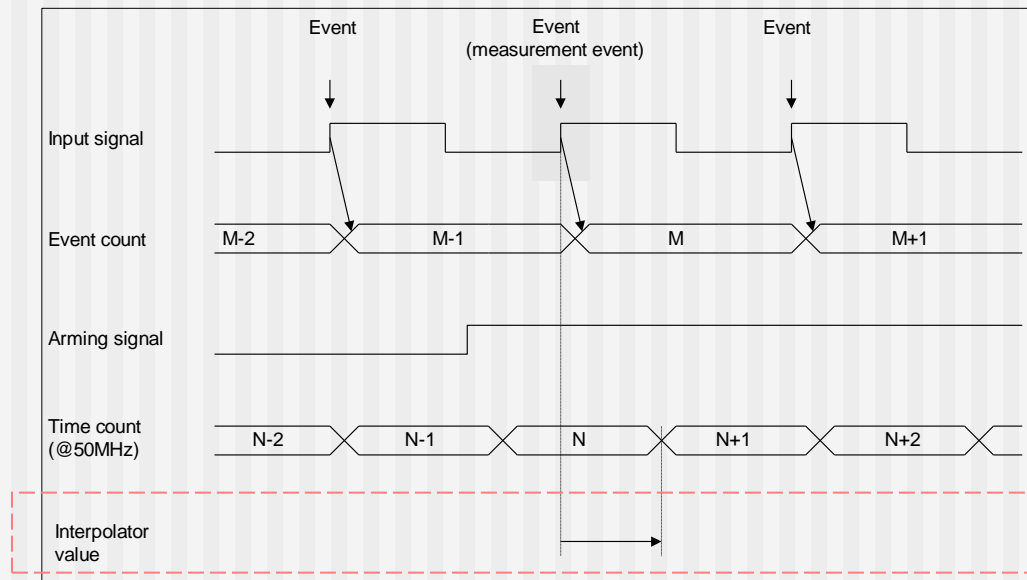
Time Counter



Every measurement channel has a **Time Counter** that is incremented after every reference timebase pulse from time T0 (system power up).

Measurement Terminology

Edge



Every measurement channel has an **Edge** that measures the time interval between a triggered measurement (timetag) event and the next rising edge of the timebase clock.

The edge measures this interval by starting a precision voltage ramp at the triggered measurement event, then stopping the ramp at the next rising edge of the timebase clock.

Measurement Terminology

Arming Signals

Arming Modes

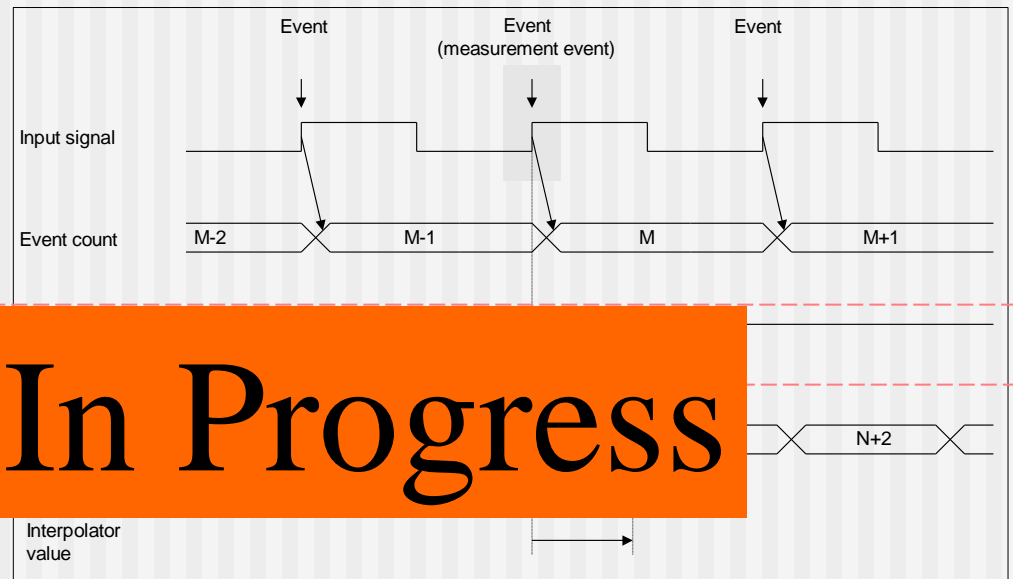
-

External Block Arm Signals

-

Time Tag Arming

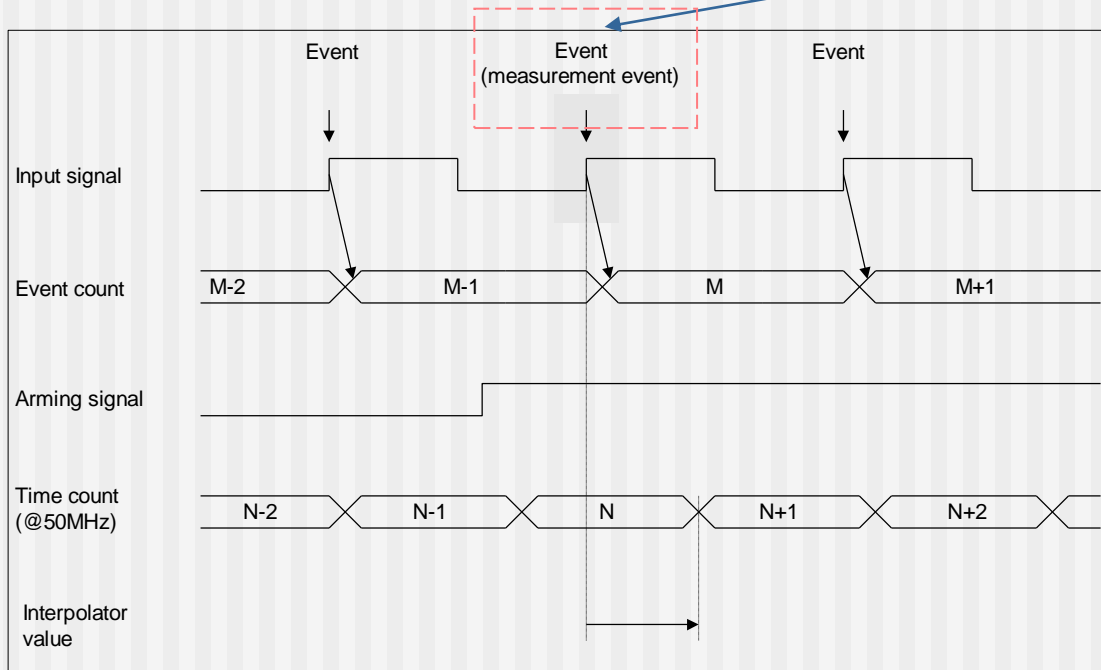
-



Slide In Progress

Measurement Terminology

Timetags



Timetag =

- Event Count
- Time value

The Time Interval Analyzer uses timetags to calculate time intervals between measured events. Since the Event Location is preserved in each timetag, the measurement results from a TIA can include the Event Count at which each measurement was taken as shown below:

<u>Period</u>	<u>Event Count</u>
1us	0
1.1us	100
0.9us	200

Measurement Terminology

Timing Diagram Notations

Femto-2000 measurements can be categorized by the number of Edges needed to generate the Time Tags for each measurement.

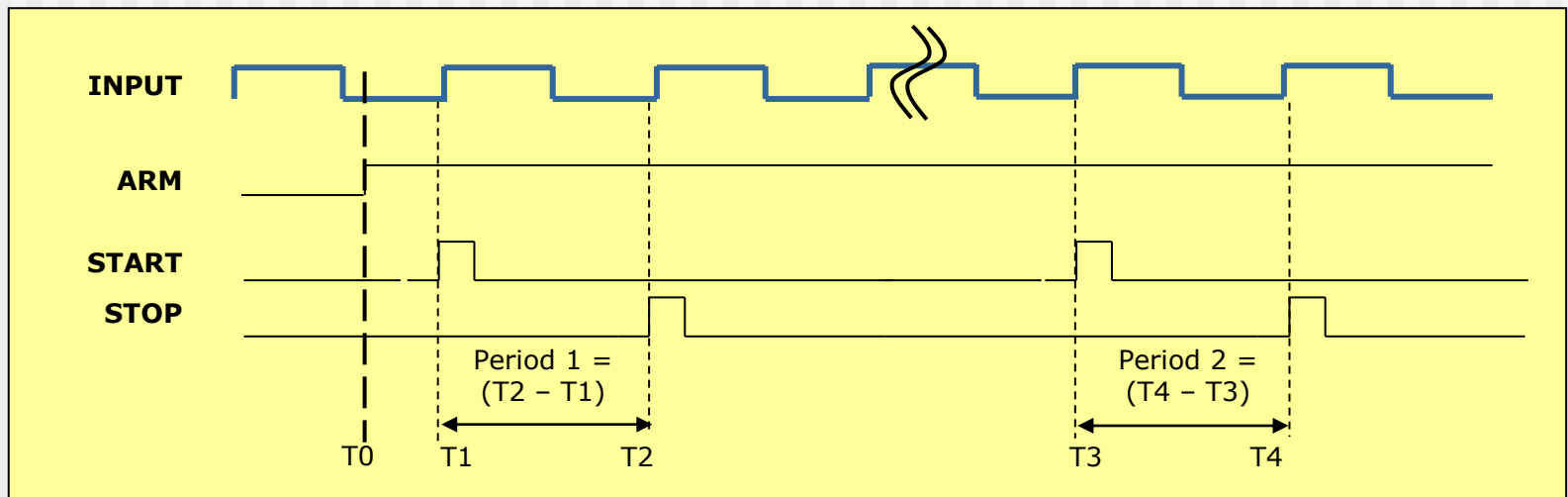
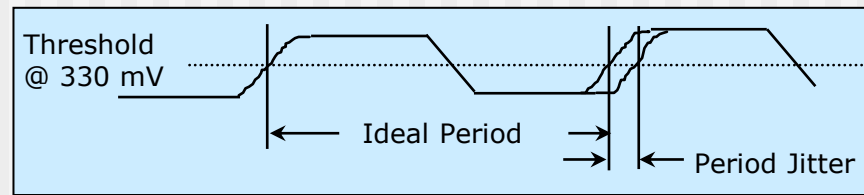
In each of the following measurement descriptions:

- **EC_n** represents the *Event Count* for measurement event *n*
- **T_n** represents the *time at which measurement event n occurs*
- **A0, A1, B0** and **B1** represent the *edges* used to generate the Time Tags for each measurement

Jitter Test

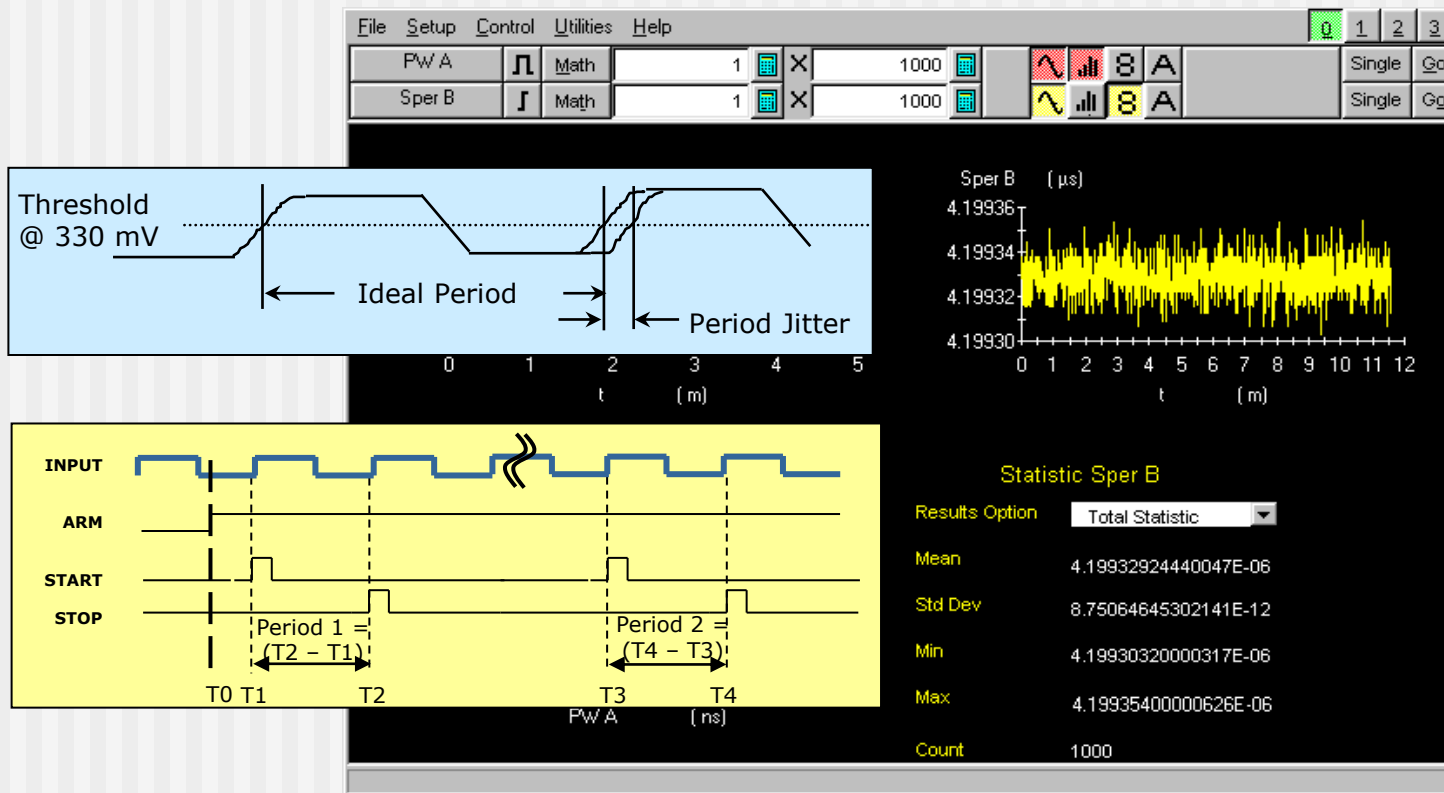
Using Single Period Measurement Mode

Jitter = change in period over time



Jitter Test

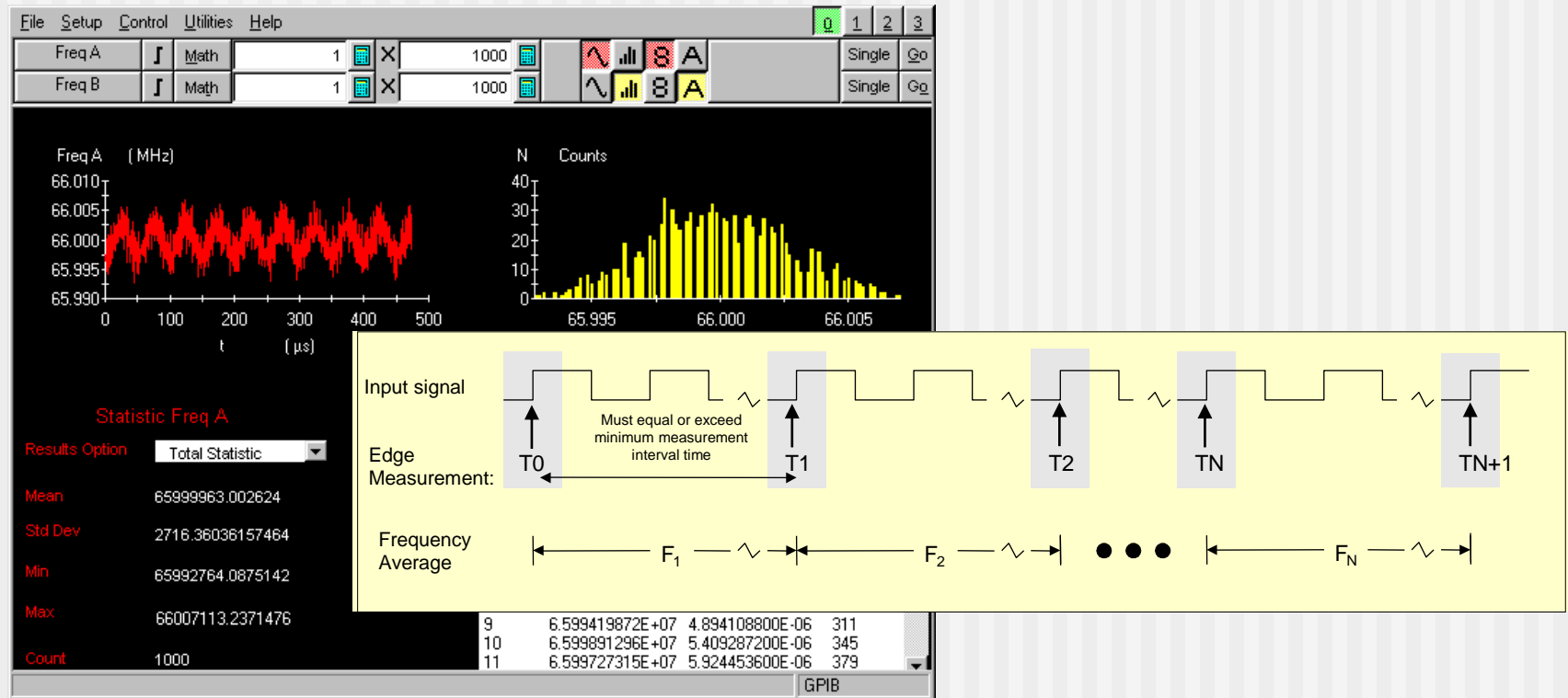
Using Single Period Measurement Mode



Jitter = STANDARD DEVIATION of Single Period Measurement

Frequency Test

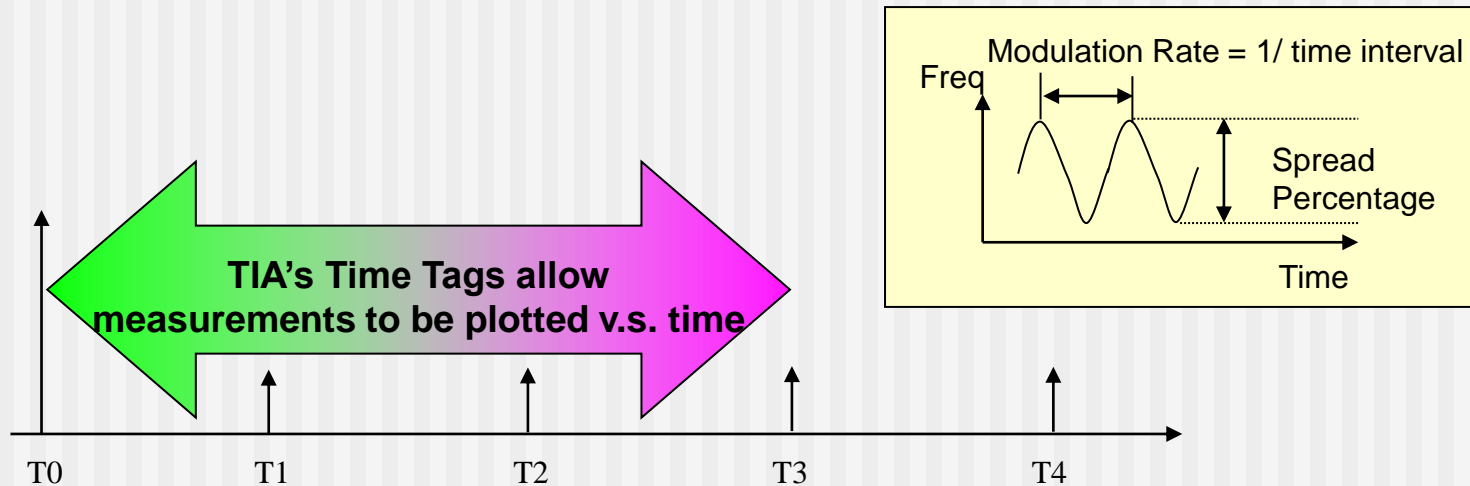
Using Frequency Average Measurement Mode



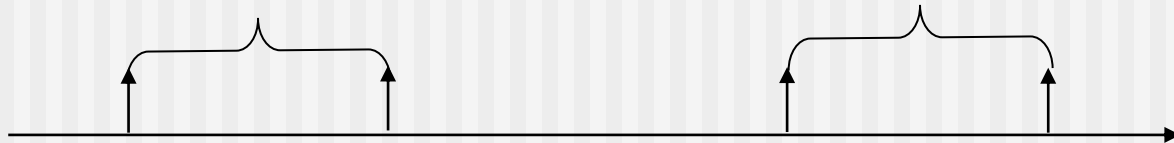
Frequency = MEAN of the Frequency Average Measurement

TIA Measurement Theory

Frequency Modulation Measurement Example



Time Counters provide Time Interval values with no reference to time

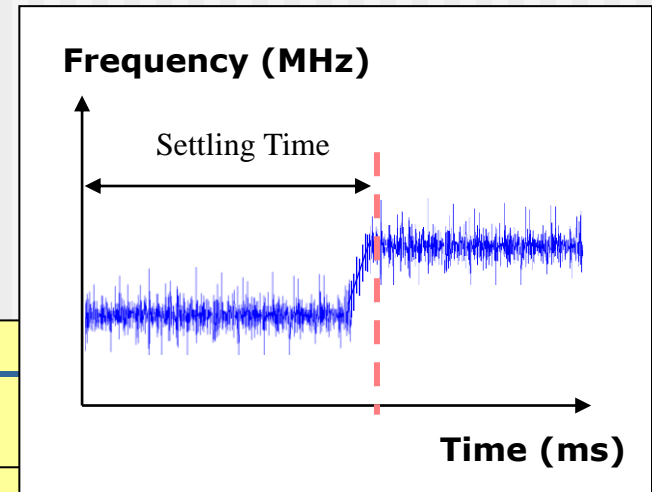
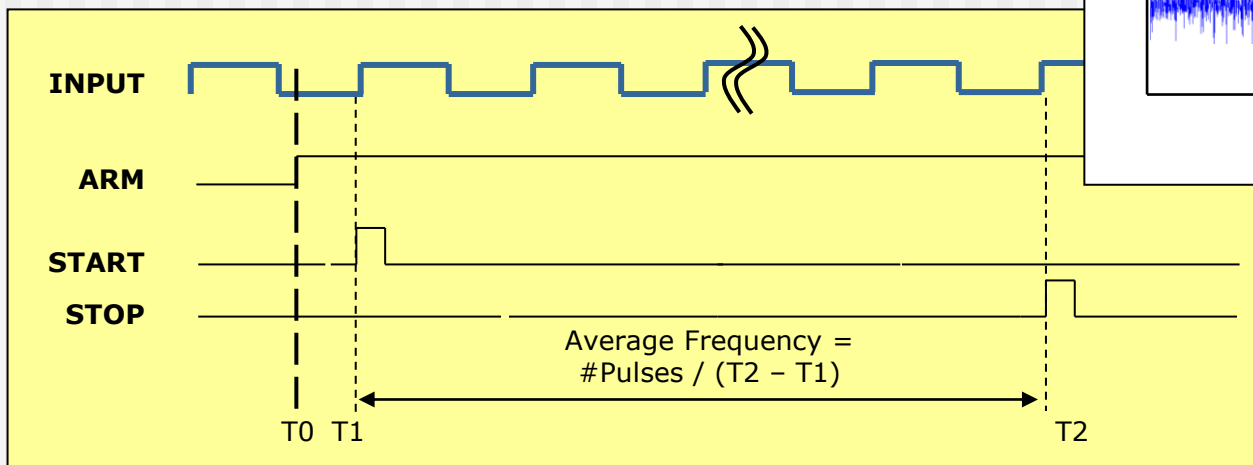


Frequency Settling Time Test

Using Frequency Measurement Mode, Ext ARM

Set an **EXTERNAL ARM** to trigger a Frequency measurement at the time of a change in the PLL input frequency.

Frequency Settling Time is calculated by searching the measurement result data array for the time when the **MEAN** values of the Frequency measurement result array corresponds with the final frequency expected.



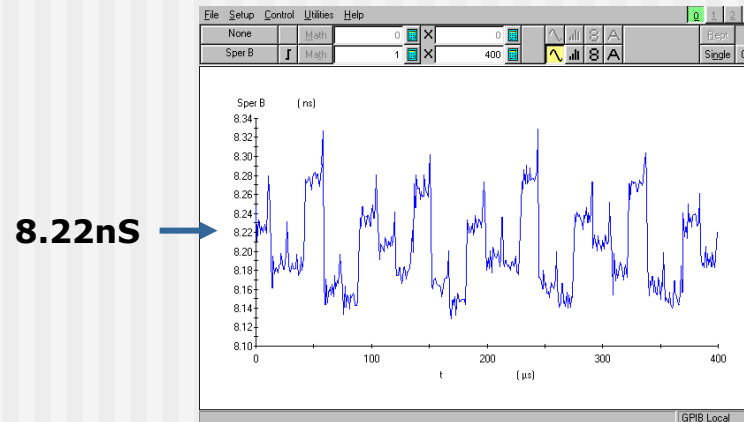
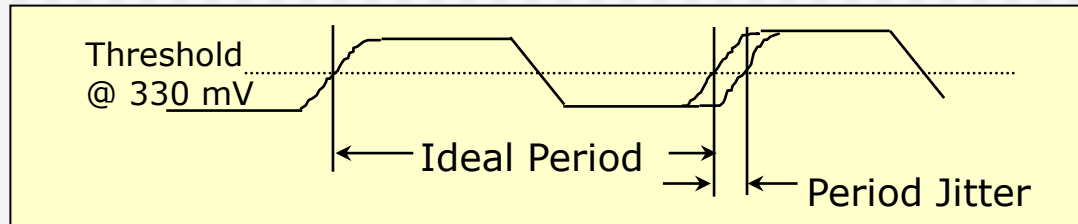
Short-Term Jitter Test

Using Single Period Measurement Mode

Objective: Verify the amount of deviation of clock output edges from the ideal position (i.e. the amount of *deviation* from the *ideal period*) on the PLL output

TIA Measurement Mode: Single Period

Period Jitter = Standard Deviation of Single Period measurement



Cycle Time: 8.22ns (+ jitter)

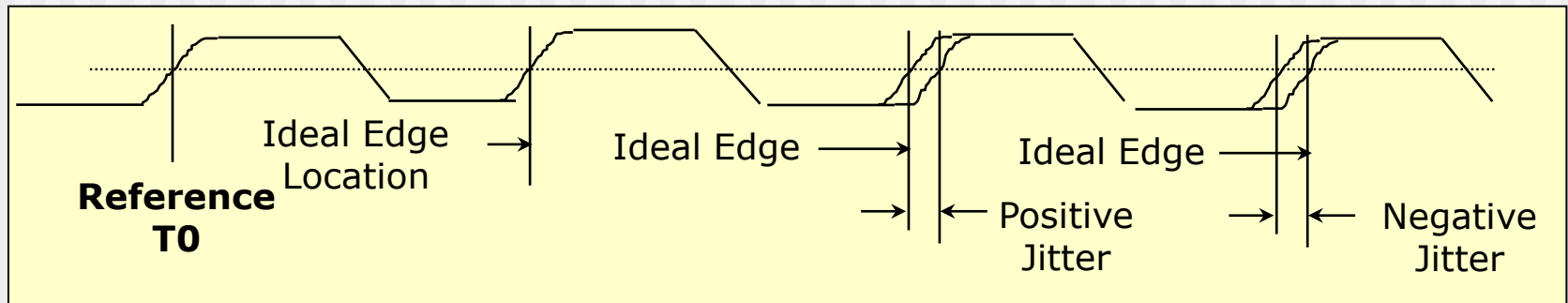
Long-Term Jitter Test

Using Time Interval Error Measurement Mode

Objective: Verify the amount of deviation of clock output edges over many cycles from the ideal position at reference time T_0 (i.e. the amount of *deviation* from the *ideal edge location* over a long period of time) on the PLL output

TIA Measurement Mode: Time Interval Error (TIE)

Long-Term Jitter = Standard Deviation of TIE measurement



Single-Edge Measurement Modes

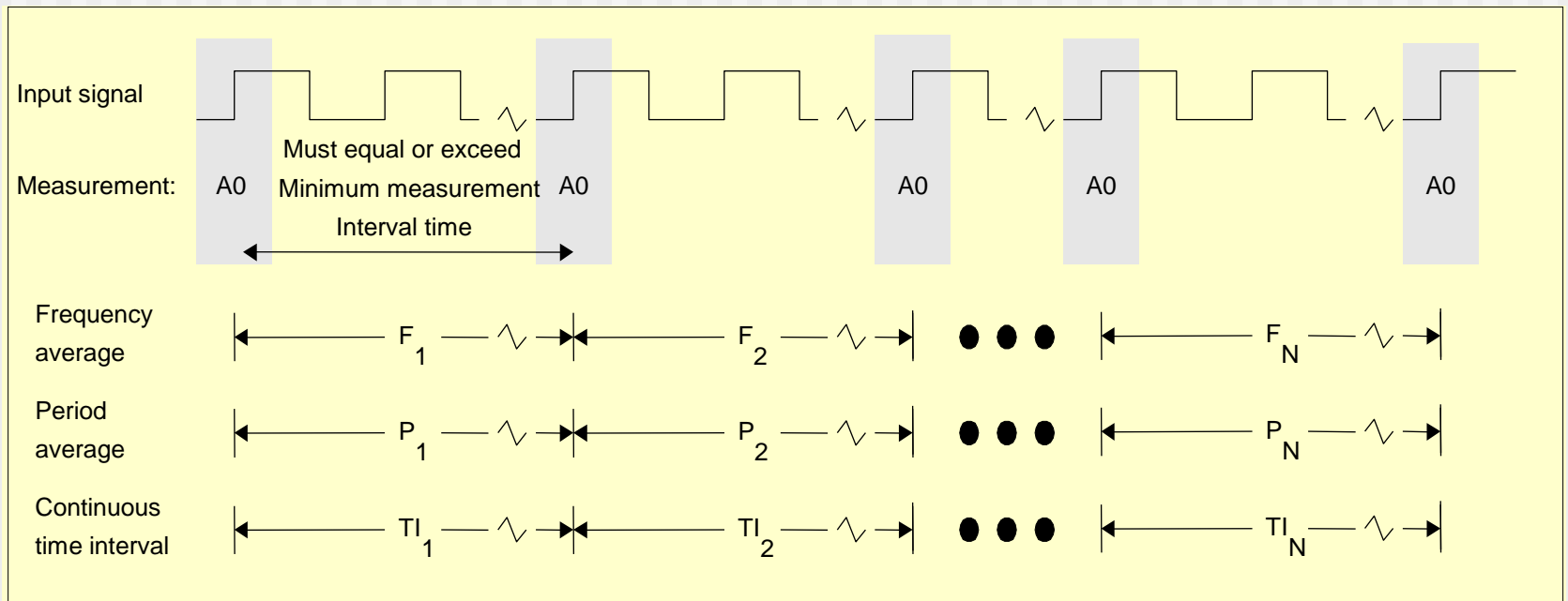
Introduction

Single-edge measurements:

- Require only a single input signal (e.g. Channel A or Channel B)
- Use only one edge (e.g. A0 or B0)

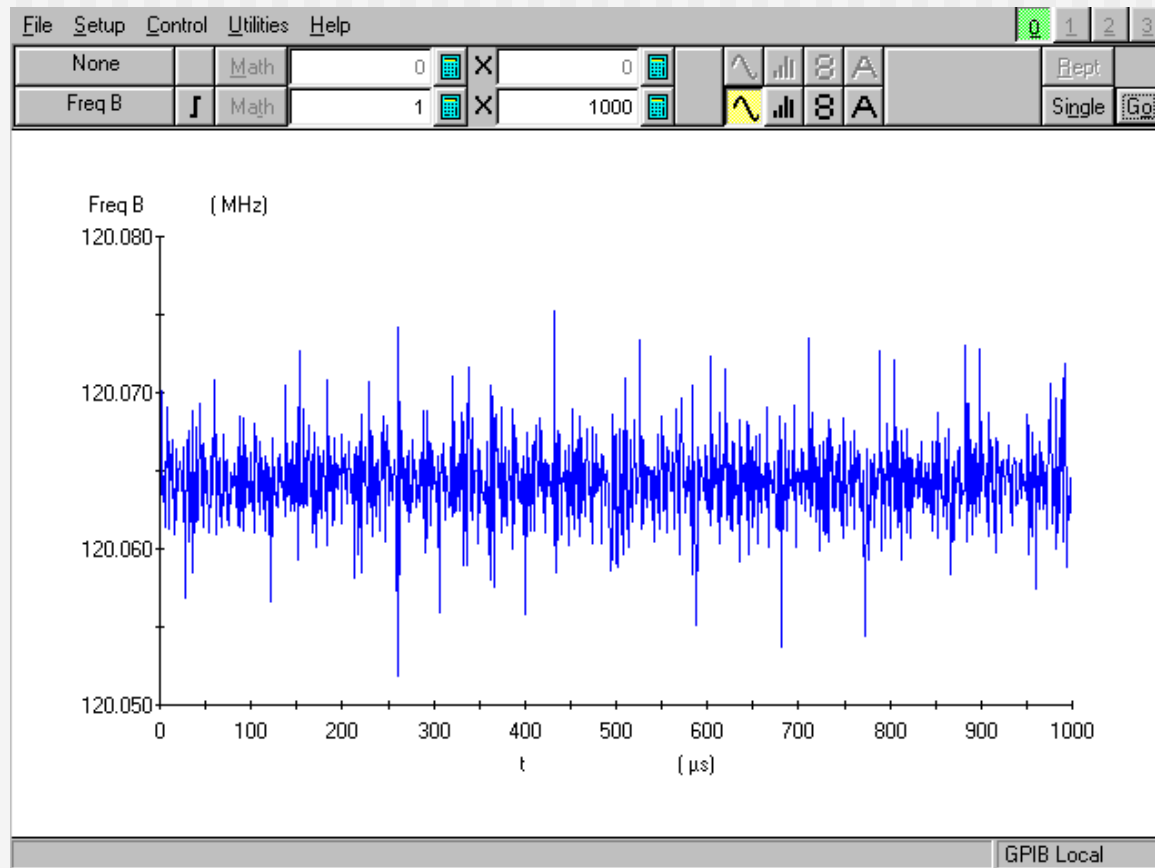
Single-Edge Measurement Modes

Frequency Averaging



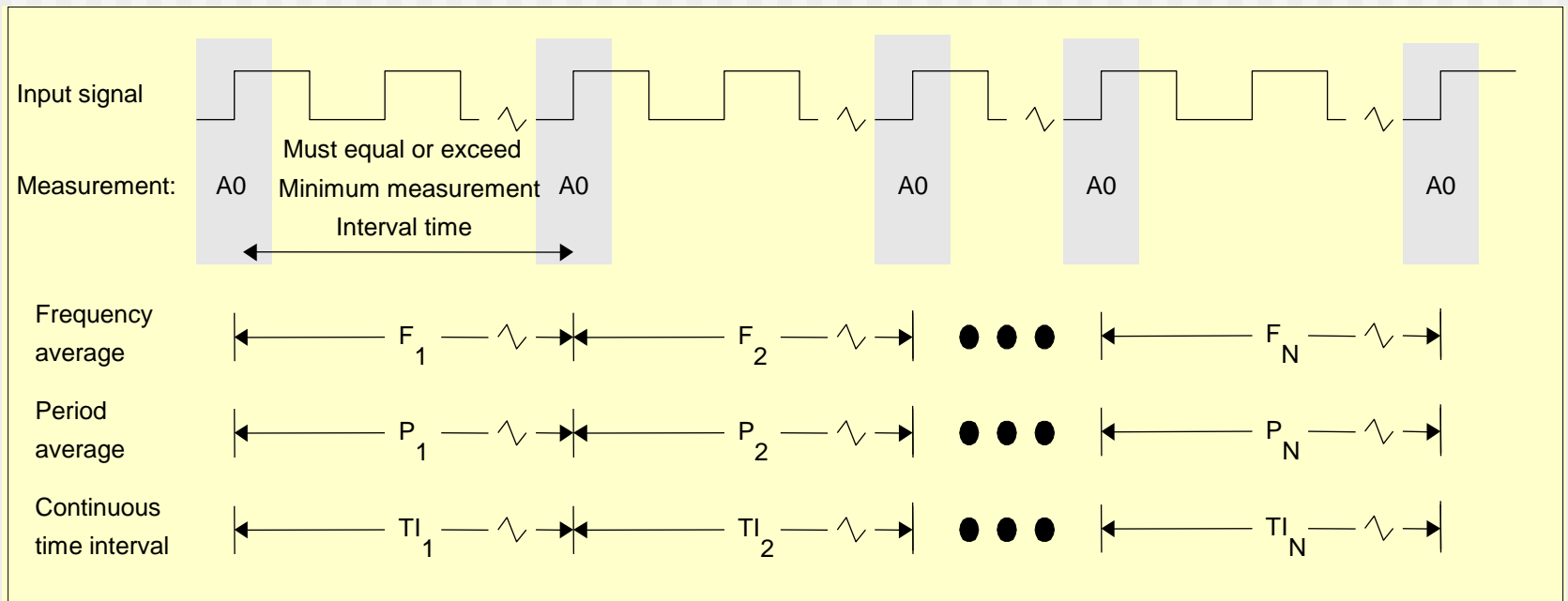
Single-Edge Measurement Modes

Frequency Averaging



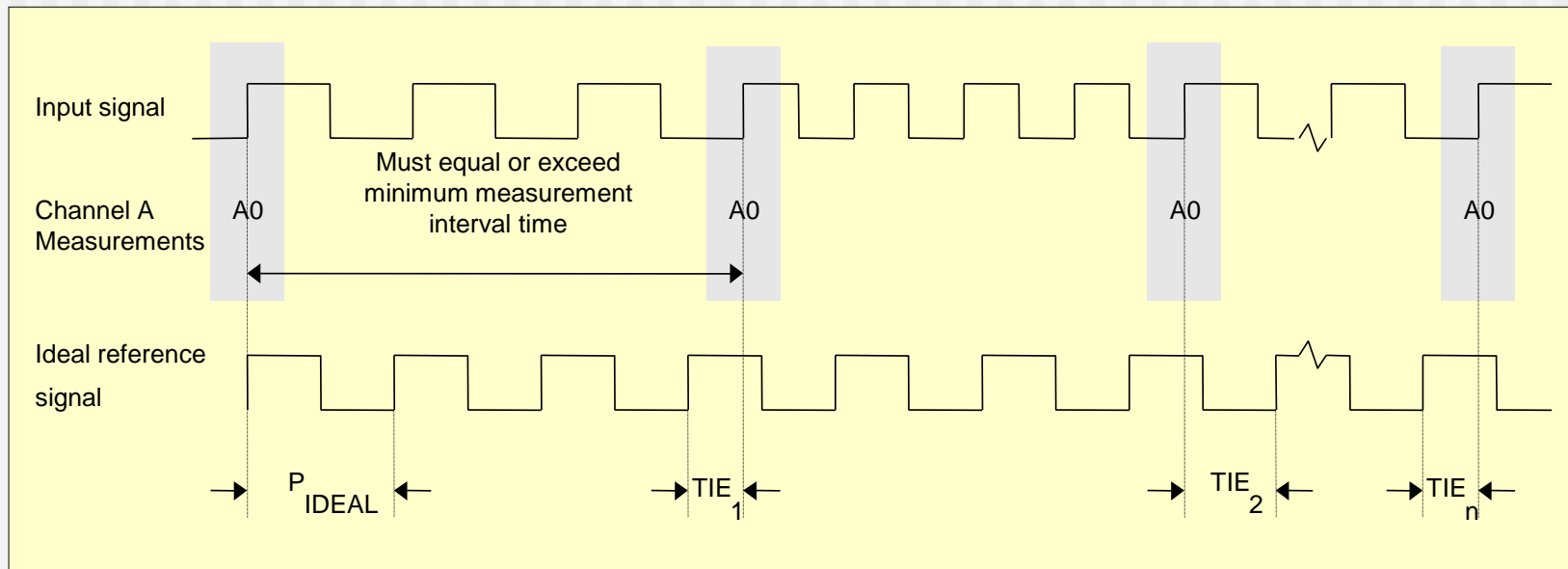
Single-Edge Measurement Modes

Period Averaging



Single-Edge Measurement Modes

Time Interval Error (TIE)



Two-Edge Measurement Modes

Introduction

Single-edge measurements have a fundamental limitation:

The minimum time between successive single-edge measurements is limited by the edge measurement circuit recovery time.

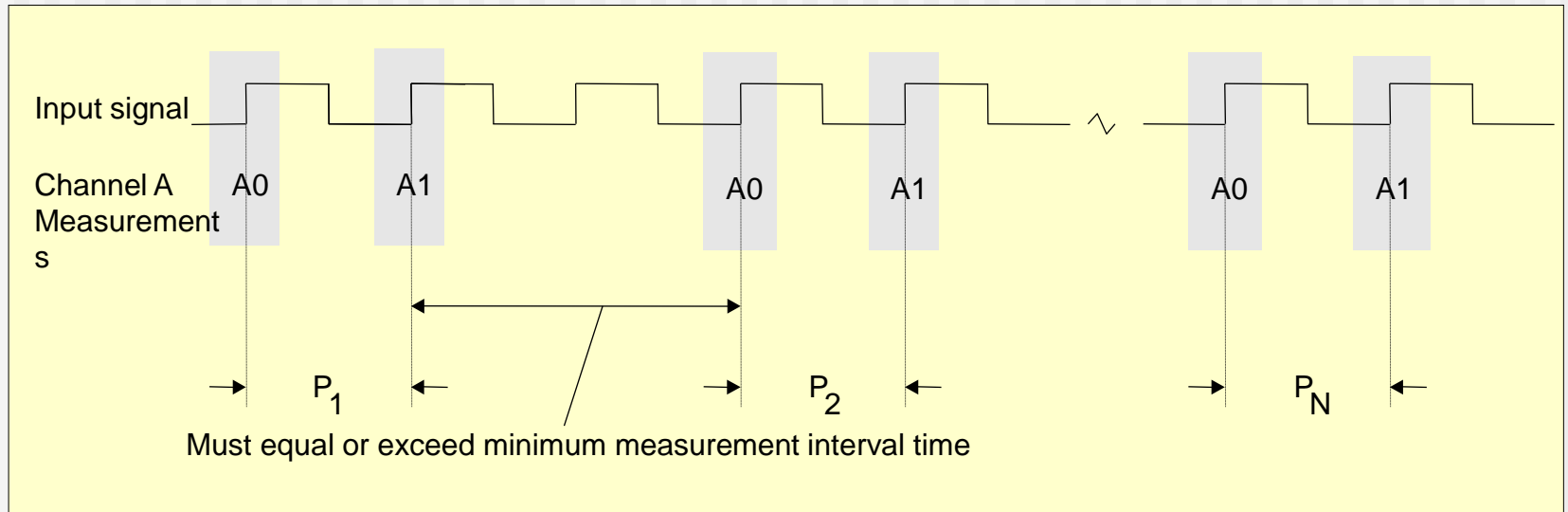
By using two edge measurement circuits, the time measurement between close successive edges can be dramatically reduced.

Two-edge measurements can measure very small intervals:

- Require two edge measurements (e.g. A0 & A1, A0 & B0 or B0 & B1)
- Two edges can be measured on a single channel (e.g. A0 & A1)
- Two edges can be measured between two different channels (e.g. A0 & B0)

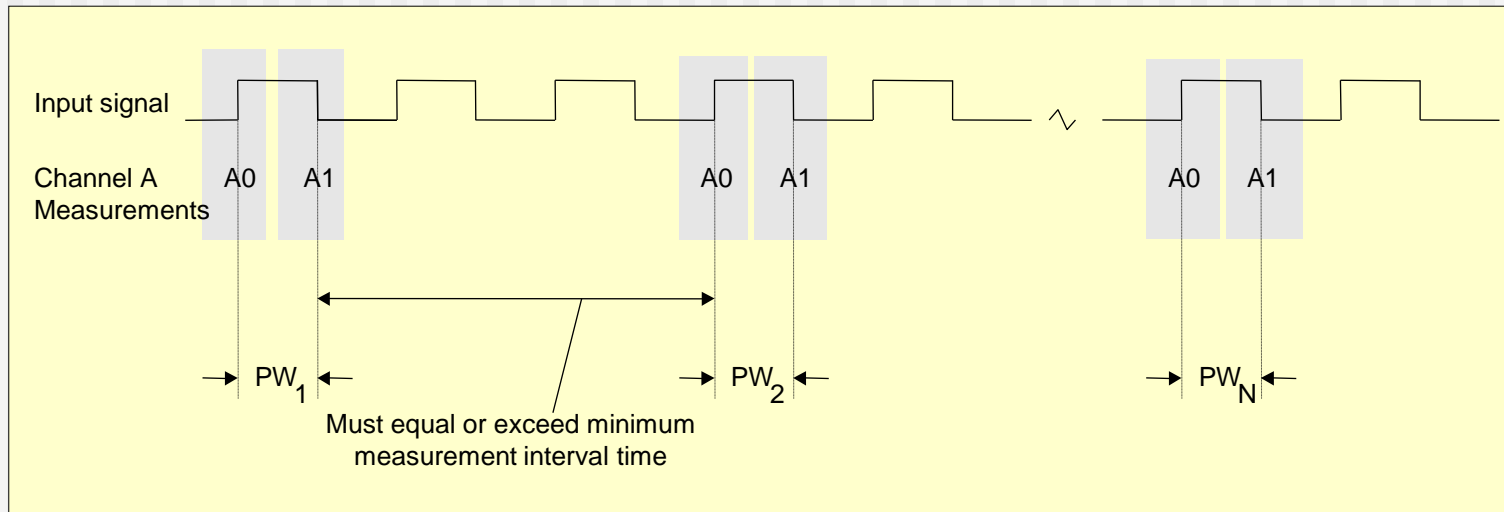
Two-Edge Measurement Modes

Single Period



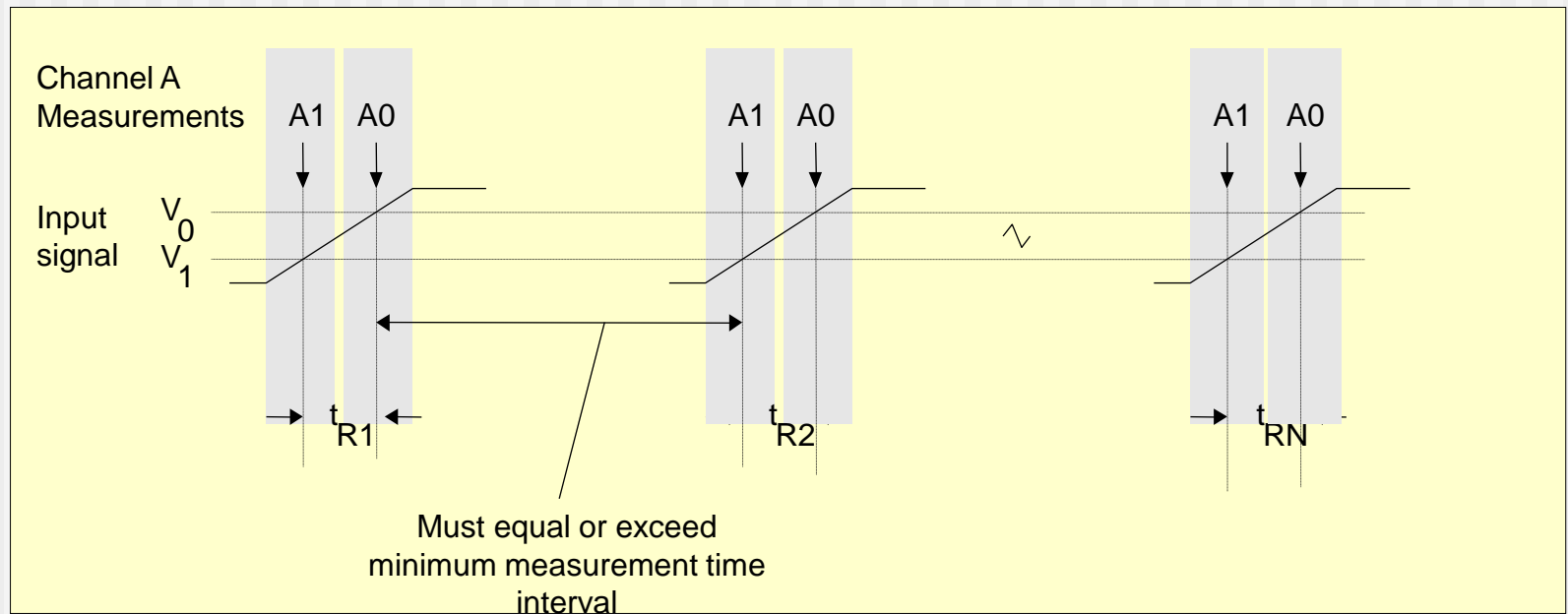
Two-Edge Measurement Modes

Pulse Width (PW)



Two-Edge Measurement Modes

Risetime / Falltime



Two-Edge Measurement Modes

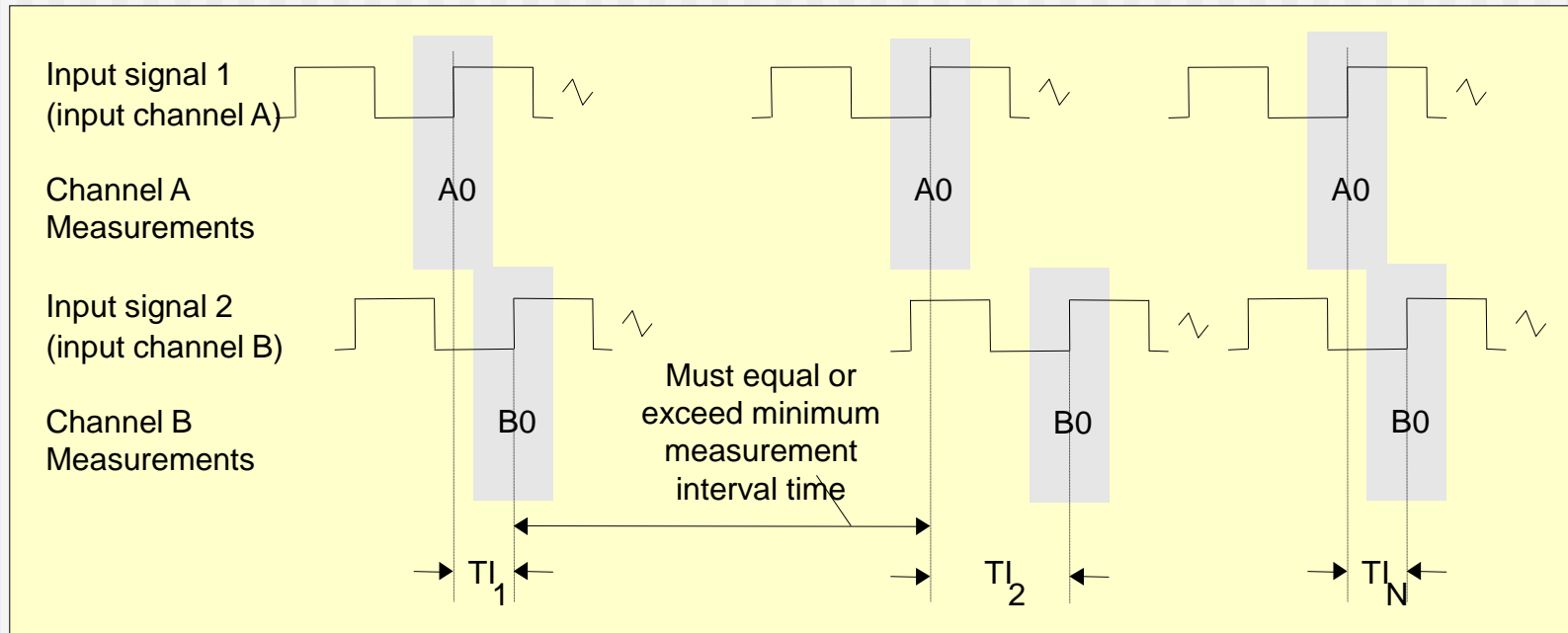
Time Interval (Single-Channel)

Time Interval (Single-channel) – This two-edge measurement mode is a more general form of the single-period, single-pulse-width, and Rise Time/Fall Time measurement modes above. In this mode, the time intervals between pairs of events on an input channel are reported, but with flexible arming of several types:

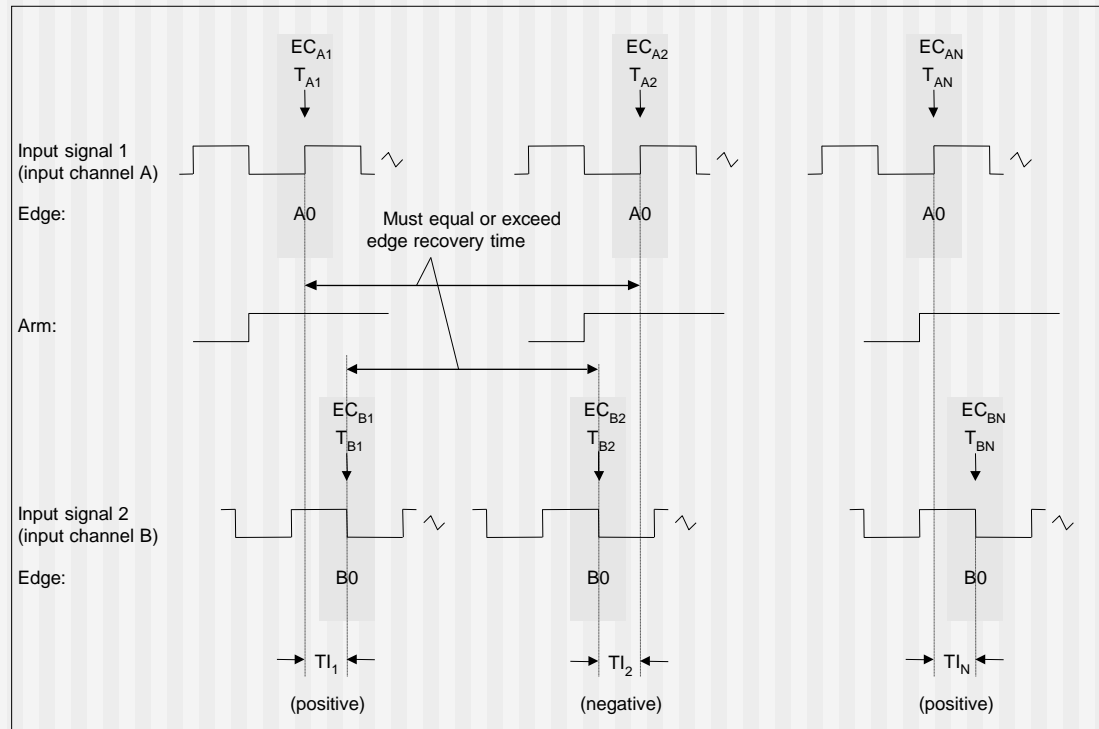
- Each measurement event can be armed by an external arming signal
- The second measurement event of each pair can be armed with the divide-by-N counter, so that the instrument measures the time between N events. If, for example, the measured events are rising edges, the instrument could measure the distance between a rising edge and the Nth subsequent rising edge
- Arming of the types used in the single-period, single-pulse-width, or Risetime/Falltime measurements

Two-Edge Measurement Modes

Time Interval (Two-Channel)



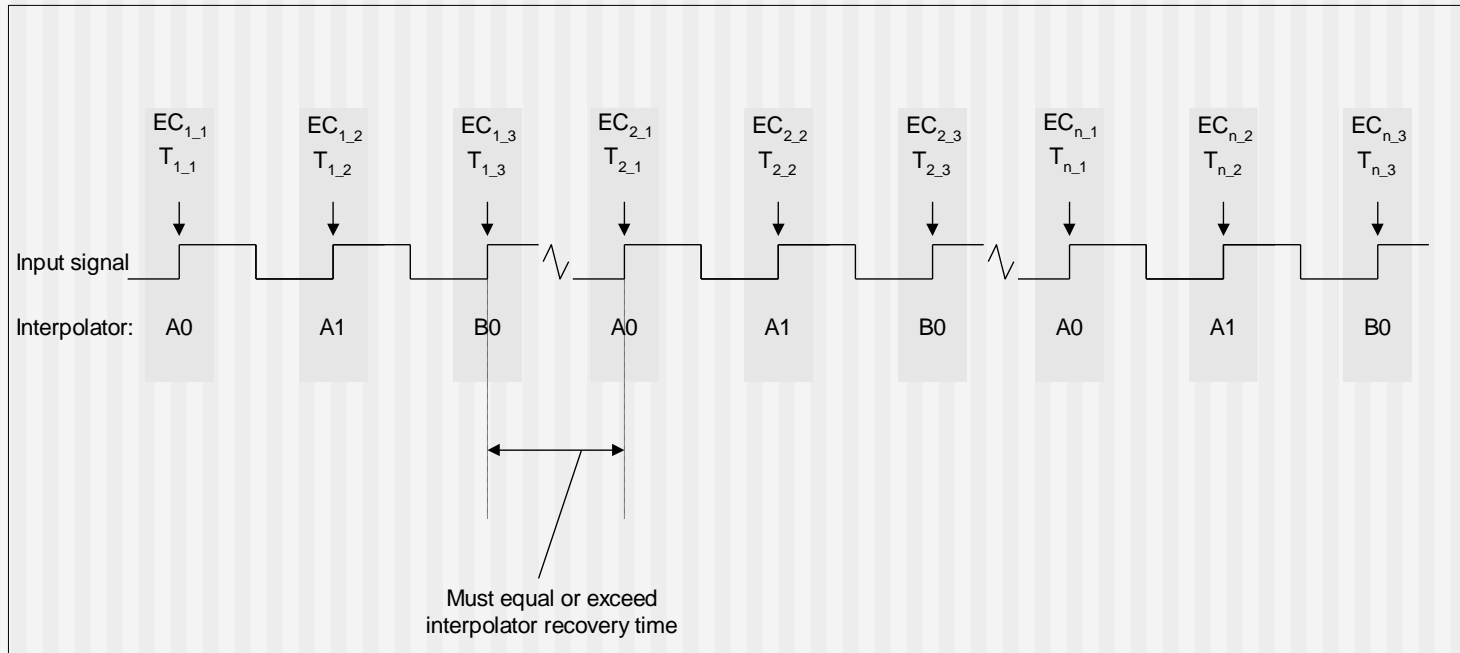
Two-Edge Measurement Modes +/- Time Interval



$$TI_n = T_{Bn} - T_{An}, \quad n=1..N \quad (\text{for TI Ch_A to Ch_B})$$

where T_{An} are the time measurements for the input signal on input channel A and T_{Bn} are the time measurements for the input signal on input channel B

Three-Edge Measurement Mode Cycle-to-Cycle (ΔP)



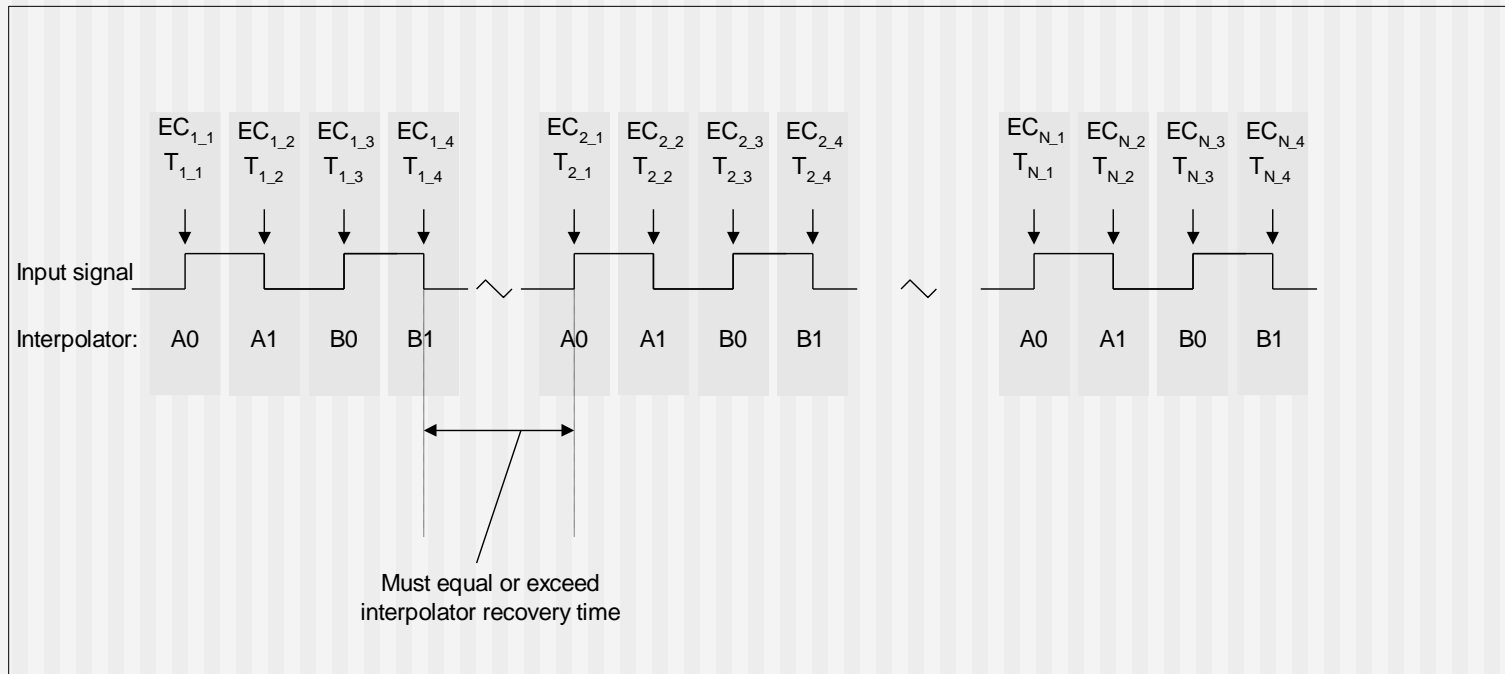
$$\Delta P_n = (T_{n-3} - T_{n-2}) - (T_{n-2} - T_{n-1}), \quad n = 1..N$$

$$= T_{n-3} - 2T_{n-2} + T_{n-1}$$

where T_{n-1} , T_{n-2} , and T_{n-3} are the times of the first, second, and third edge measurements.

Four-Edge Measurement Mode

Pulse-Width-to-Pulse-Width (ΔPW)



$$\Delta PW_n = (T_{n_4} - T_{n_3}) - (T_{n_2} - T_{n_1}), \quad n = 1..N$$

where $T_{n,1}$, $T_{n,2}$, $T_{n,3}$, and $T_{n,4}$ are the times of the first, second, third, and fourth edge measurements.



Geosynchronous LRA performance analysis with NP data

Daniel Kucharski¹, David A. Arnold²

¹The University of Texas at Austin, TX

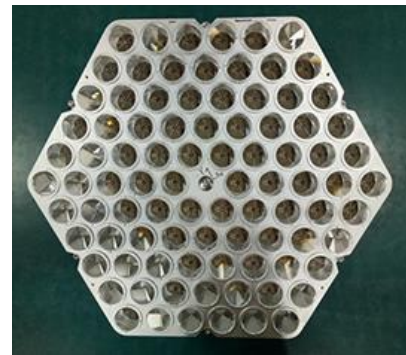
²Smithsonian Astrophysical Observatory, Cambridge, MA (retired)

GEO SLR: satellites

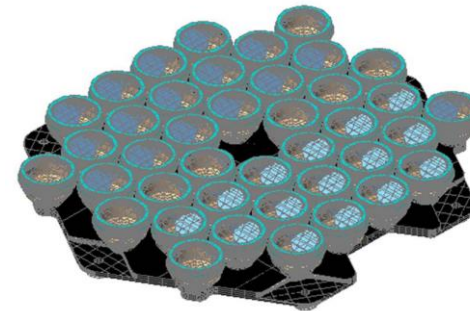
Mission	Satellites (18)	Orbit altitude [km]	Orbit inclination	Data	LRA
ETS-8	1	36,000	0°	Legacy NP data (pre-CRD)	Planar, 36 CCRs, 1.6" (41 mm)
COMPASS	5: G1, I3, I5, I6B, IS1	35,680-35,790	55.5°	NP CRD	Hexagonal, 90 CCRs, 1.5" (38 mm)
IRNSS	7: 1A, 1B, 1C, 1D, 1E, 1F, 1I	35,790-42,290	5°, 29.5°, 30°	NP CRD	Hexagonal, 40 CCRs, 1.5" (38 mm)
QZSS	5: 1, 2, 3, 4, 1R	32,000-40,000, 36,000	0°, 45°	NP CRD	Planar, 56 CCRs, 1.6" (41 mm)



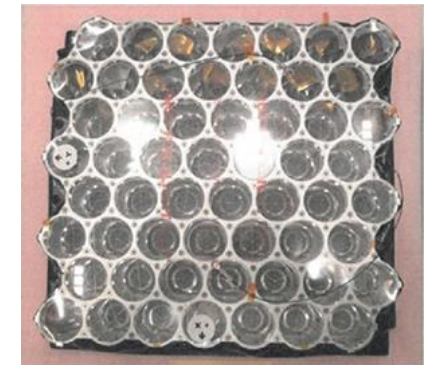
ETS-8 (JAXA)



COMPASS
(Chinese Academy of Sciences)



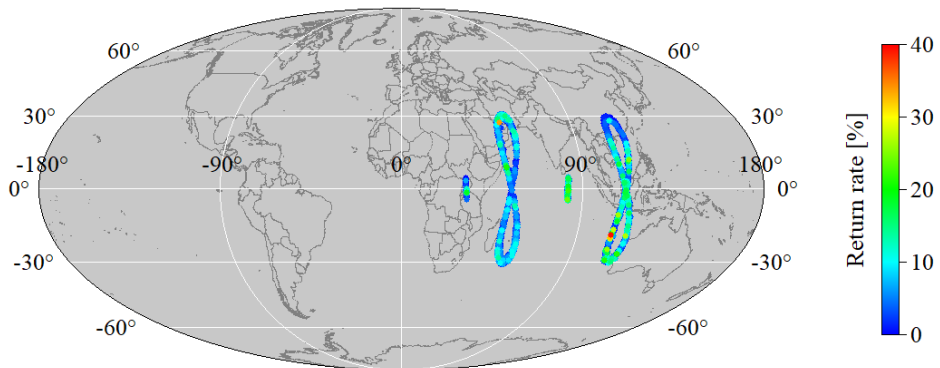
IRNSS (ISRO)



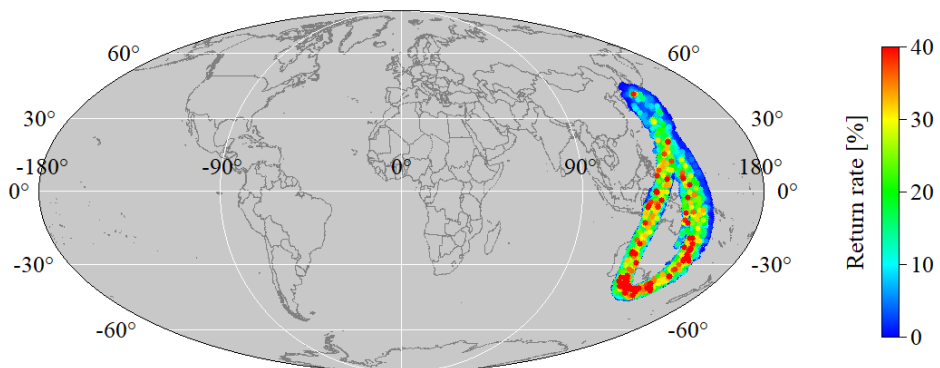
QZSS (JAXA)

GEO SLR: NP data

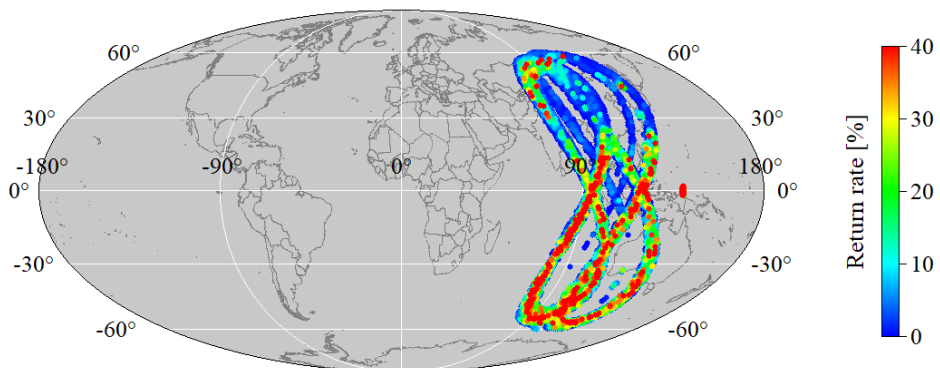
IRNSS



QZSS



COMPASS



Earth-fixed (ECEF) distribution of NP CRD, color coded by return rate.

The NP data of GEO-synchronous satellites can be analyzed in Sun-Earth-satellite frame with respect to the argument of satellite latitude Δu and the elongation angle ϵ .

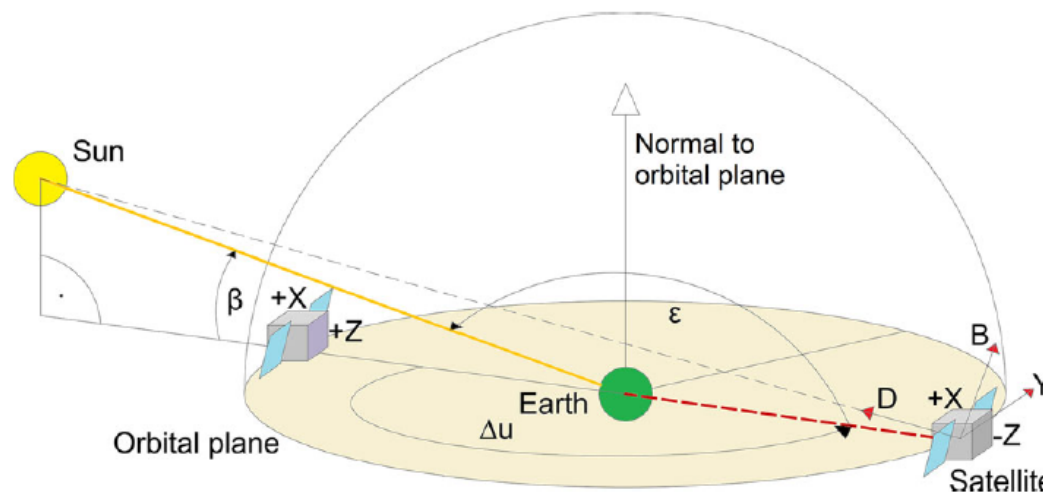
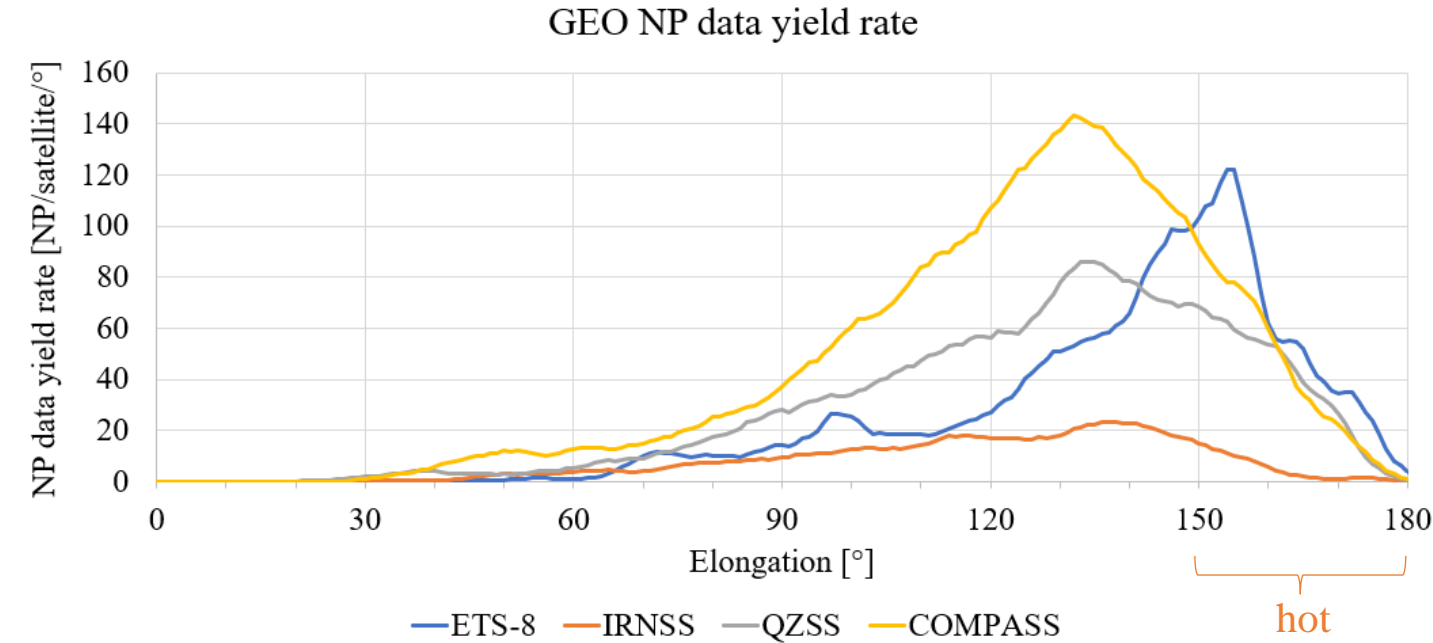


Fig. 2 Sun–Earth–satellite reference frame showing the elevation angle of the Sun over orbital plane β , argument of satellite latitude with respect to the Sun Δu and the elongation angle ϵ

Ref: Validation of Galileo orbits using SLR with a focus on satellites launched into incorrect orbital planes, Sosnica et al., 2017.

GEO SLR: NP data yield rate comparison



Moving average trends represent number of NPs collected at different elongation angles.

The orbits are slightly different, but the IRNSS trend significantly deviates from the group – especially at high elongation angles where the retroreflectors are facing the Sun.

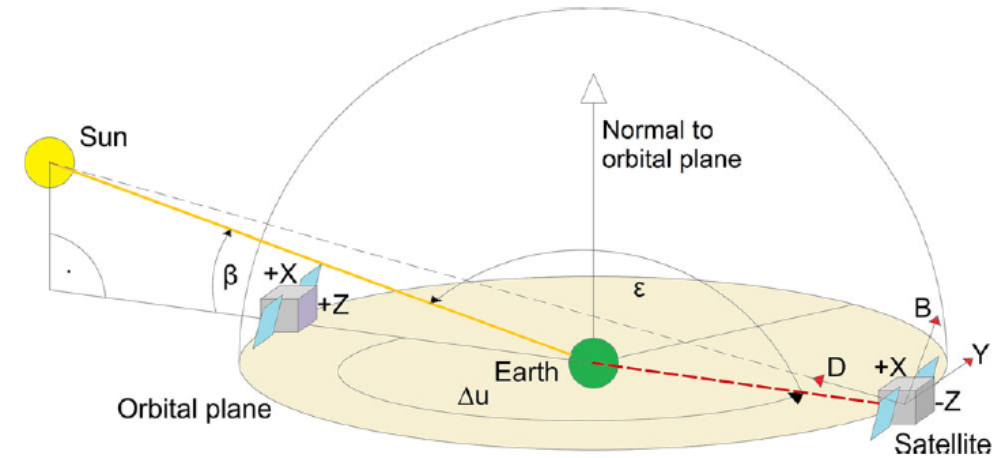
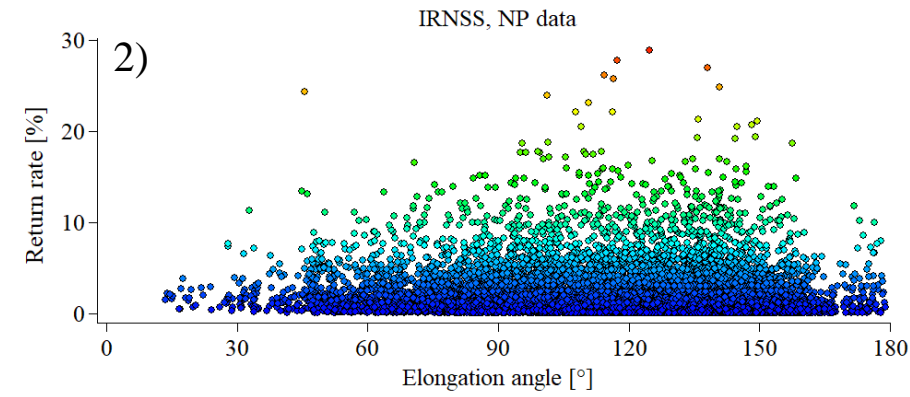
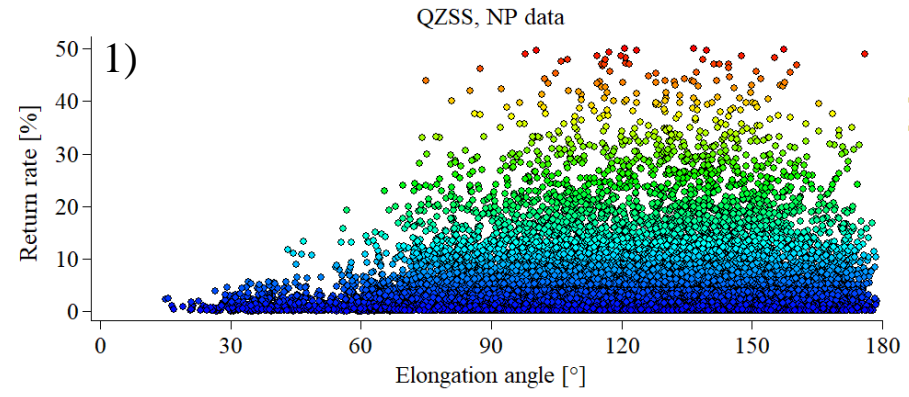


Fig. 2 Sun–Earth–satellite reference frame showing the elevation angle of the Sun over orbital plane β , argument of satellite latitude with respect to the Sun Δu and the elongation angle ϵ

Ref: Validation of Galileo orbits using SLR with a focus on satellites launched into incorrect orbital planes, Sosnica et al., 2017.

GEO SLR, NP distribution – a closer look

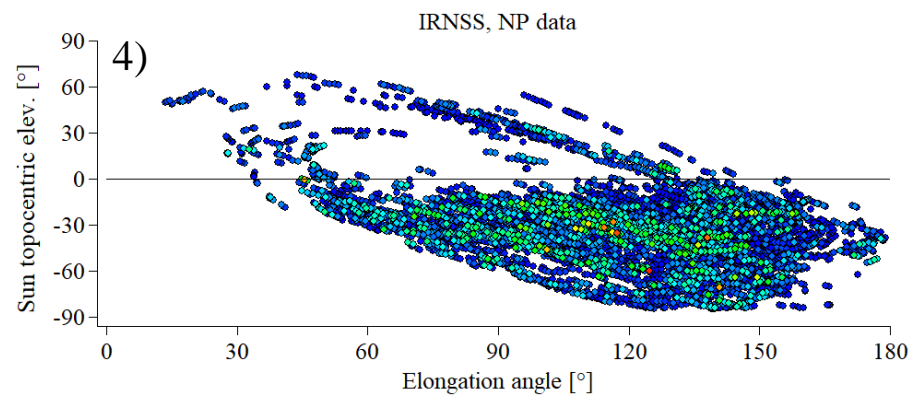
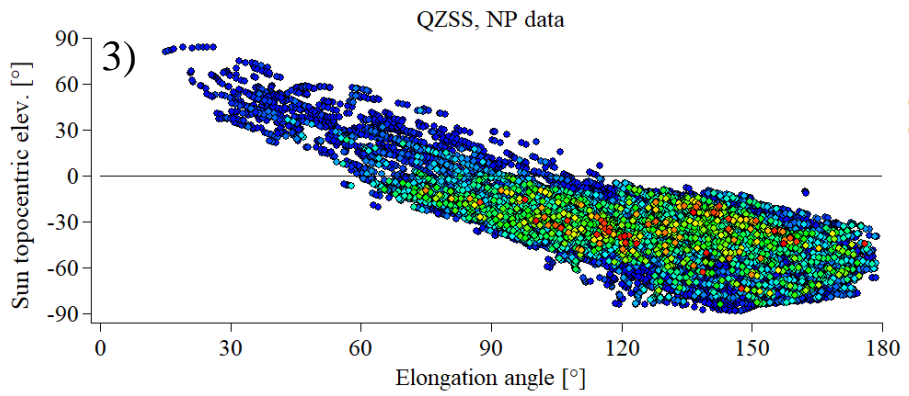
How does the elongation angle ϵ relate to day/night time tracking?



Orbital inclinations:
 QZSS: 0°, 45°
 IRNSS: 5°, 29.5°, 30°

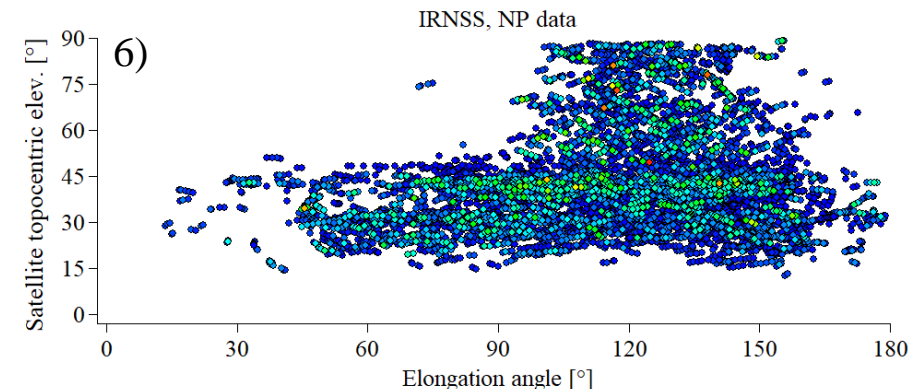
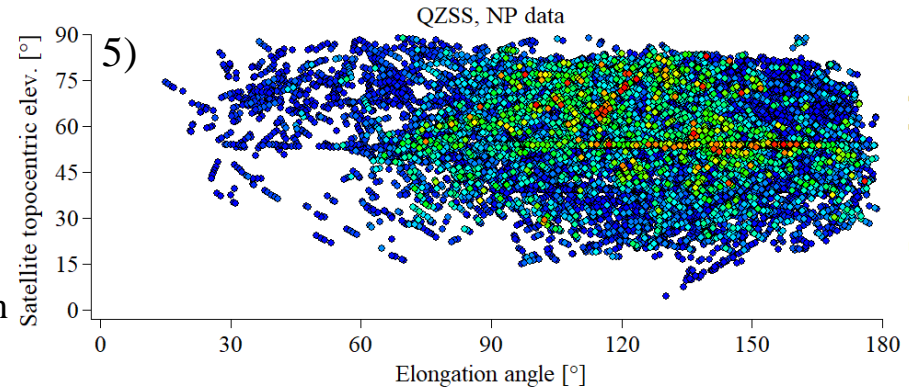
IRNSS satellites spend 3%-5% of their yearly orbital time at the elongation angles >160°.

Day



Night

Zenith



Horizon

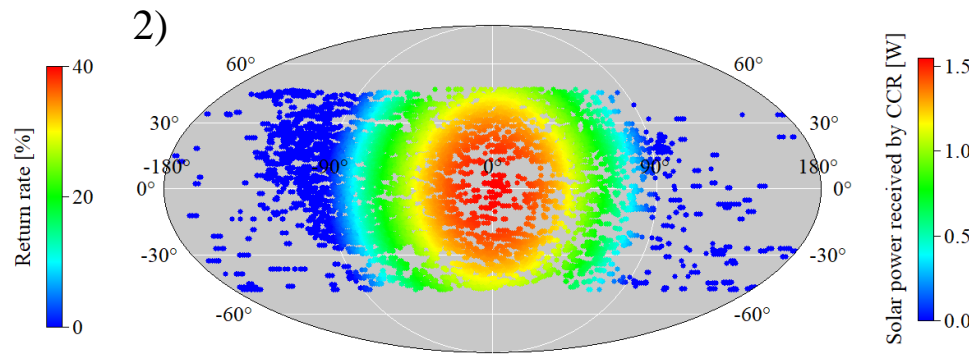
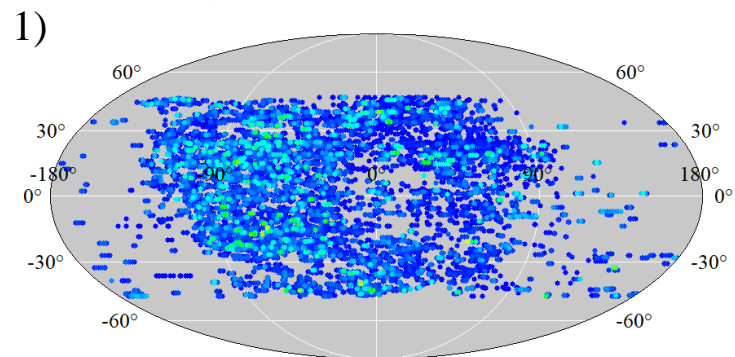
GEO SLR: NP v Sun vector

NP Return Rate

Solar power at CCR front face

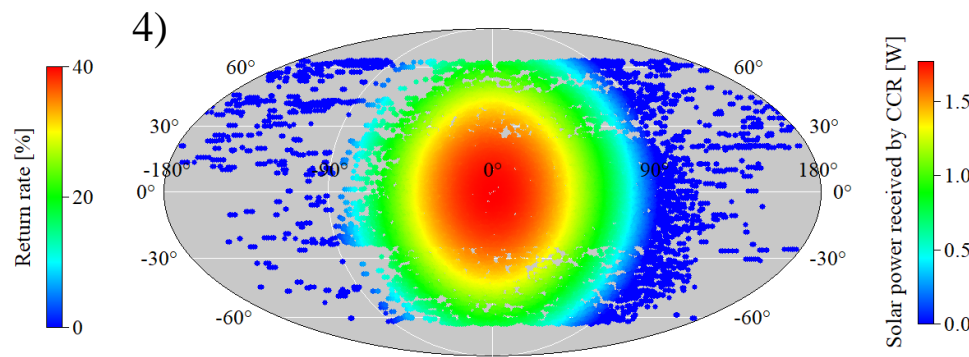
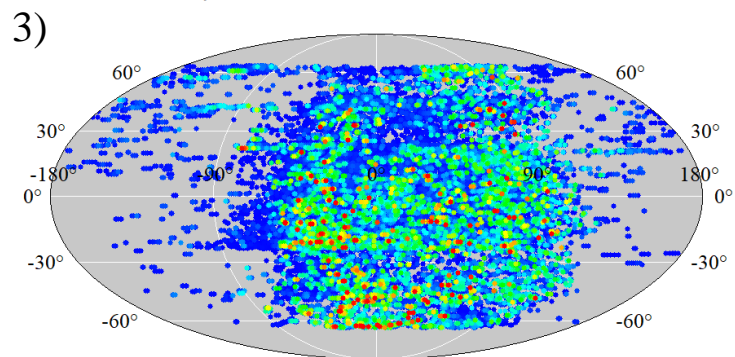
IRNSS, $(\Delta u + 180^\circ, \beta)$

IRNSS, $(\Delta u + 180^\circ, \beta)$



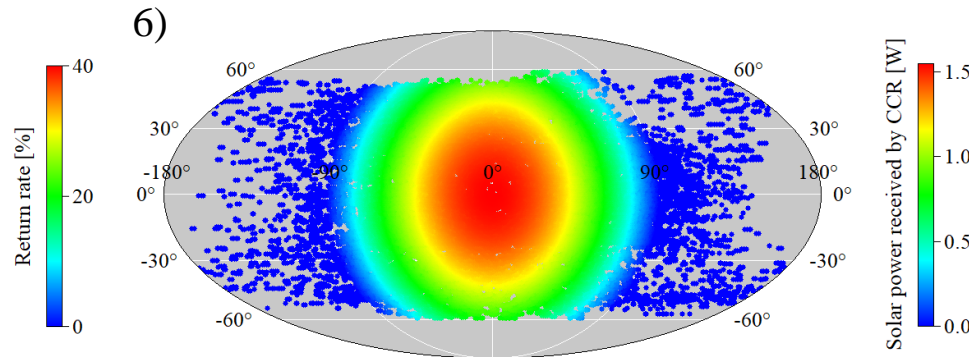
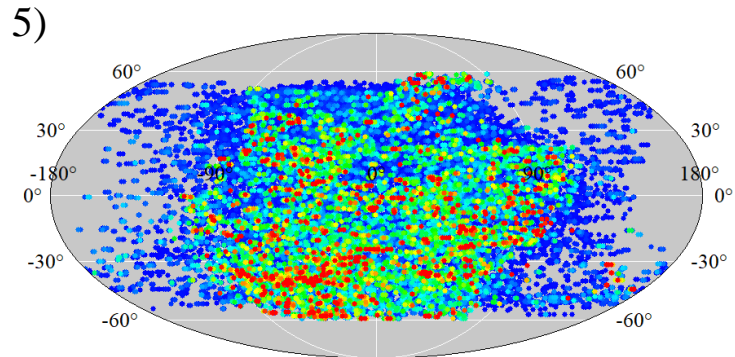
QZSS, $(\Delta u + 180^\circ, \beta)$

QZSS, $(\Delta u + 180^\circ, \beta)$



COMPASS, $(\Delta u + 180^\circ, \beta)$

COMPASS, $(\Delta u + 180^\circ, \beta)$



NPs are plotted at Sun vector coordinates of $\Delta u + 180^\circ, \beta$.

The origin $(0^\circ, 0^\circ)$ corresponds to the situation when the Sun is in normal direction of the LRA panel (“noon”).

Solar power at CCR aperture is calculated as $P = S_0 A \cos(\varphi)$, where S_0 is the solar constant, A is a CCR’s front face area and φ is an incident angle between satellite-Sun direction vector and LRA normal ($0^\circ \leq \varphi \leq 90^\circ$).

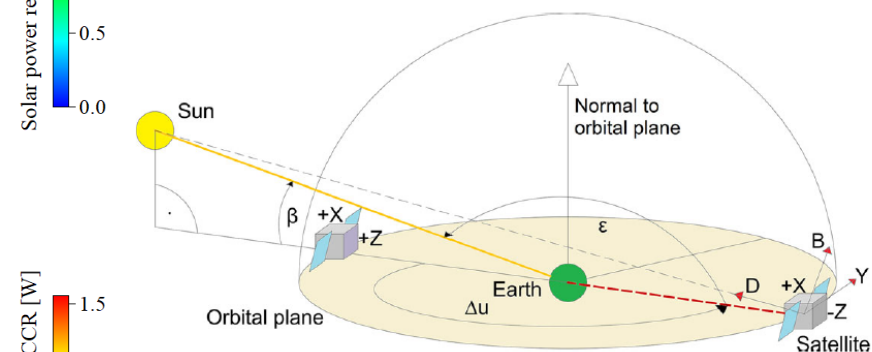


Fig. 2 Sun–Earth–satellite reference frame showing the elevation angle of the Sun over orbital plane β , argument of satellite latitude with respect to the Sun Δu and the elongation angle ϵ

Ref: Validation of Galileo orbits using SLR with a focus on satellites launched into incorrect orbital plane Sosnica et al., 2017.

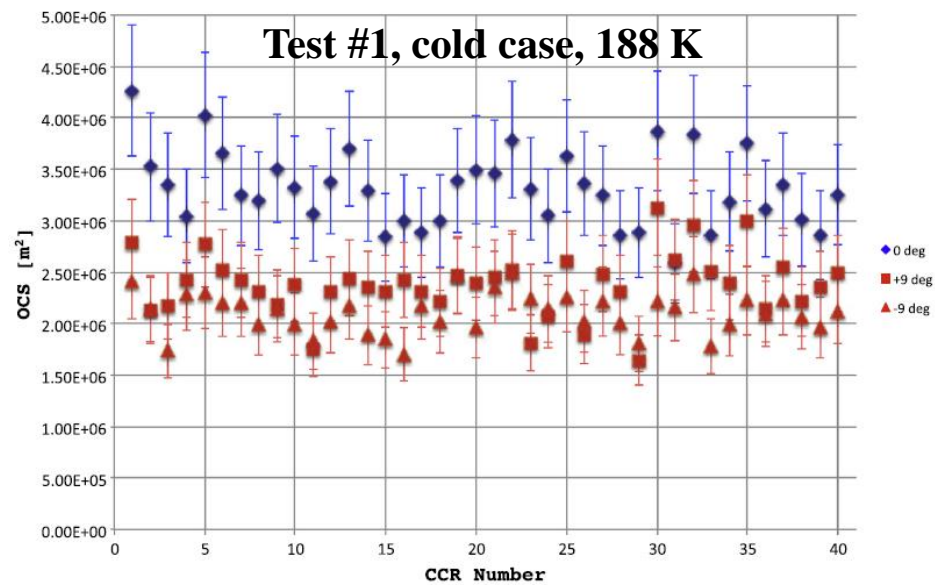


Fig. 5. Average intensities at 18 μrad for each IRNSS CCR for the *Thermal test #1*.

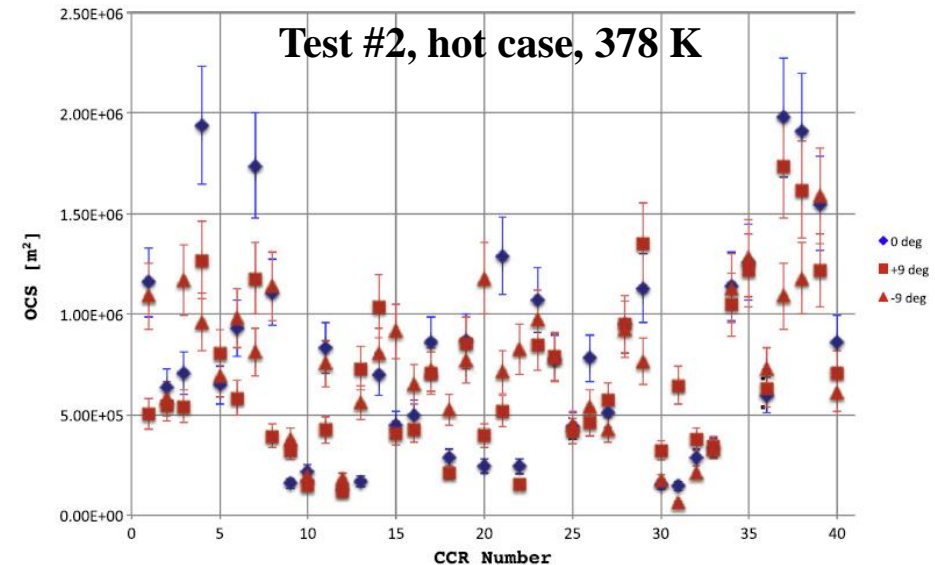


Fig. 6. Average intensities at 18 μrad for each IRNSS CCR for the *Thermal test #2*.

IRNSS LRA: pre-launch thermo-optical tests at Frascati



Advances in Space Research
Volume 60, Issue 5, 1 September 2017, Pages 1054-1061



Thermo-optical vacuum testing of IRNSS laser retroreflector array qualification model

L. Porcelli ^a, A. Boni ^a, E. Ciocci ^a, S. Contessa ^a, S. Dell'Agnello ^a, G. Delle Monache ^a, N. Intaglietta ^a, M. Martini ^a, C. Mondaini ^a, G. Patrizi ^a, L. Salvatori ^a, M. Tibuzzi ^a, C. Lops ^a, C. Cantone ^a, P. Tuscano ^a, M. Maiello ^a, R. Venkateswaran ^b, P. Chakraborty ^b, C.V. Ramana Reddy ^b, K.V. Sriram ^b

^a Istituto Nazionale di Fisica Nucleare – Laboratori Nazionali di Frascati (INFN-LNF), Via E. Fermi 40, 00044 Frascati, Rome, Italy

^b Indian Space Research Organisation – Laboratory for Electro-Optics Systems (ISRO-LEOS), First Cross, First Phase, Peenya Industrial Estate, Bangalore 560 058, India



Test #1: “cold case” in vacuum at 188 K (-85 C, -121 F), w/o solar simulator illumination. Thermal gradients inside the solid CCRs are contained and retroreflection is highly efficient.

Test #2: “hot case” in vacuum at 378 K (105 C, 221 F), w/o solar simulator illumination. OCS decreases significantly when the CCRs are hot. FFDPs are highly deformed. This “hot case” is the worst-case scenario for IRNSS LRA operations.

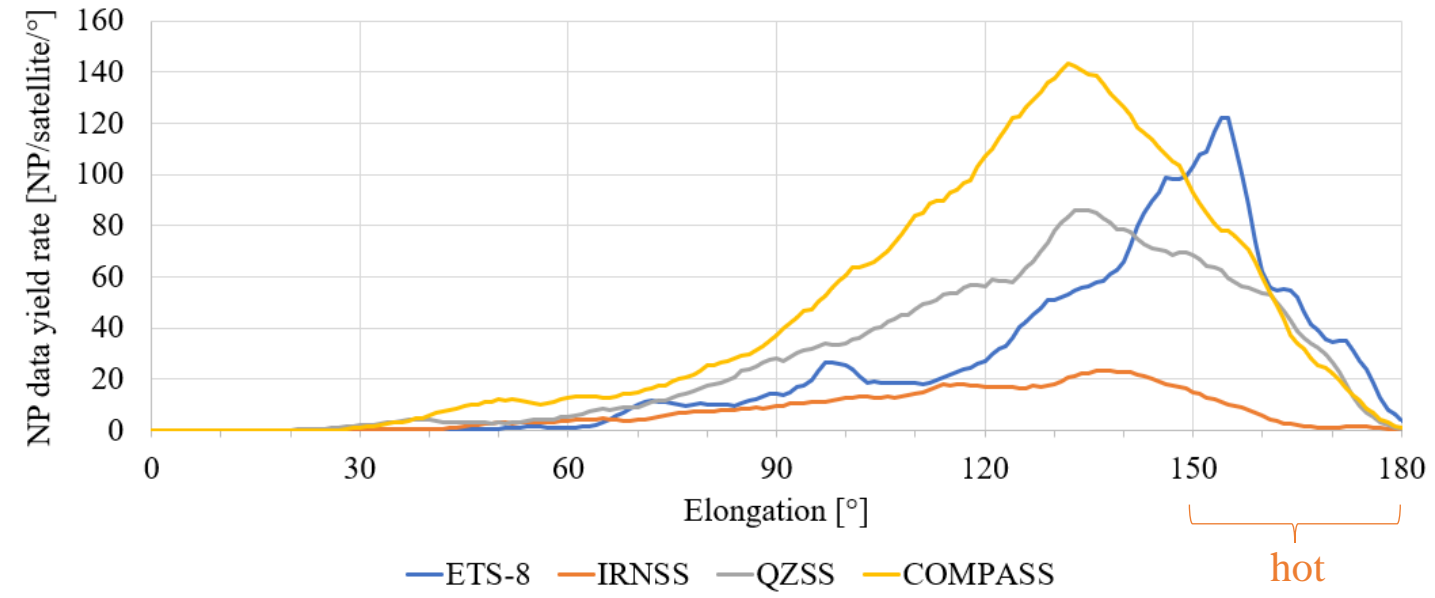
Another paper reports on “thermal breakthrough” effect that can occur at specific orientations of the CCRs with respect to the direction of incoming solar flux. In such cases the total internal reflection is broken as rays of sunlight pass through the glassy cubes and heat up the internal surfaces of the housing.

For uncoated CCRs this effect can occur at the Sun incident angles above 17° with respect to the cube’s optical axis.

Conclusions/remarks

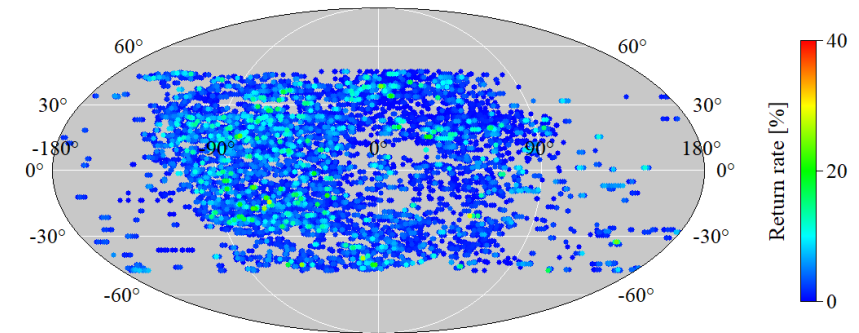
- High temperature causes thermal gradients within the solid retroreflectors. The thermal gradients cause the distortion of the FFDP that weakens Optical Cross Section of an LRA. Additionally, loss of total internal reflection causes thermal breakthrough at specific incidence angles of the incoming solar flux.
- The thermo-optical LRA design of ETS-8 (by David Arnold) leads in the hot-zone of high elongation angles.
- The NP data indicates relatively low performance of IRNSS LRAs, especially under the hot conditions when the retroreflectors are facing the Sun.

GEO NP data yield rate

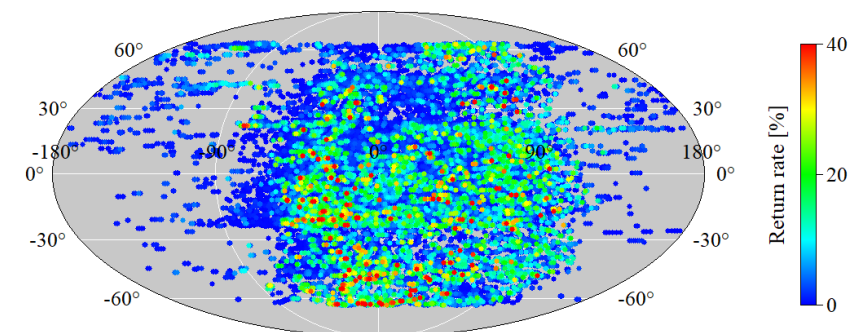


NP Return Rate

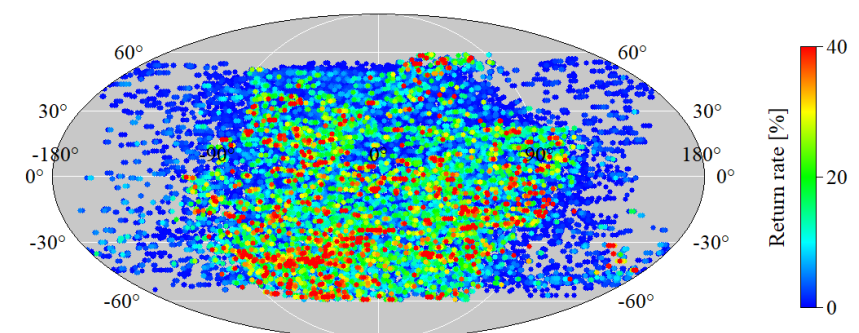
IRNSS, ($\Delta u+180^\circ, \beta$)



QZSS, ($\Delta u+180^\circ, \beta$)



COMPASS, ($\Delta u+180^\circ, \beta$)





Station Barometric Comparisons using the Vienna Mapping Function (1993 to 2019: VMF3o_EI)

Van S. Husson

vhusson@peraton.com

ILRS Network and Engineering Standing Committee Meeting

07-Jul-2022



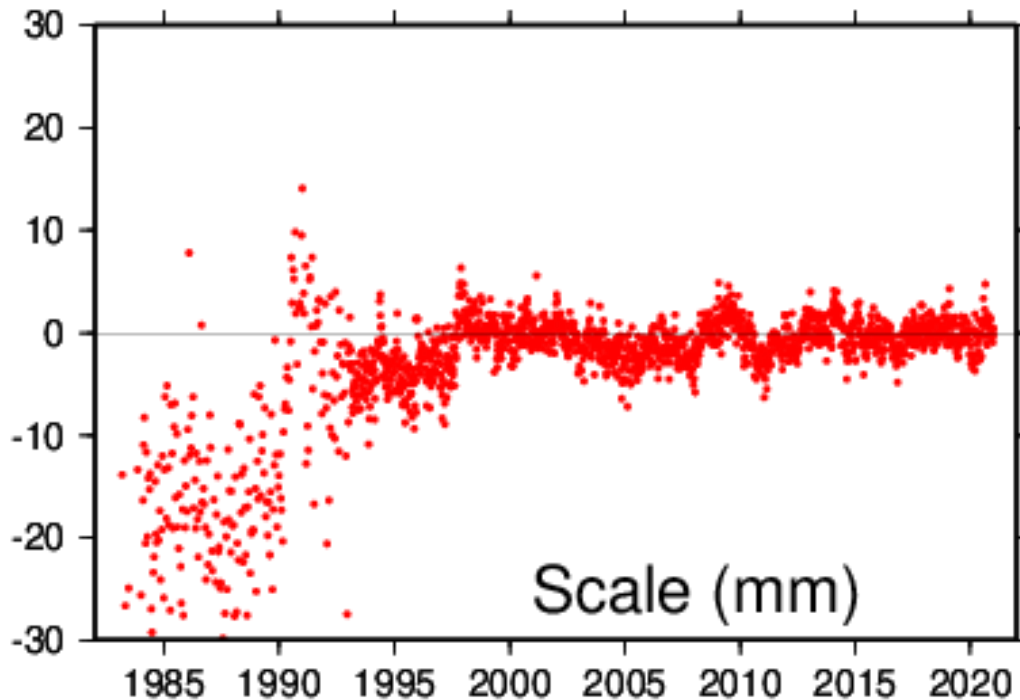
Vienna Mapping Function (VMF)



- ❑ VMF Reference: re3data.org: VMF Data Server; editing status 2020-12-14; re3data.org - Registry of Research Data Repositories. <http://doi.org/10.17616/R3RD2H>
- ❑ VMF data is available on the VMF Data Server at https://vmf.geo.tuwien.ac.at/trop_products/SLR/VMF3o/VMF3o_EI/ and [VMF Data Server \(tuwien.ac.at\)](#)
 - VMF3o: the Vienna Mapping Functions for optical frequencies. Reference: [VMF3o: the Vienna Mapping Functions for optical frequencies | SpringerLink](#)
 - ◆ There are meteorological measurements every six hours for 186 unique SLR monuments. Some sites (e.g. Greenbelt, Wettzell) have more than one SLR monument.
 - ◆ There are **semi-diurnal signals with amplitudes of a few millibars in pressure** differences between the station's barometric measurements and the VMF
- ❑ **There are 3 flavors of VMF3o data**
 - VMF3o_EI: VMF3o parameters are based on ray-traced delays using European Centre for Medium-Range Weather Forecast (ECMWF) **ERA-Interim** Numerical Weather Models (NWM) data (**a climate reanalysis**). Time Span: **January 1, 1990, to August 31, 2019.**
 - VMF3o_FC: ECMWF **forecasted** NWM
 - VMF3o_OP: ECMWF **operational** NWM. Data is available next day. Time Span: **January 1, 2008 to present.**
- ❑ **Note: Erricos mentioned caution using the operational data (VMF3o_OP) because it is not as accurate as the climate reanalysis (VMF3o_EI). He also cautioned that for sites near large bodies of water, the ray tracing technique is not as accurate.**



SLR Scale from ITRF2020



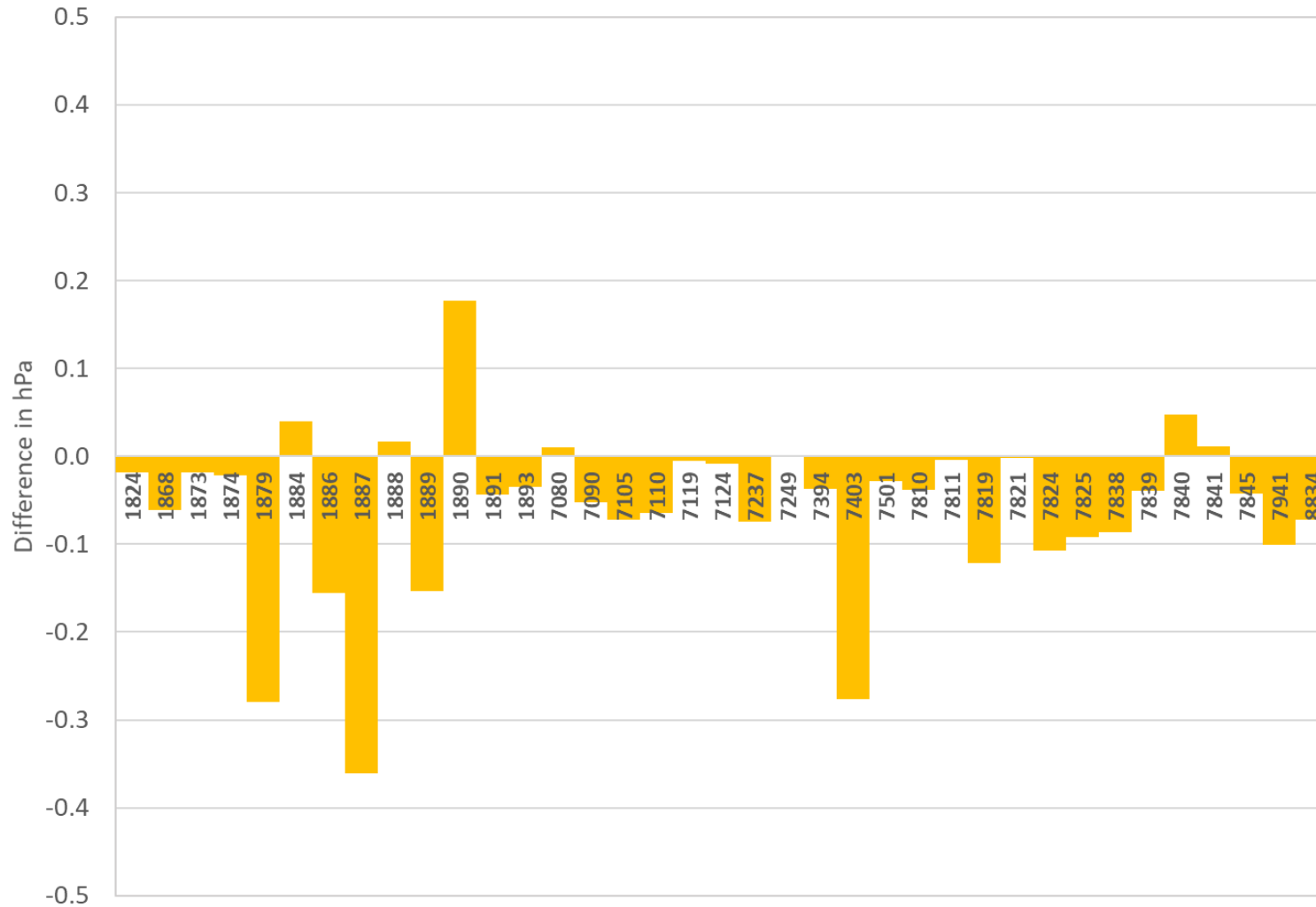
- ❑ Adding a second LAGEOS satellite in 24-Oct-1992 improved the ITRF scale derived from SLR
- ❑ The SLR scale from 1993 to 1997 appears to be biased short. Were barometric errors within the SLR network a root cause?
- ❑ To achieve one mm absolute ranging accuracies, the ILRS need to reduce systematic errors to <1 mm [Prochazka, ILRS Technical Workshop 2015]
- ❑ Based on this, the following SLR barometric requirement can be derived:
 - Absolute barometric accuracies better than 0.10 to 0.15 millibars dependent upon the site's minimum tracking elevation angle



VMF System Characterization (EI versus OP)



VMF Average Differences (EI-OP 2008-2019)



Mark	Location
1824	Golosiiv, Russia
1868	Komsomolsk-na-Amure, Russia
1873	Simeiz, Ukraine
1874	Mendeleevo, Russia
1879	Altay, Russia
1884	Riga, Latvia
1886	Arkhyz, Russia
1887	Baikonur, Kazakhstan
1888	Svetloe, Russia
1889	Zelenchukskya, Russia
1890	Badary, Russia
1891	Irkutsk, Russia
1893	Katzively, Ukraine
7080	McDonald, TX, USA
7090	Yarragadee, Australia
7105	Greenbelt, MD, USA
7110	Monument Peak, CA, USA
7119	Haleakala, HI, USA
7124	Tahiti, French Polynesia
7237	Changchun, China
7249	Beijing, China
7394	Sejong City, Republic of Korea
7403	Arequipa, Peru
7501	Hartebeesthoek, South Africa
7810	Zimmerwald, Switzerland
7811	Borowiec, Poland
7819	Kunming, China
7821	Shanghai, China
7824	San Fernando, Spain
7825	Mt Stromlo, Australia
7838	Simosato, Japan
7839	Graz, Austria
7840	Herstmonceux, United Kingdom
7841	Potsdam, Germany
7845	Grasse, France
7941	Matera, Italy
8834	Wetzell, Germany

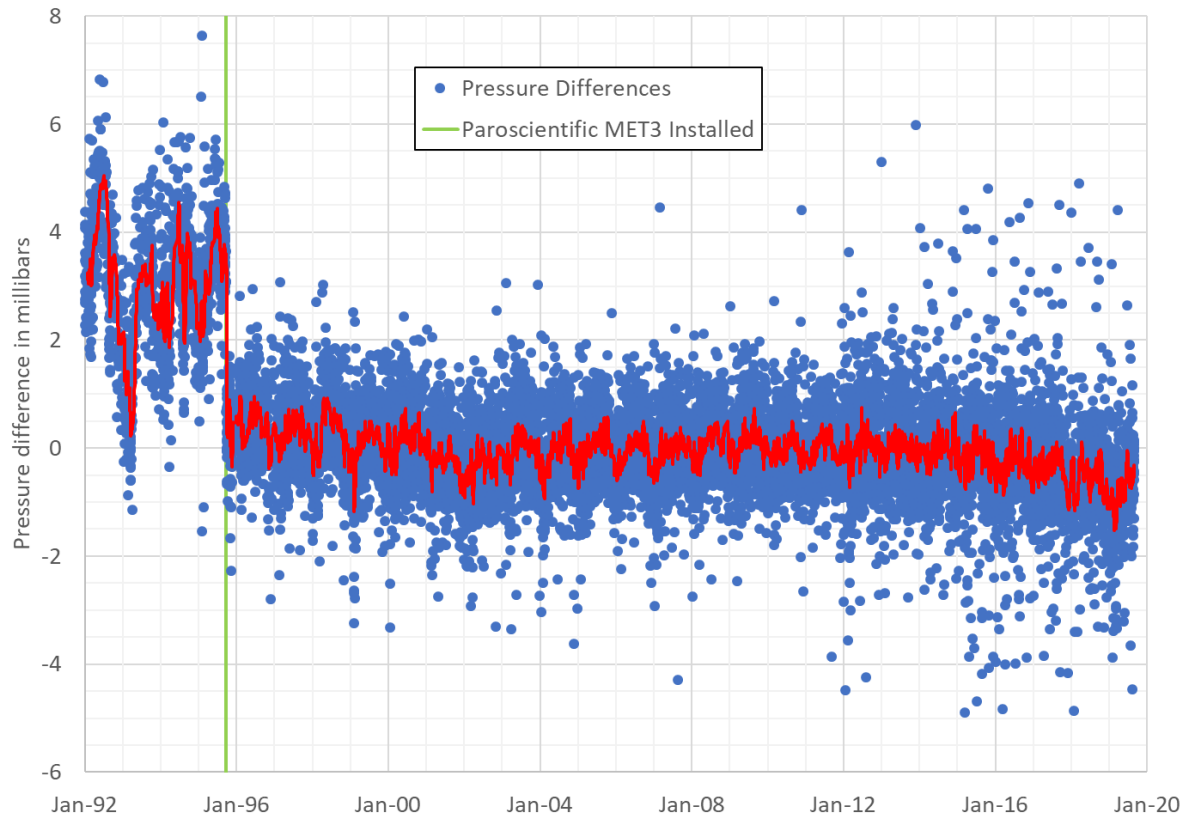
- The mean difference between VMF3o_EI and VMF3o_OP for all 186 SLR monuments for the 12 years is minus 0.07 hPa (EI-OP).
- Listed here are most of the current active sites.



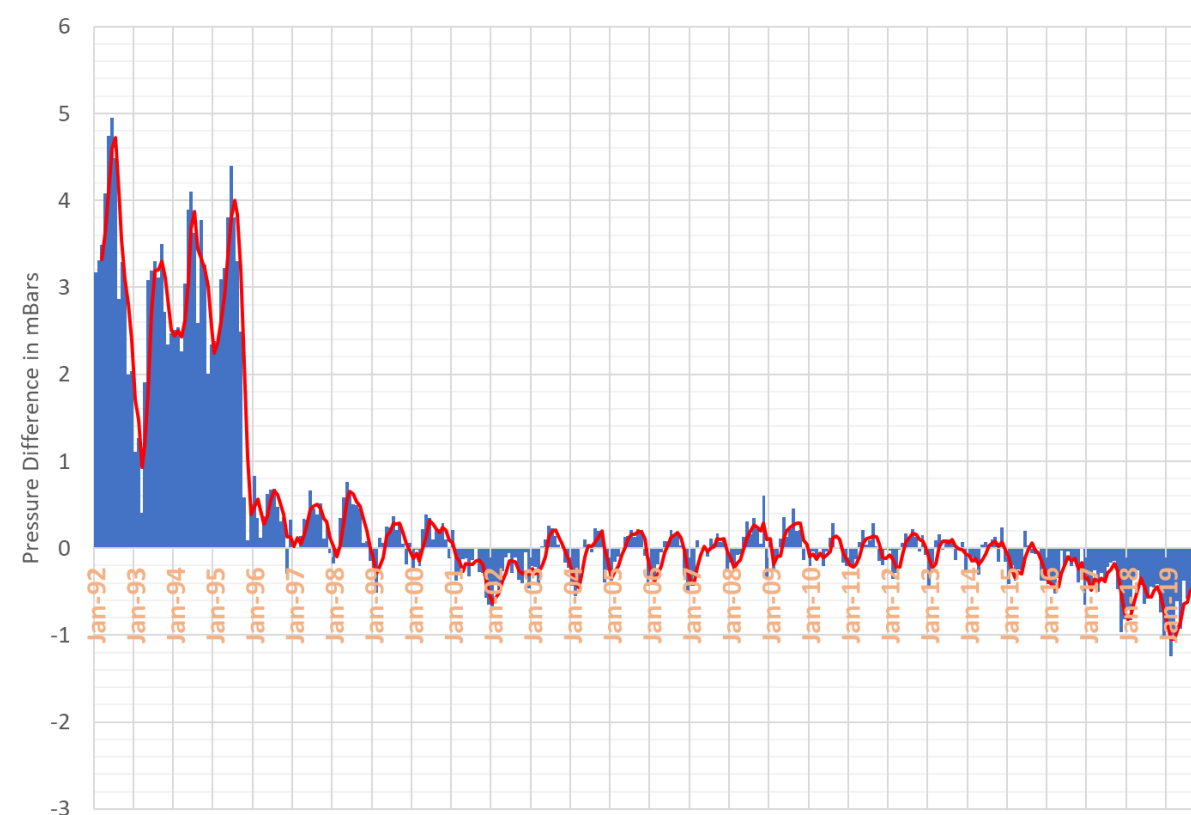
7839 GRZL Pressure Analysis



7839 GRZL Pressure Differences (Station-VMF)



7839 GRZL Monthly Pressure Differences (Station-VMF)



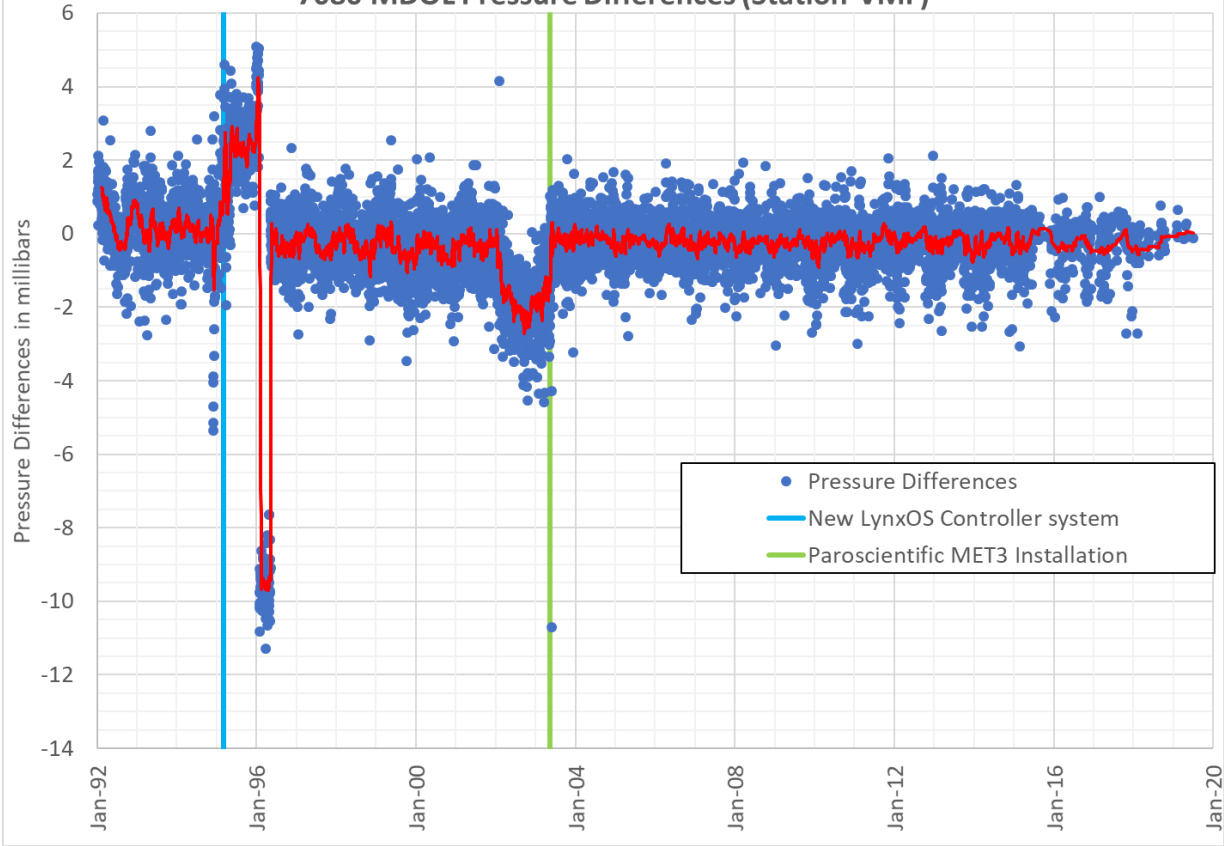
- ❑ Left & right charts are pressure differences (Station-VMF3oEI) aggregated every 6 hours and monthly; respectively.
- ❑ **Red lines** on the left & right chart are a 20-point running average and a 3-month running average; respectively.
- ❑ On the left chart, there is sudden discontinuity when the Paroscientific MET3 was installed on 22-Sep-1995.
- ❑ *Note: All Graz site pressures are from the original release of data (release 0).*



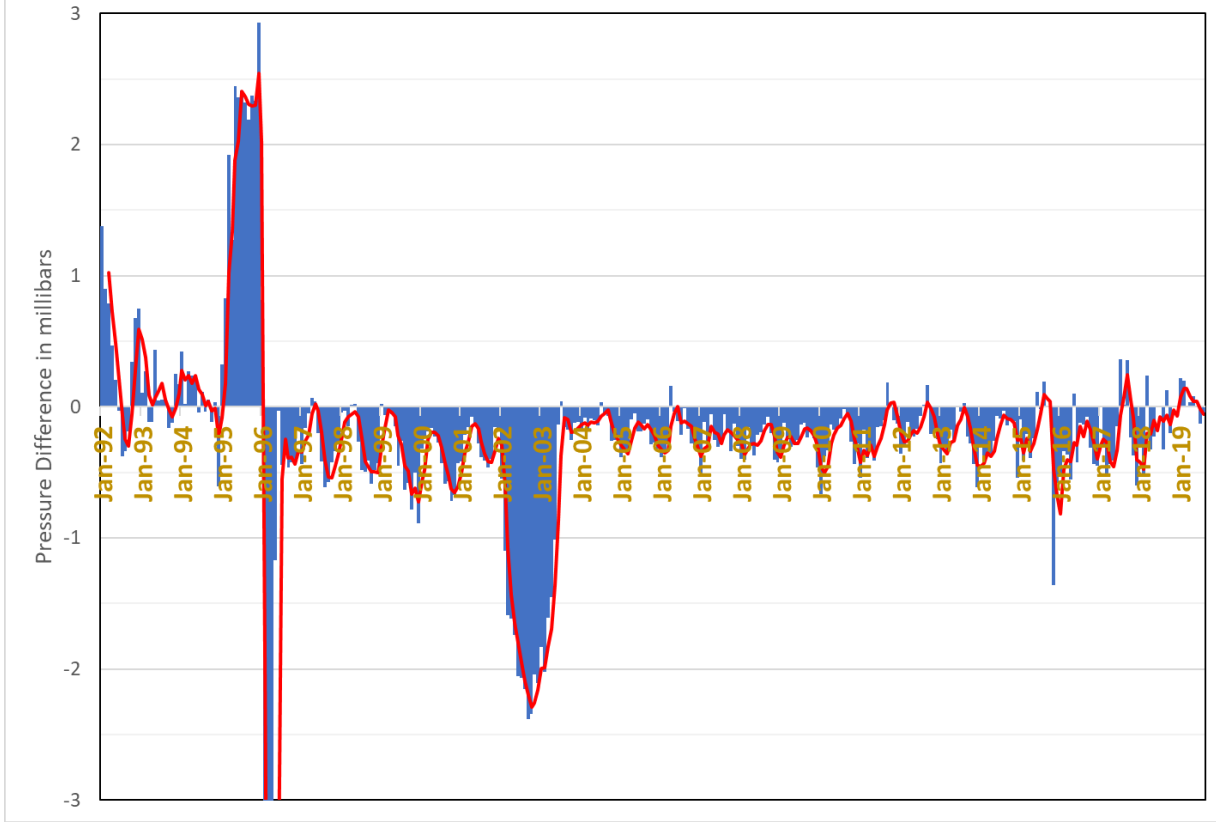
7080 MDOL Pressure Analysis



7080 MDOL Pressure Differences (Station-VMF)



7080 MDOL Monthly Pressure Differences (Station-VMF)

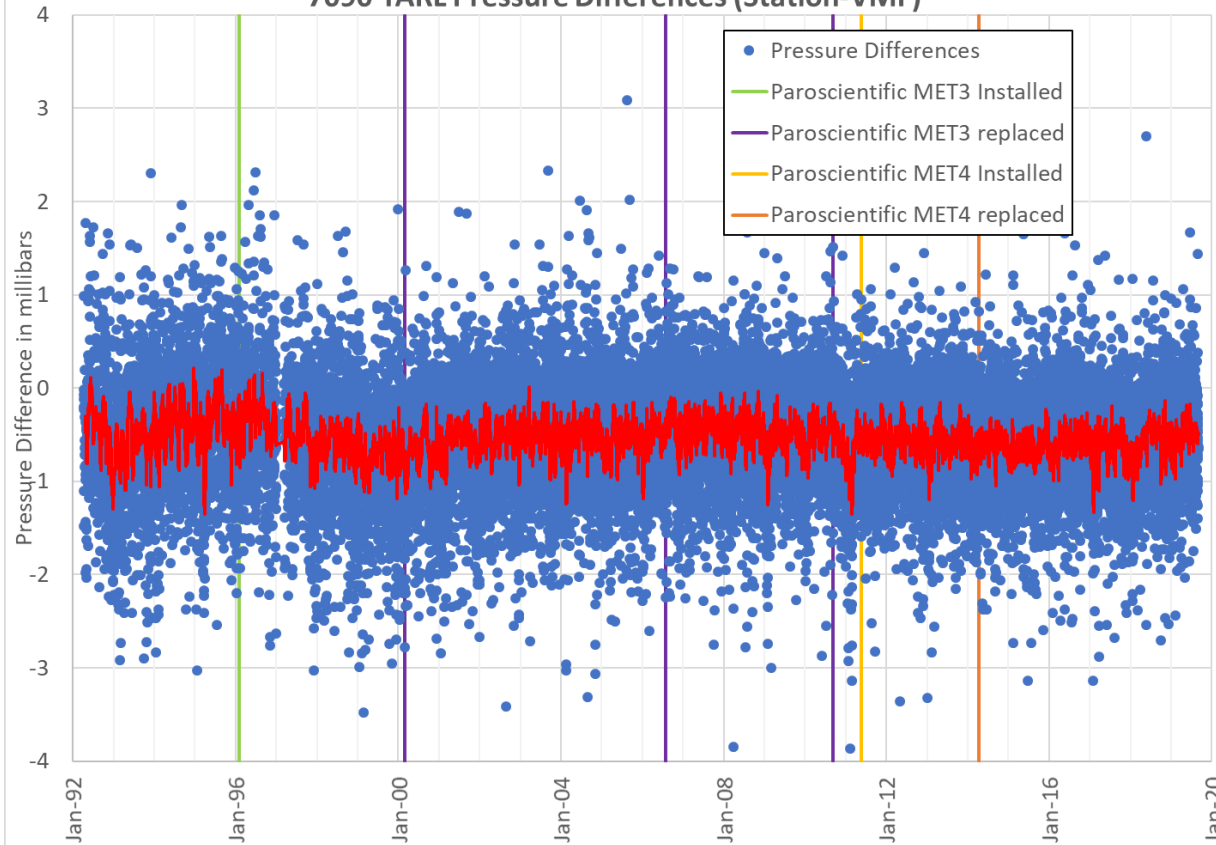




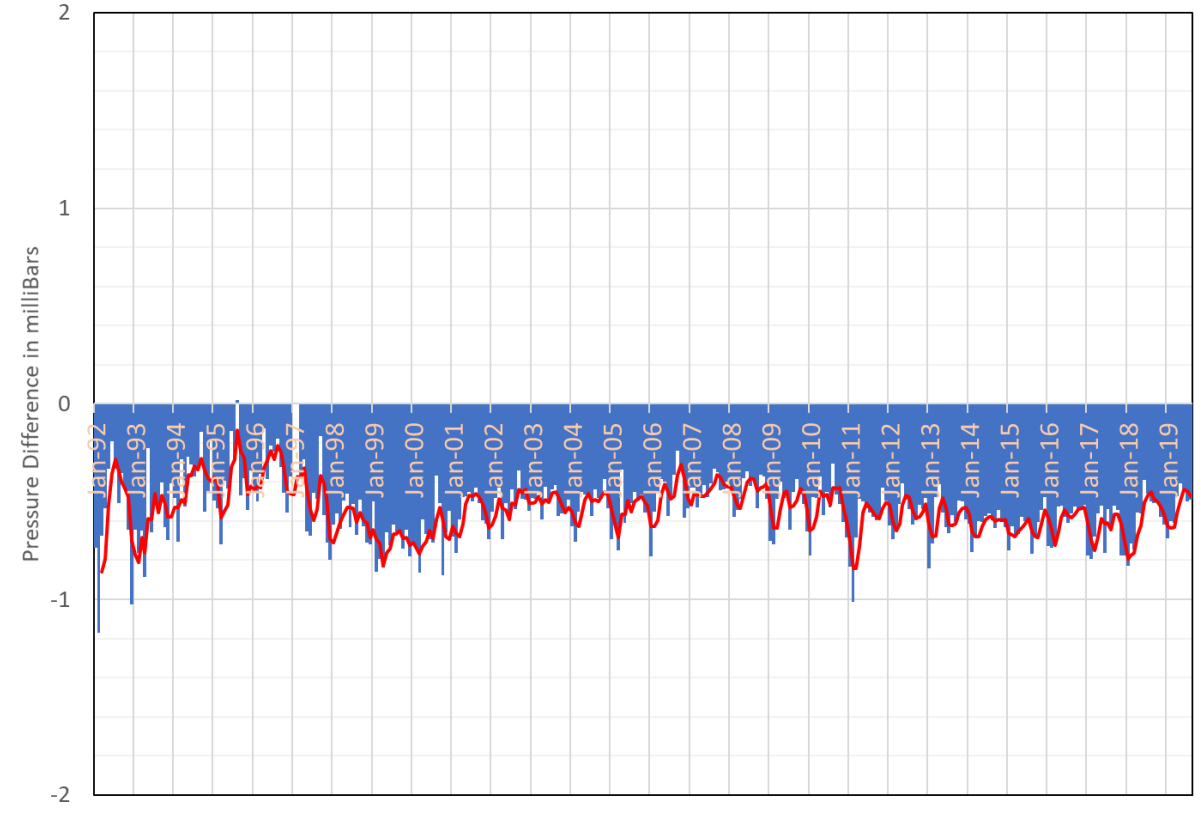
7090 YARL Pressure Analysis



7090 YARL Pressure Differences (Station-VMF)



7090 YARL Monthly Pressure Differences (Station-VMF)



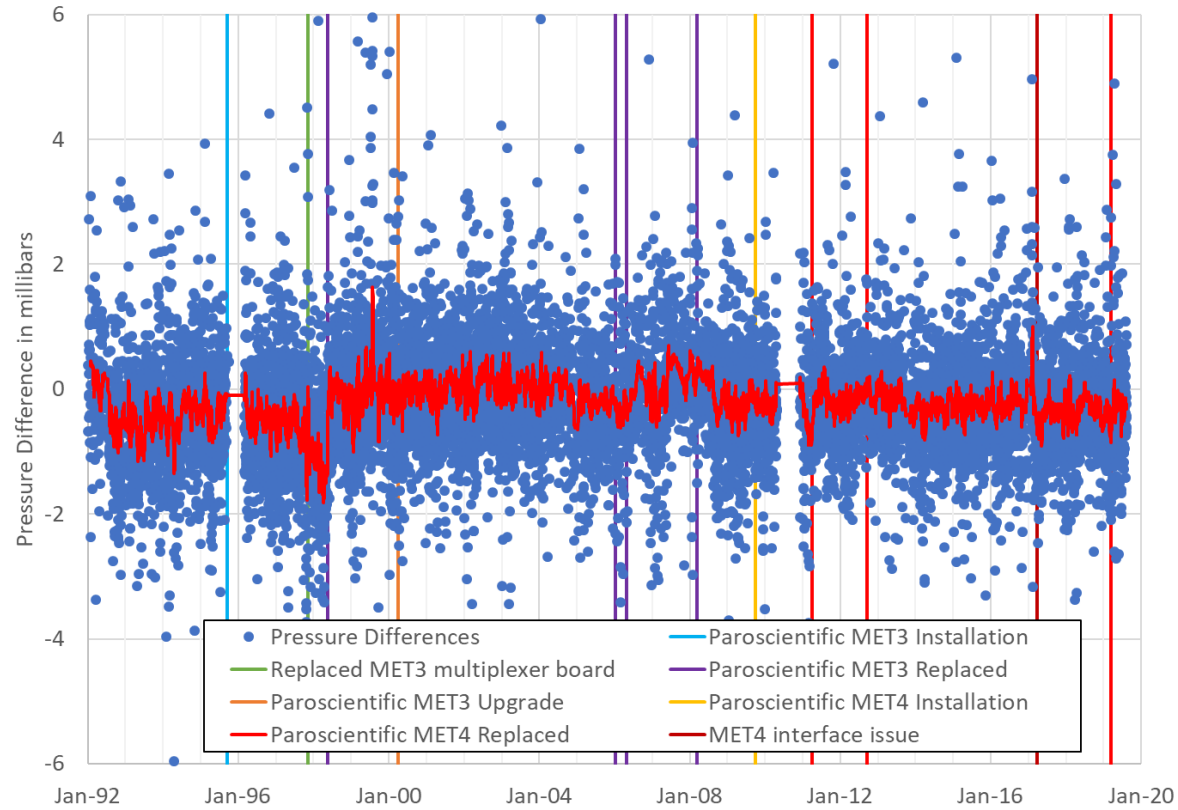
❑ There is -0.54 millibar offset between the Station and the VMF. Based on the left chart the 7090 meteorological sensors were calibrated/replaced every few years. This begs the question, **which data is more accurate?**



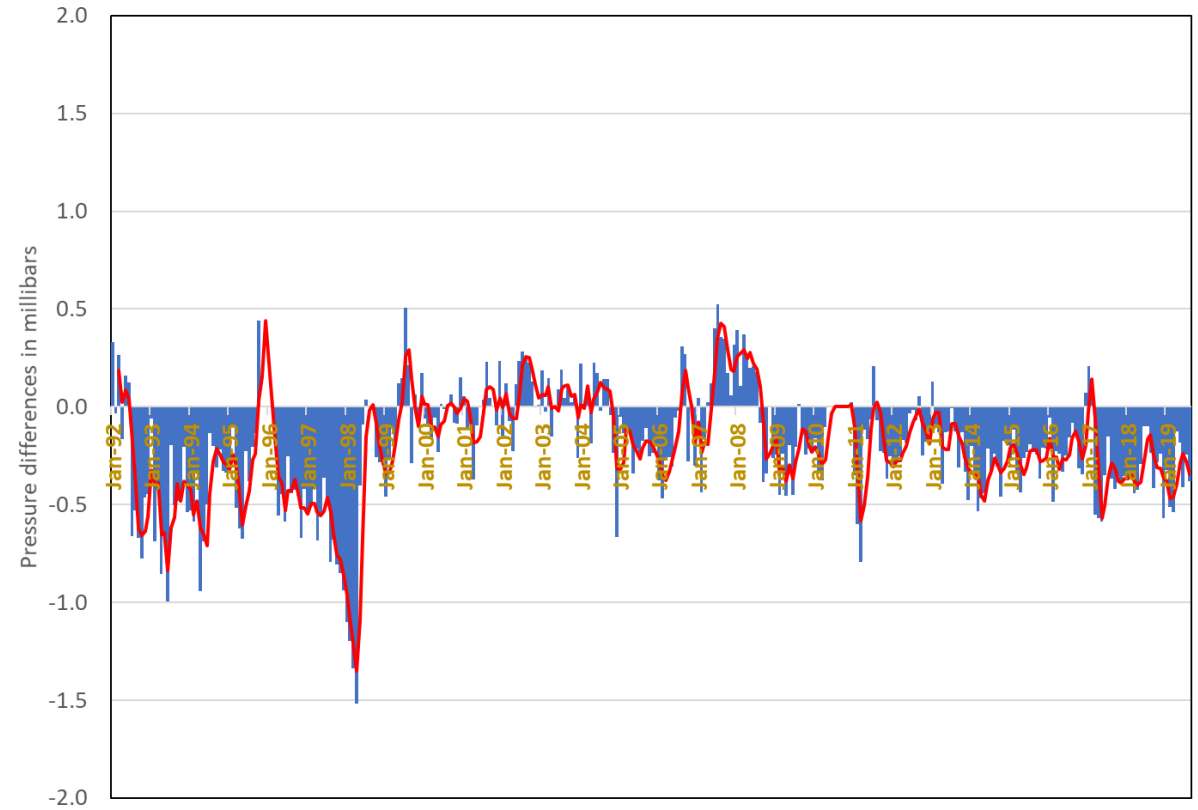
7105 GODL Pressure Analysis



7105 GODL Pressure Differences (Station-VMF)



7105 GODL Monthly Pressure Differences (Station-VMF)

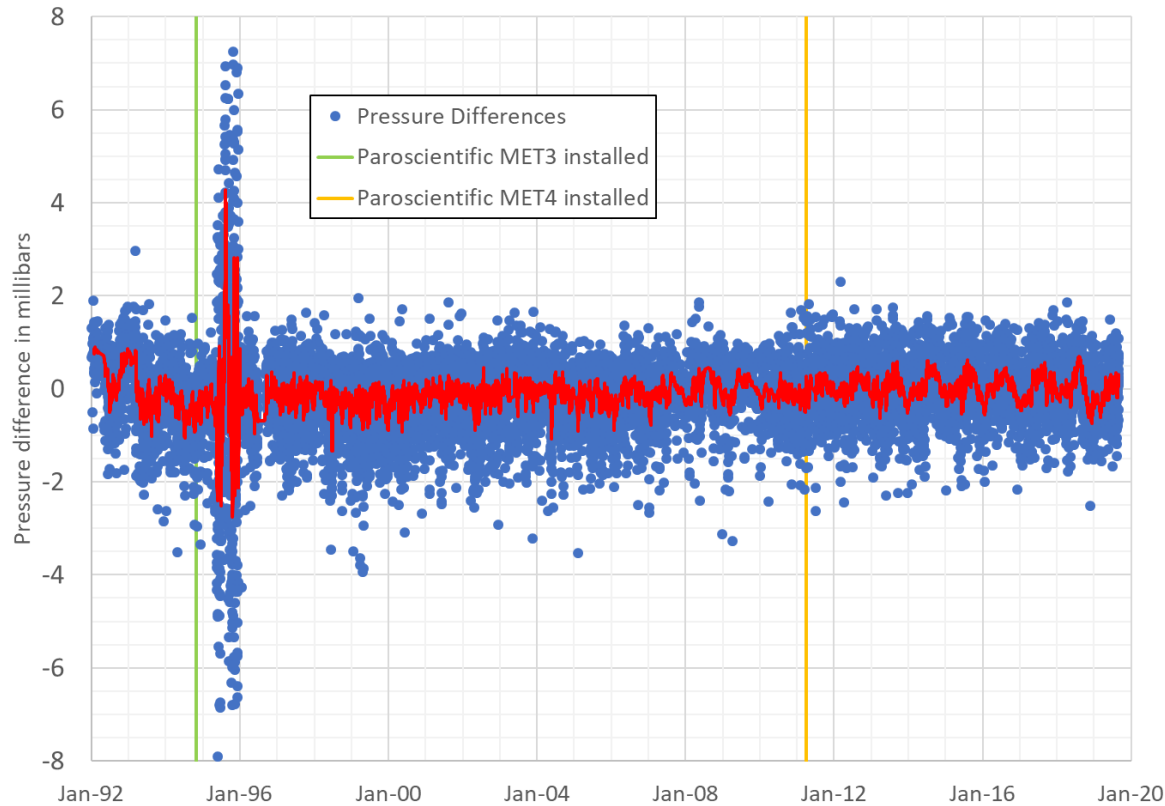




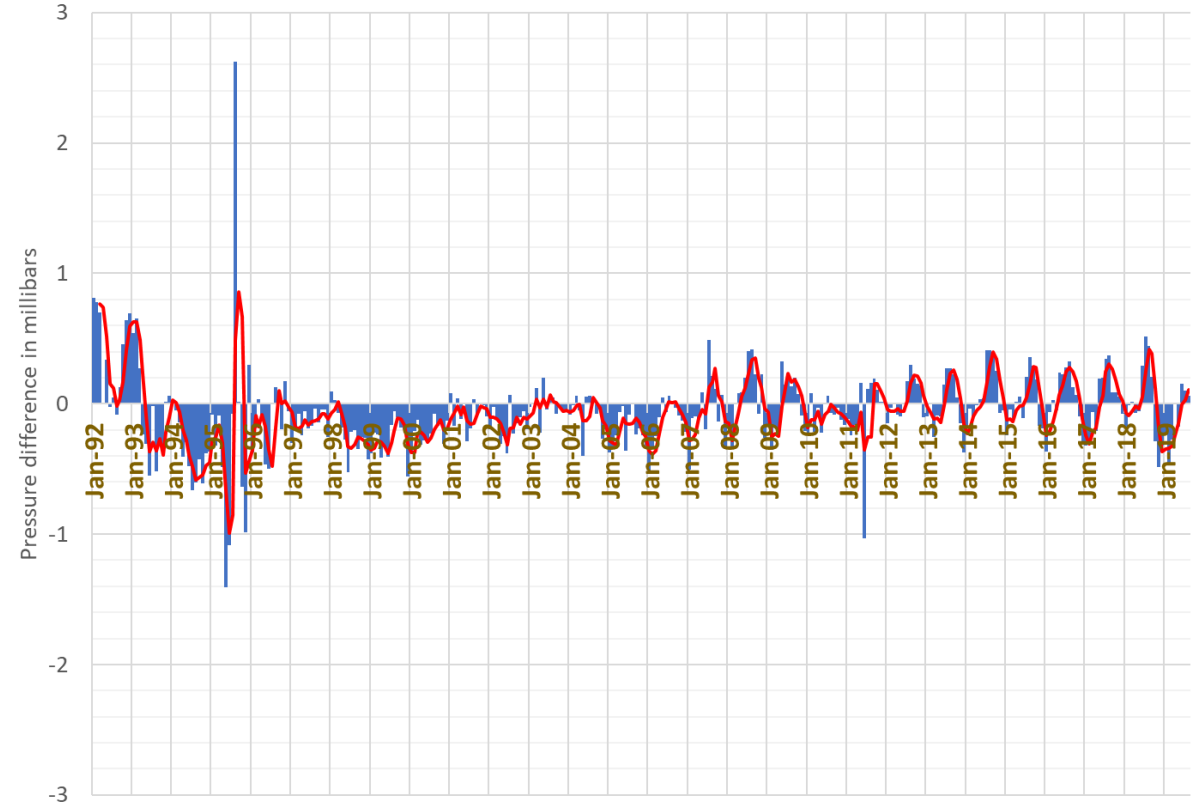
7110 MONL Pressure Analysis



7110 MONL Pressure Differences (Station-VMF)



7110 MONL Monthly Pressure Differences (Station-VMF)



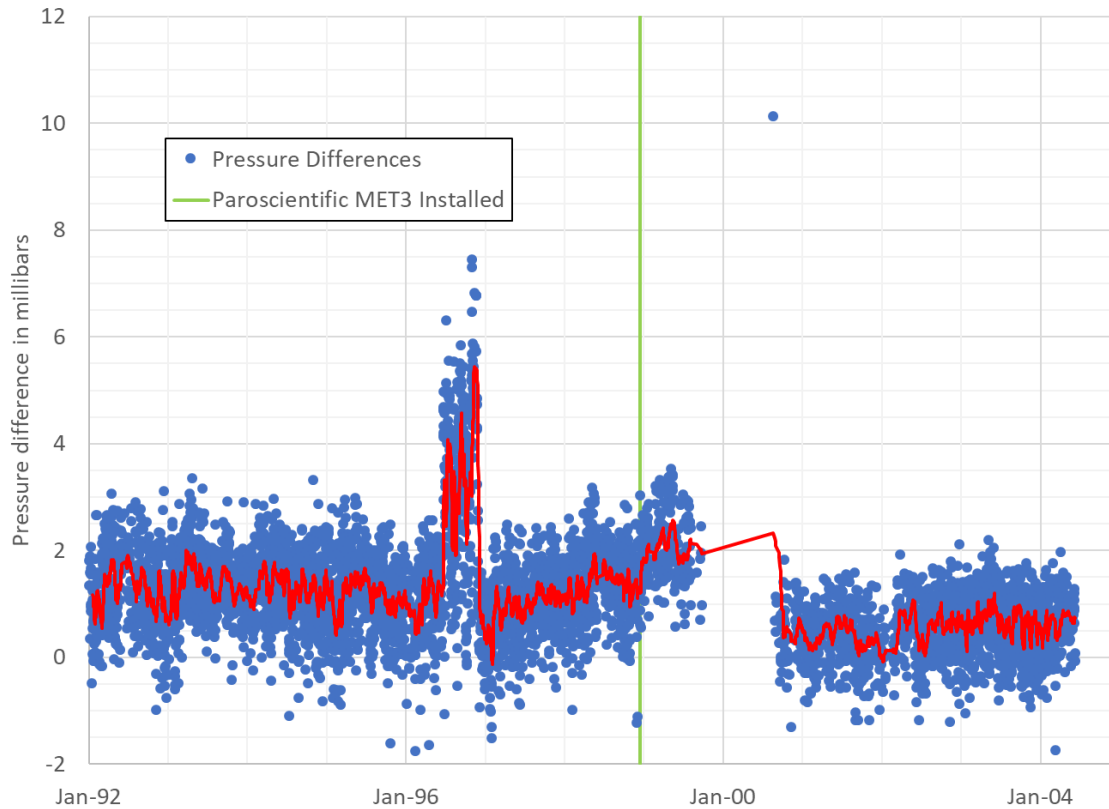
❑ There was an issue with the 7110 barometer in 1995 causing an increase in the scatter and a possible bias.



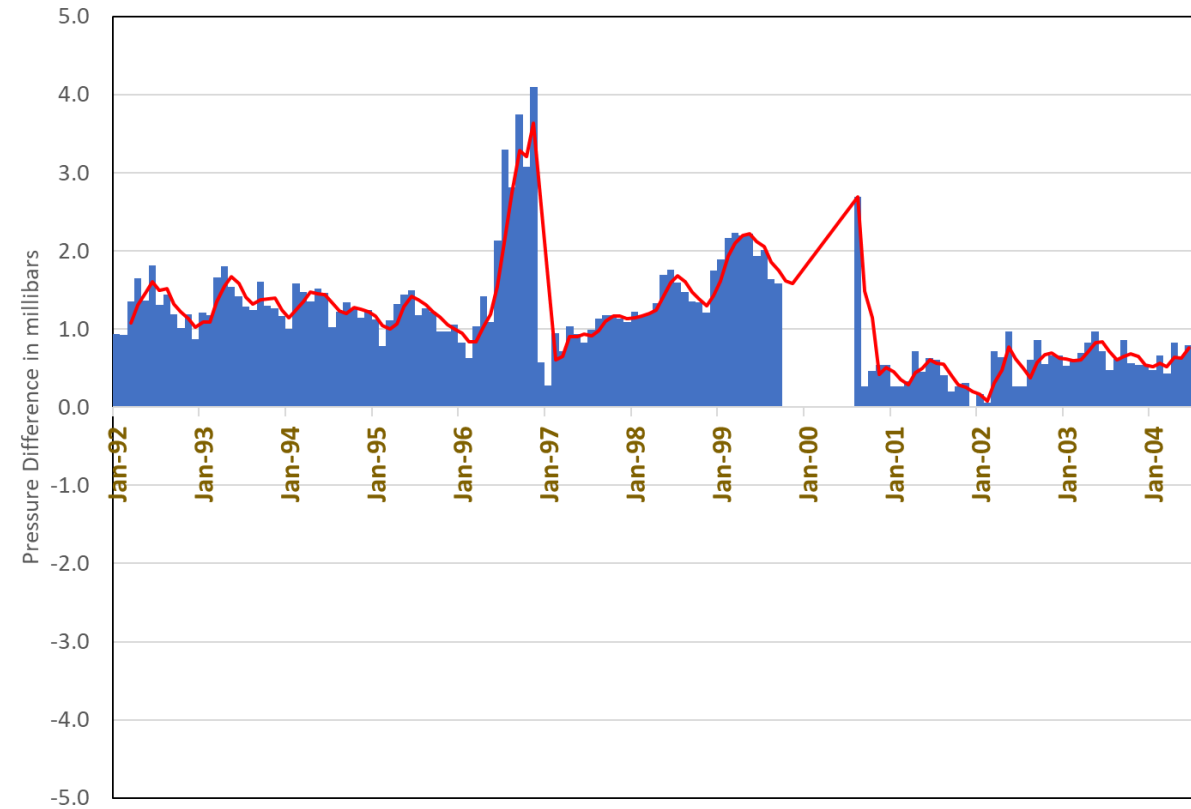
7210 HALL Pressure Analysis



7210 HALL Pressure Differences (Station-VMF)



7210 HALL Pressure Differences (Station-VMF)



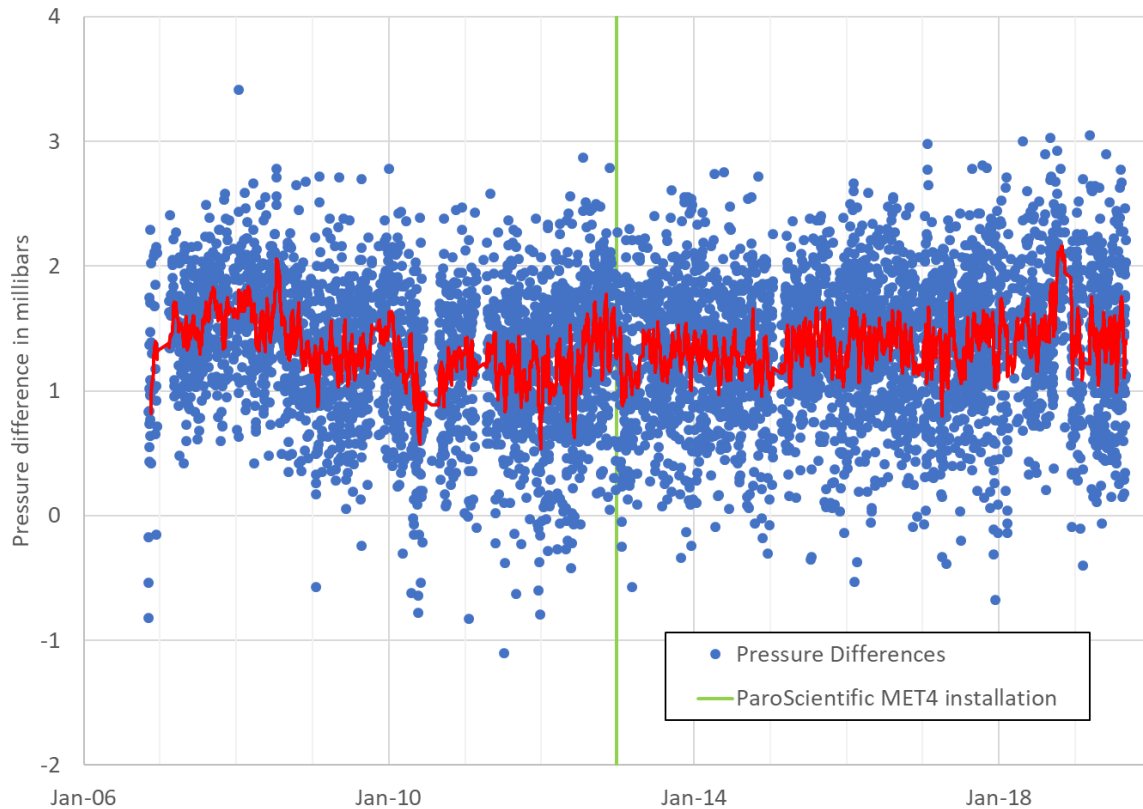
- ❑ The 7210 site log mentions there is ~2-meter height difference between the sensor and the system reference point. A 2-meter height difference equates to a 0.2 millibar pressure difference which was not modelled in the data processing.
- ❑ There is a difference in pressure before and after the data gap.



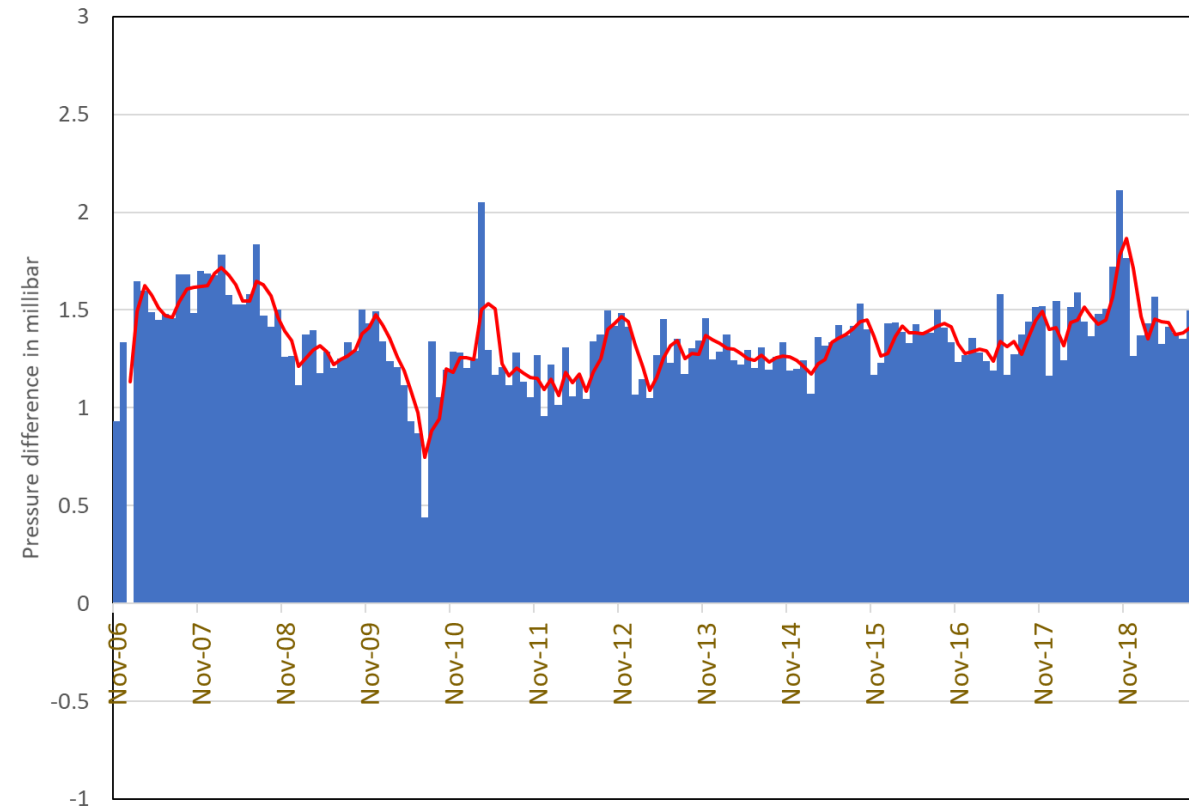
7119 HA4T Pressure Analysis



7119 HA4T Pressure Differences (Station-VMF)



7119 HA4T Monthly Pressure Differences (Station-VMF)



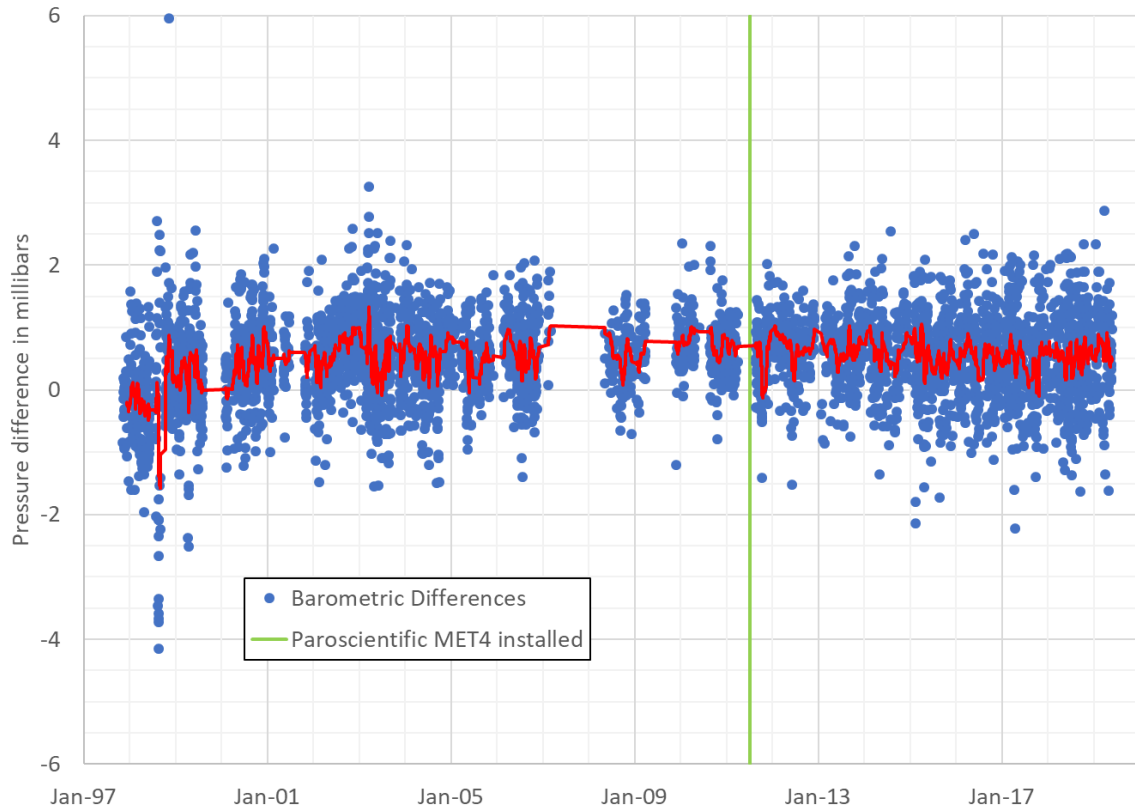
- ❑ **7210 HALL was closed in 2004 (see 7210 results on previous slide) and was replaced in 2006 with station 7119 HA4T (TLRS-4). Both stations have a positive barometric bias relative to VMF, but the apparent 7119 pressure bias is much larger. WHY?**



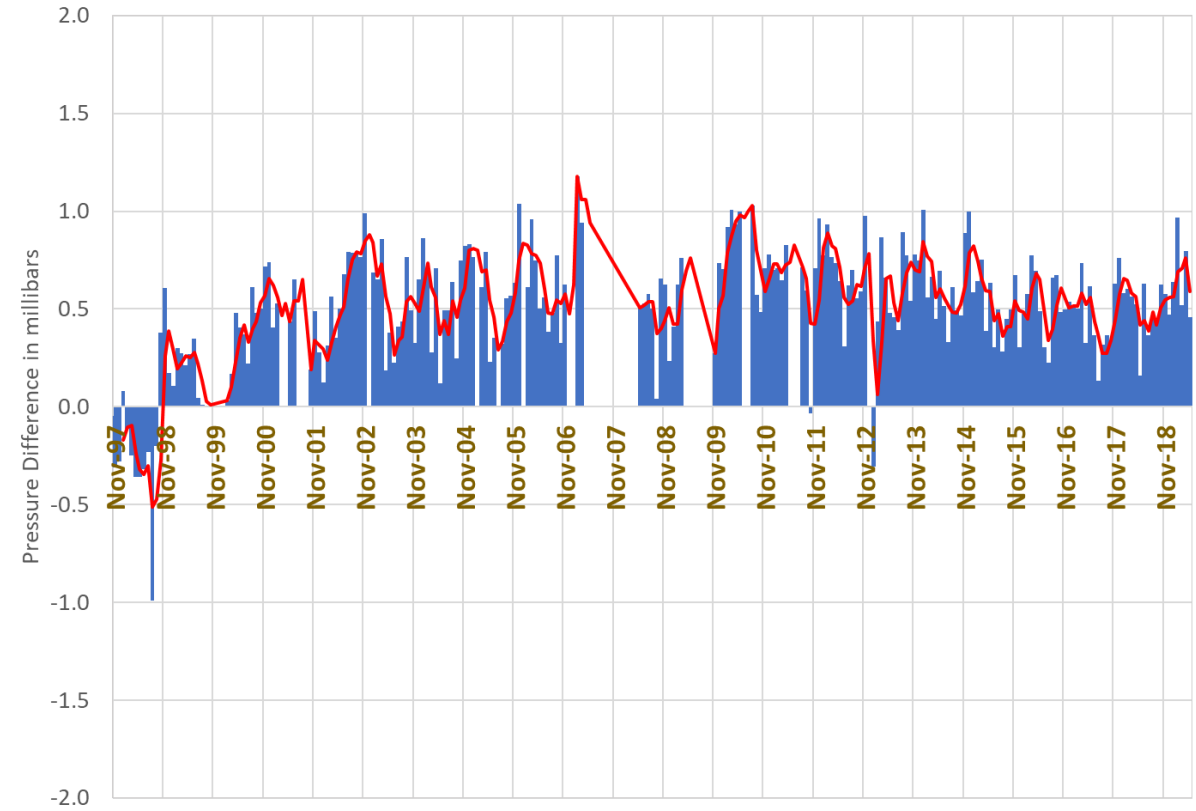
7124 THTL Pressure Analysis



7124 THTL Pressure Differences (Station-VMF)



7124 THTL Monthly Pressure Differences (Station-VMF)

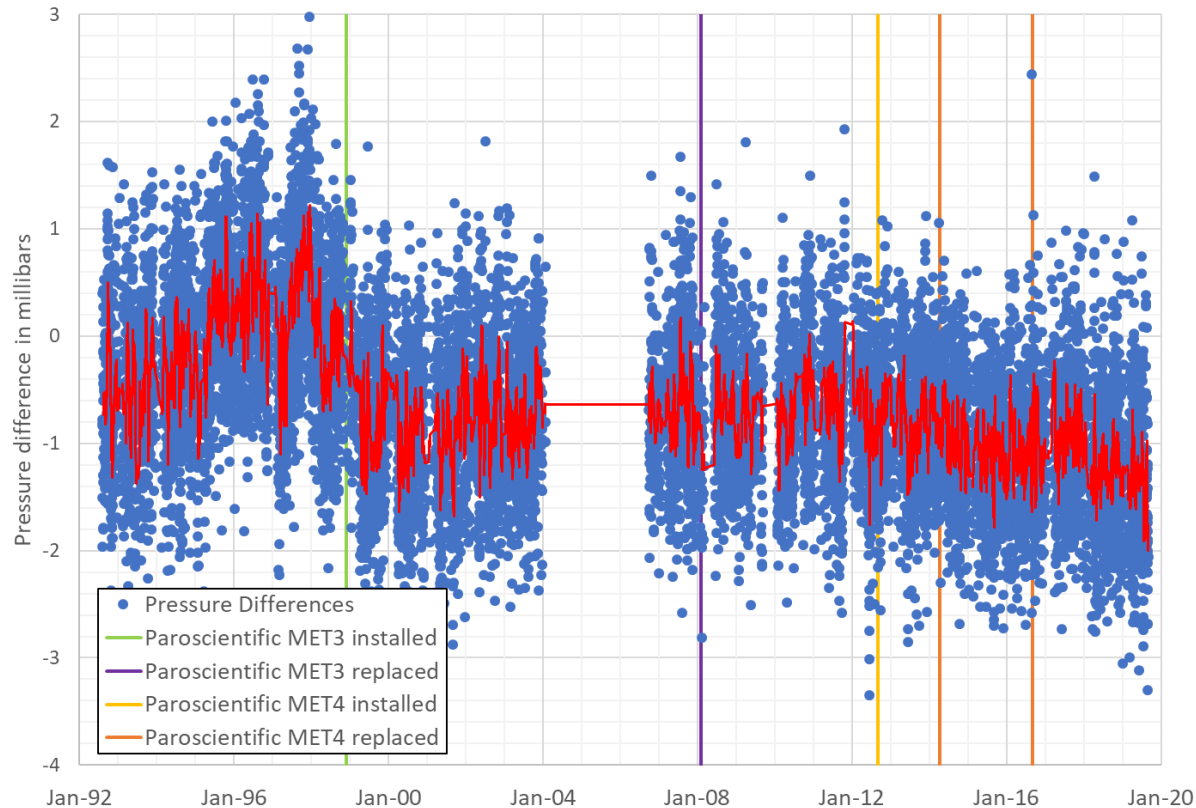




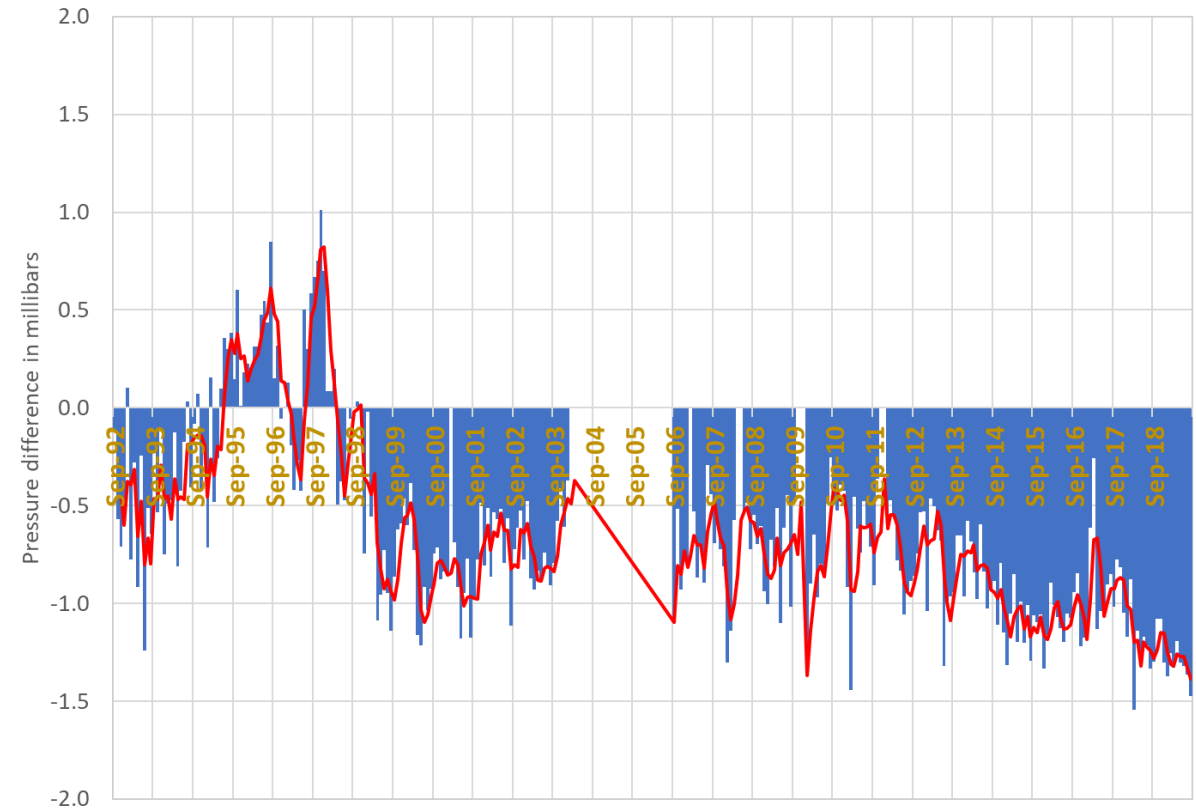
7403 AREL Pressure Analysis



7403 AREL Pressure Differences (Station-VMF)



7403 AREL Monthly Pressure Differences (Station-VMF)



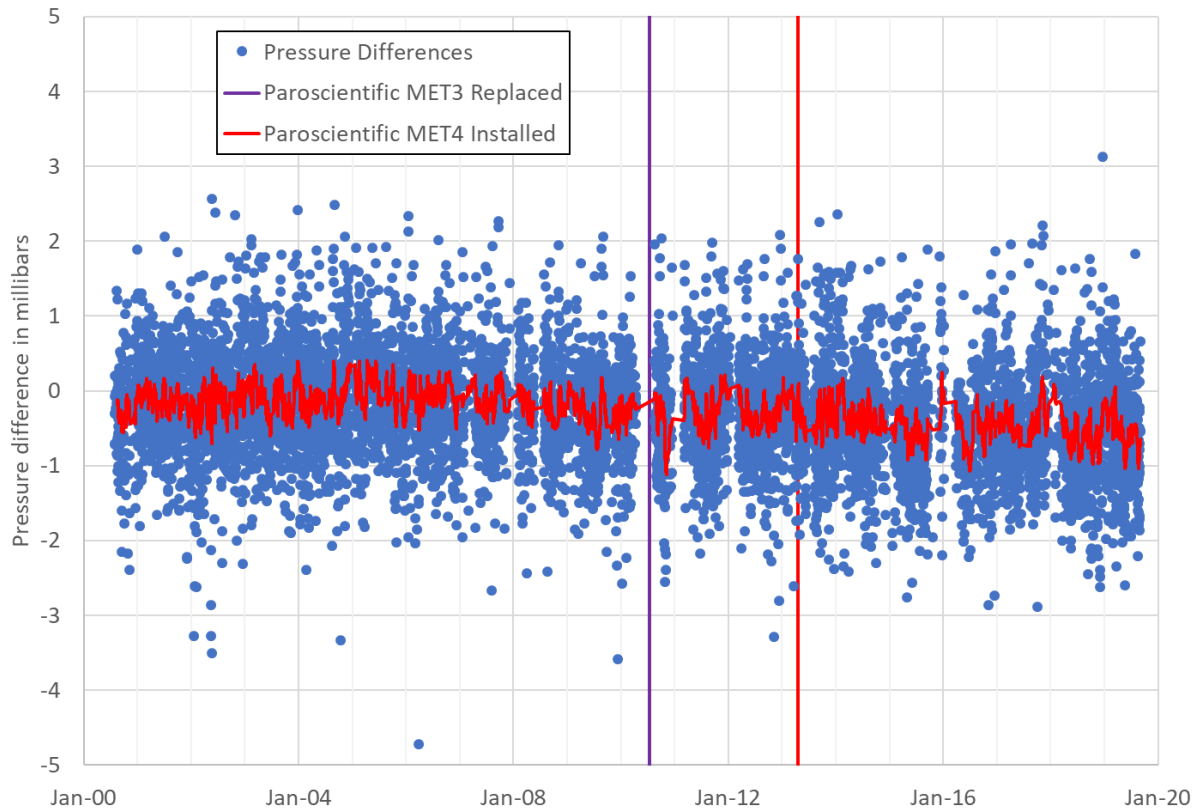
- ❑ **7403 Paroscientific MET sensors have been calibrated/replaced a few times, but there are large offsets vs VMF.**



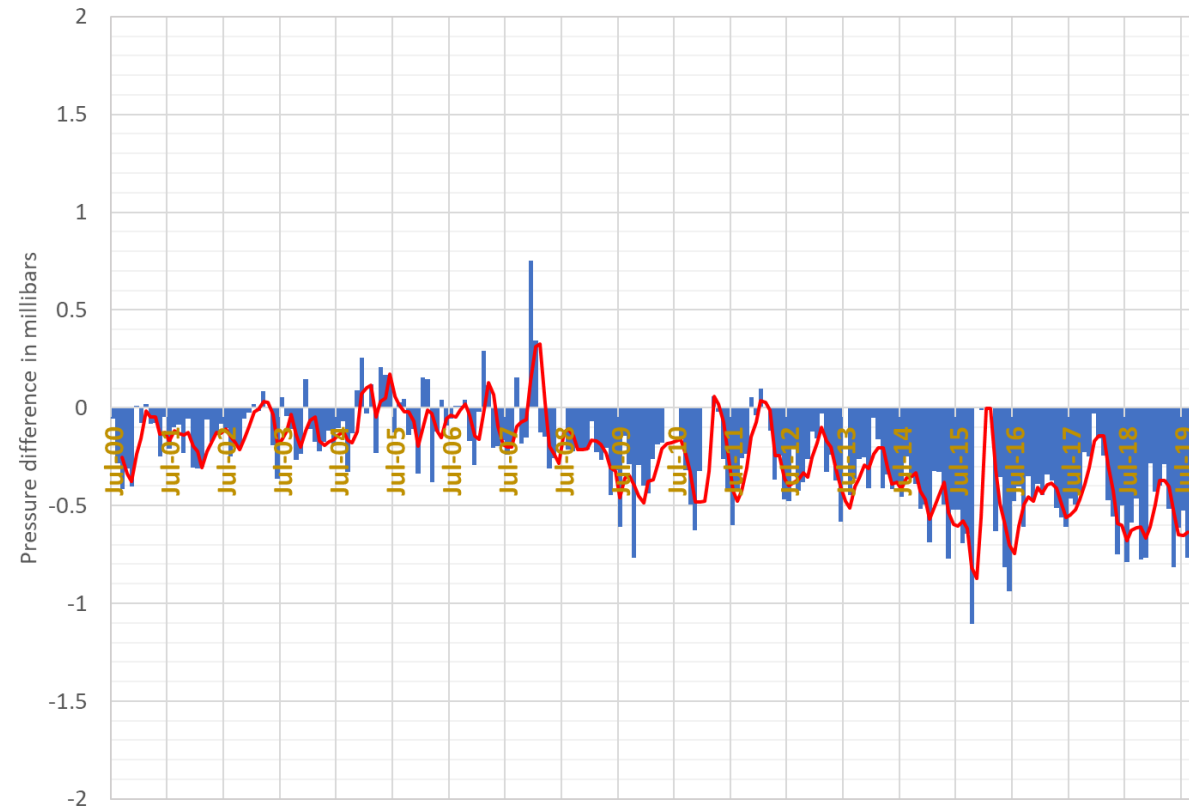
7501 HARL Pressure Differences



7501 HARL Pressure Differences (Station-VMF)



7501 HARL Monthly Pressure Differences (Station-VMF)

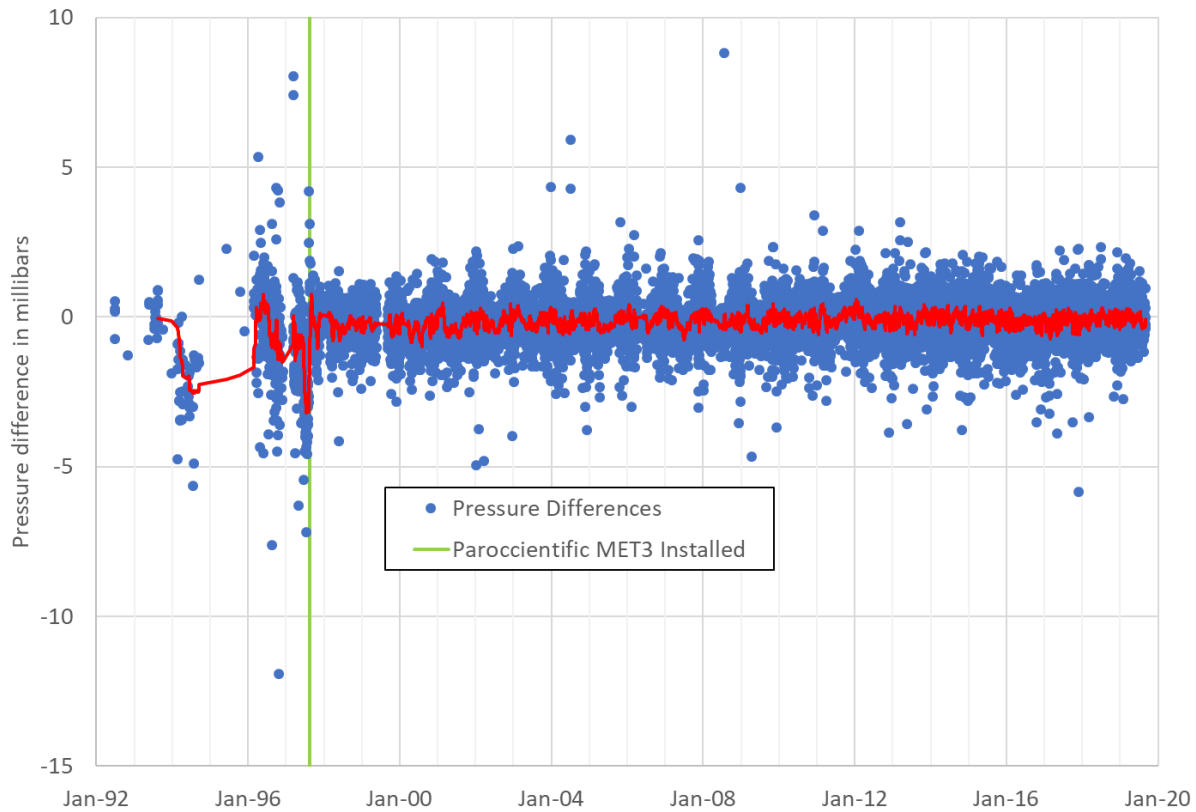




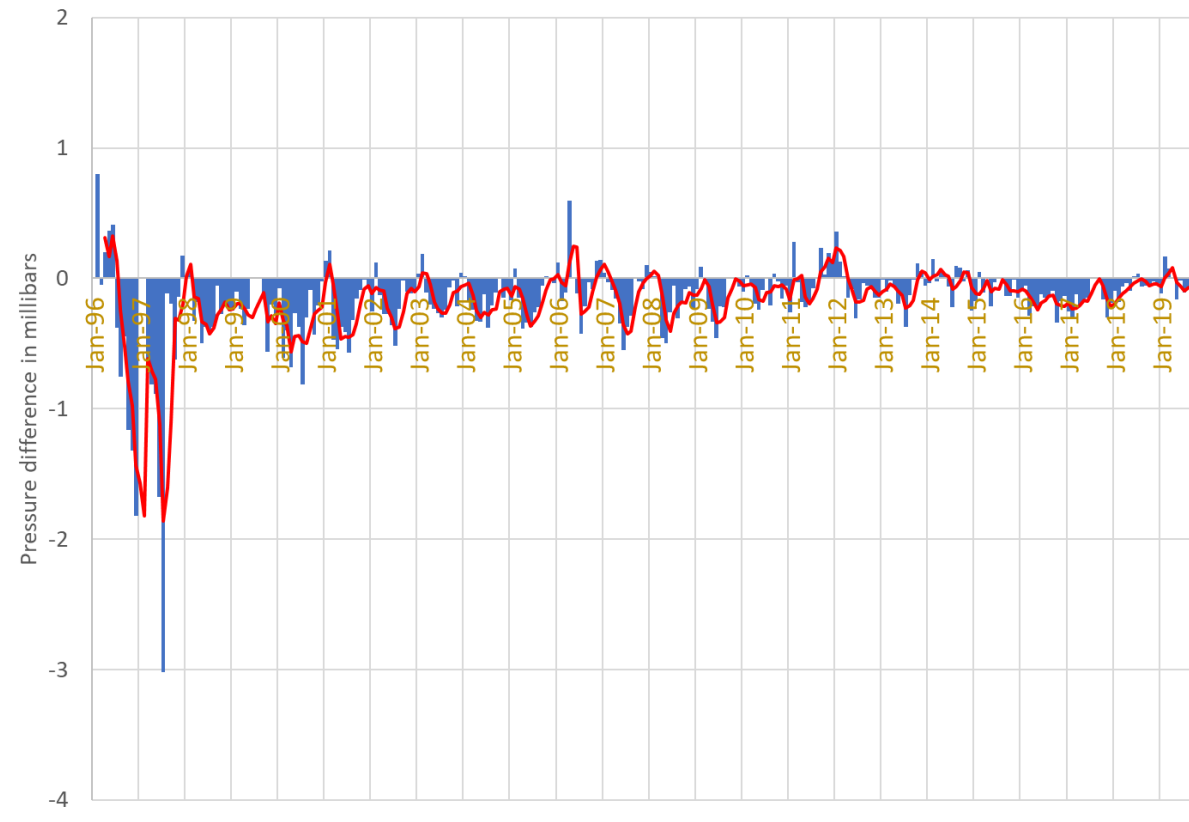
7237 CHAL Pressure Analysis



7237 CHAL Pressure Differences (Station-VMF)



7237 CHAL Monthly Pressures Differences (Station-VMF)

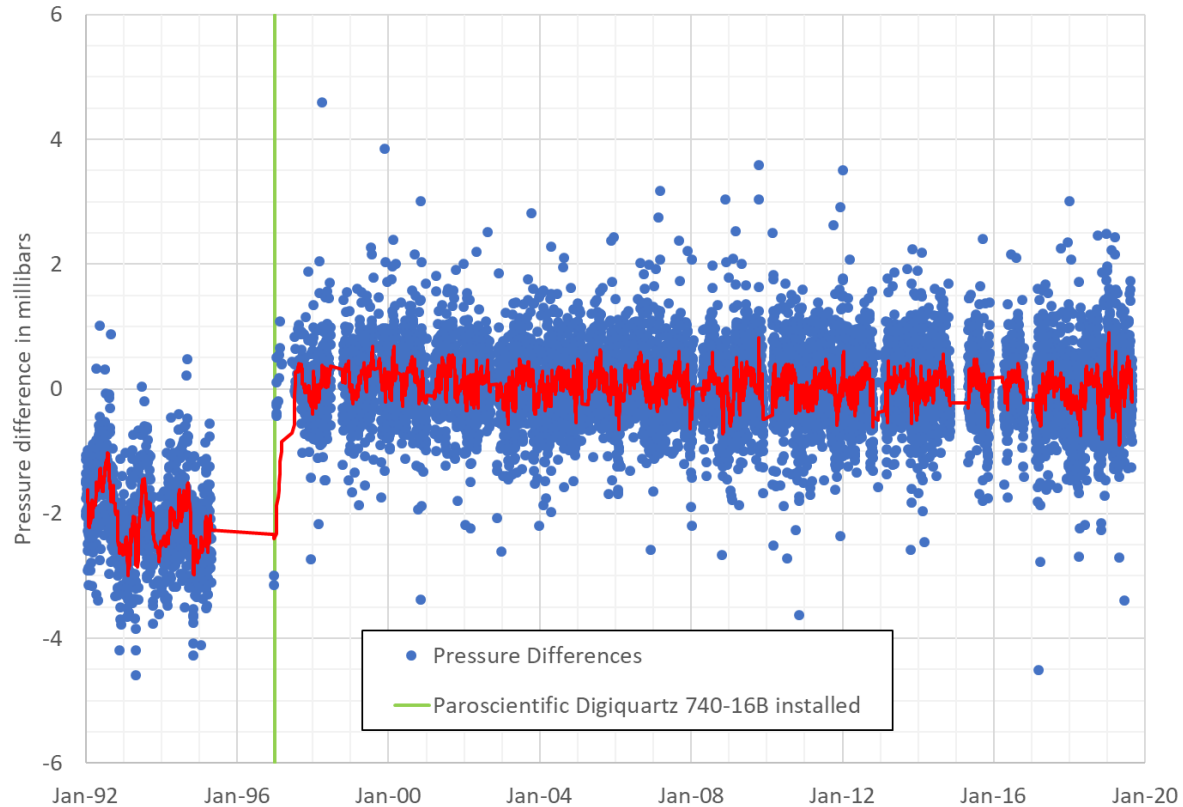




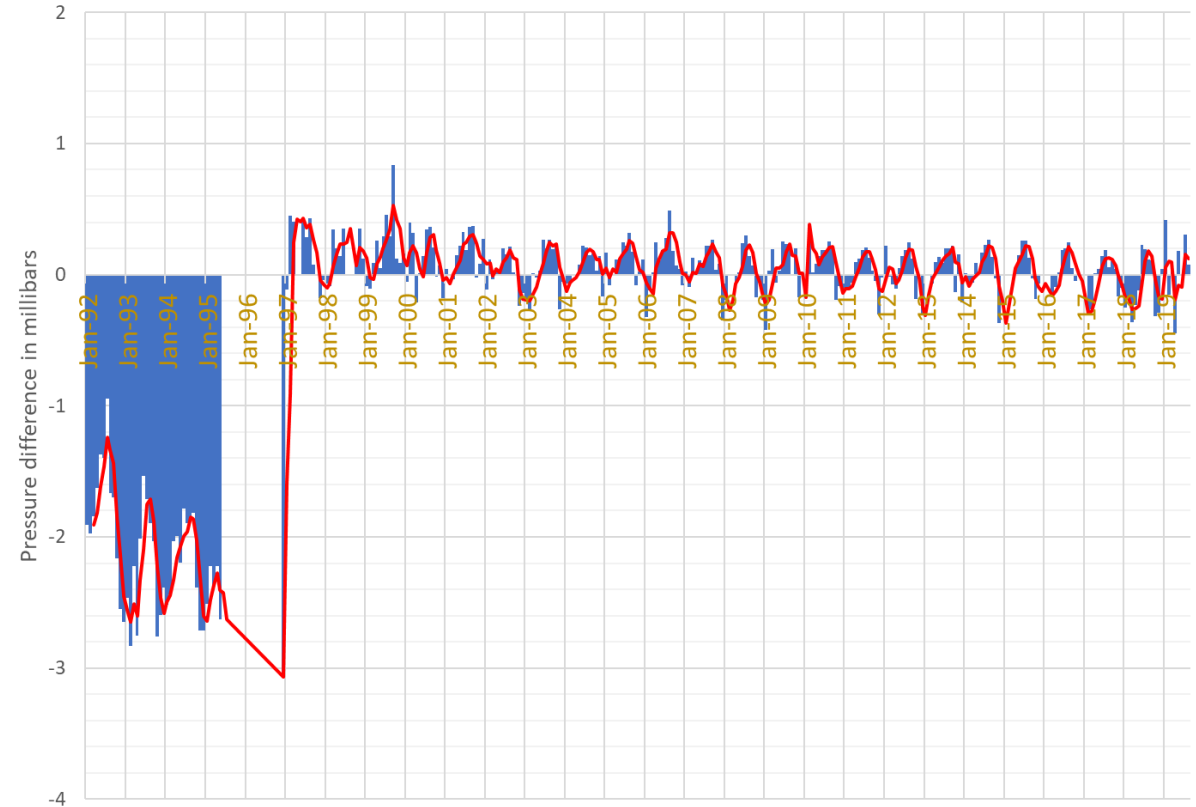
7810 ZIML Pressure Analysis



7810 ZIML Pressure Differences (Station-VMF)



7810 ZIML Monthly Pressure Differences (Station-VMF)

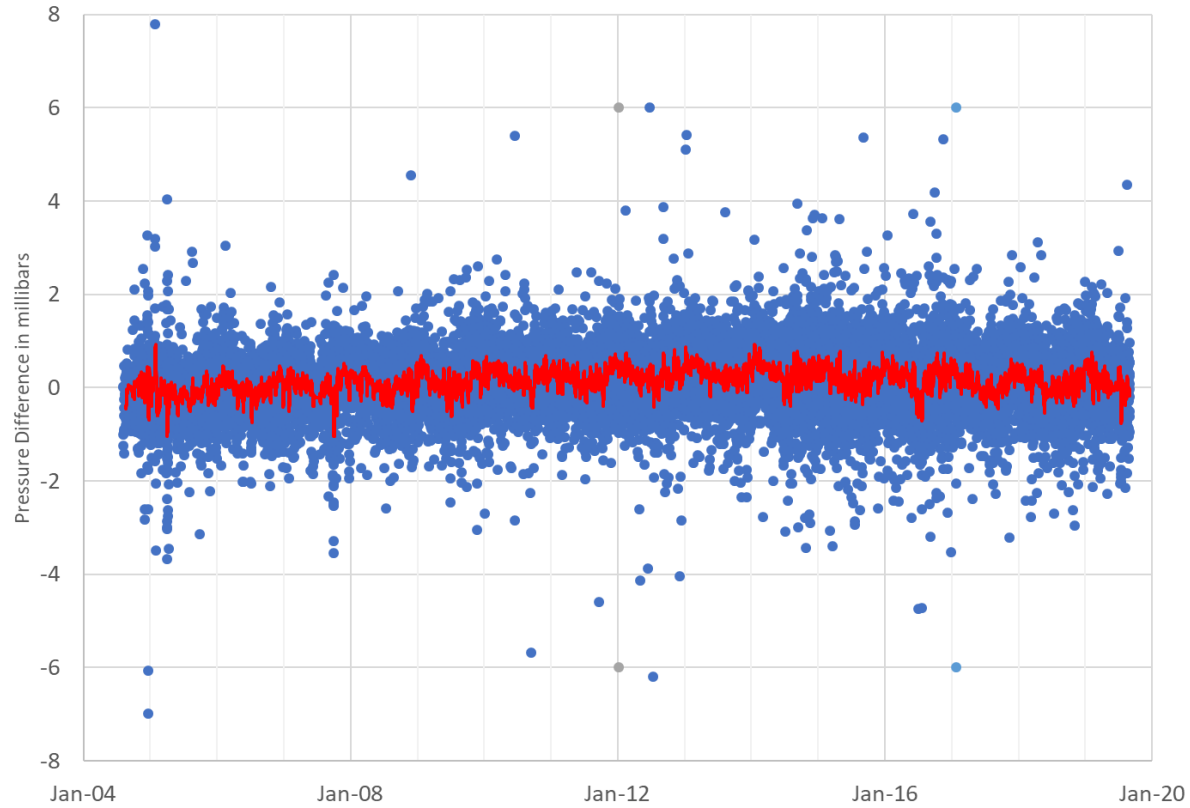




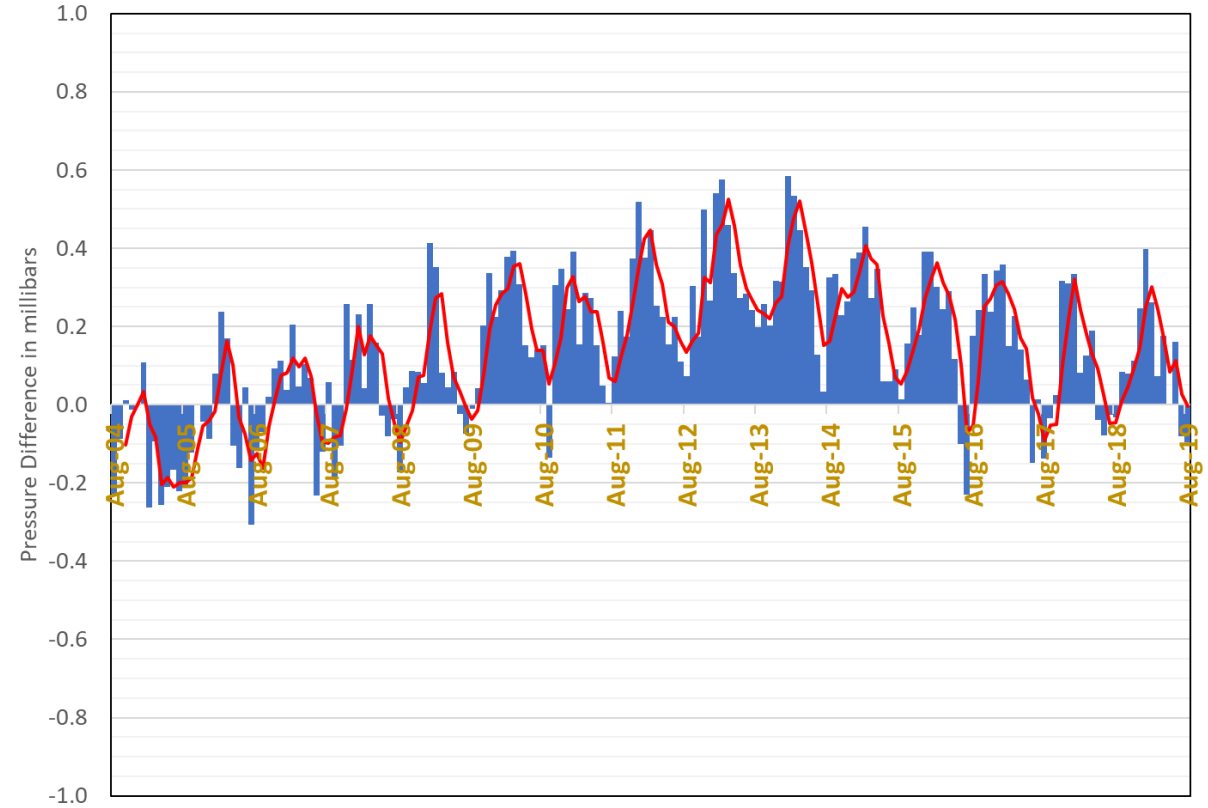
7825 STL3 Pressure Analysis



7825 STL3 Pressure Differences (Station-VMF)



7825 STL3 Monthly Pressure Differences (Station-VMF)

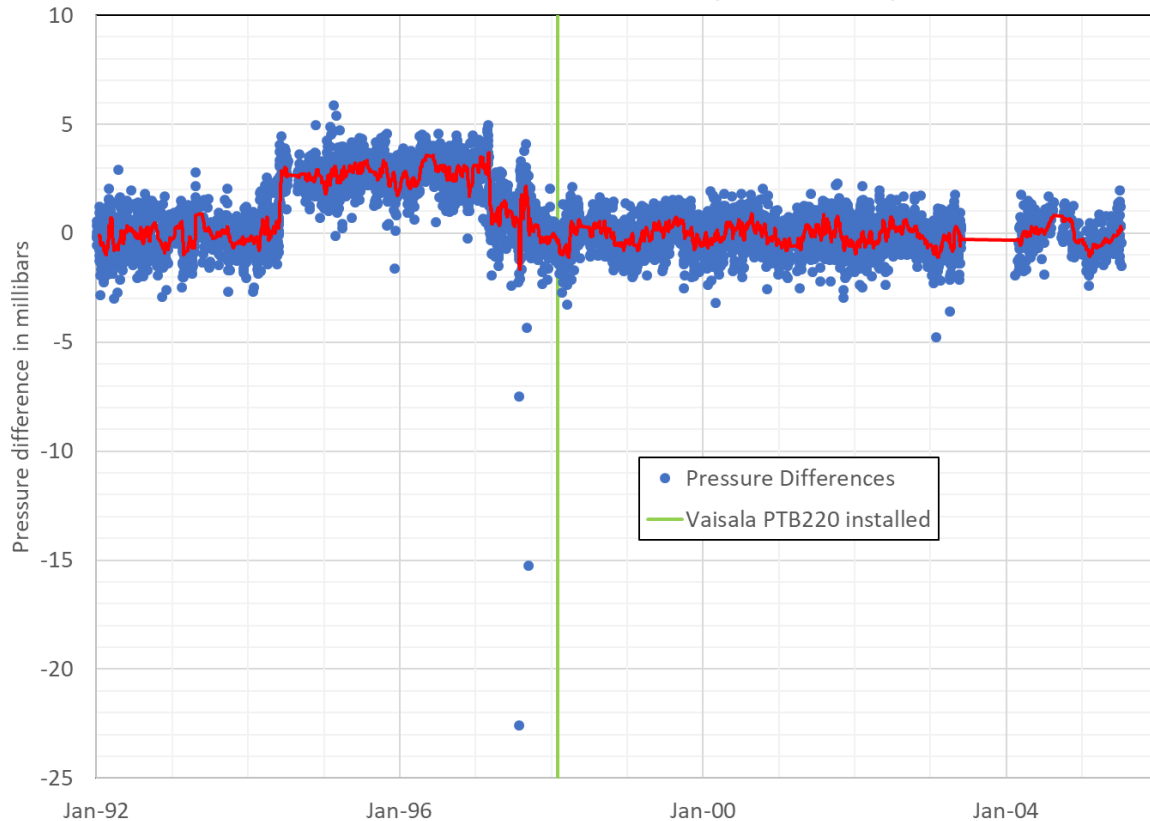




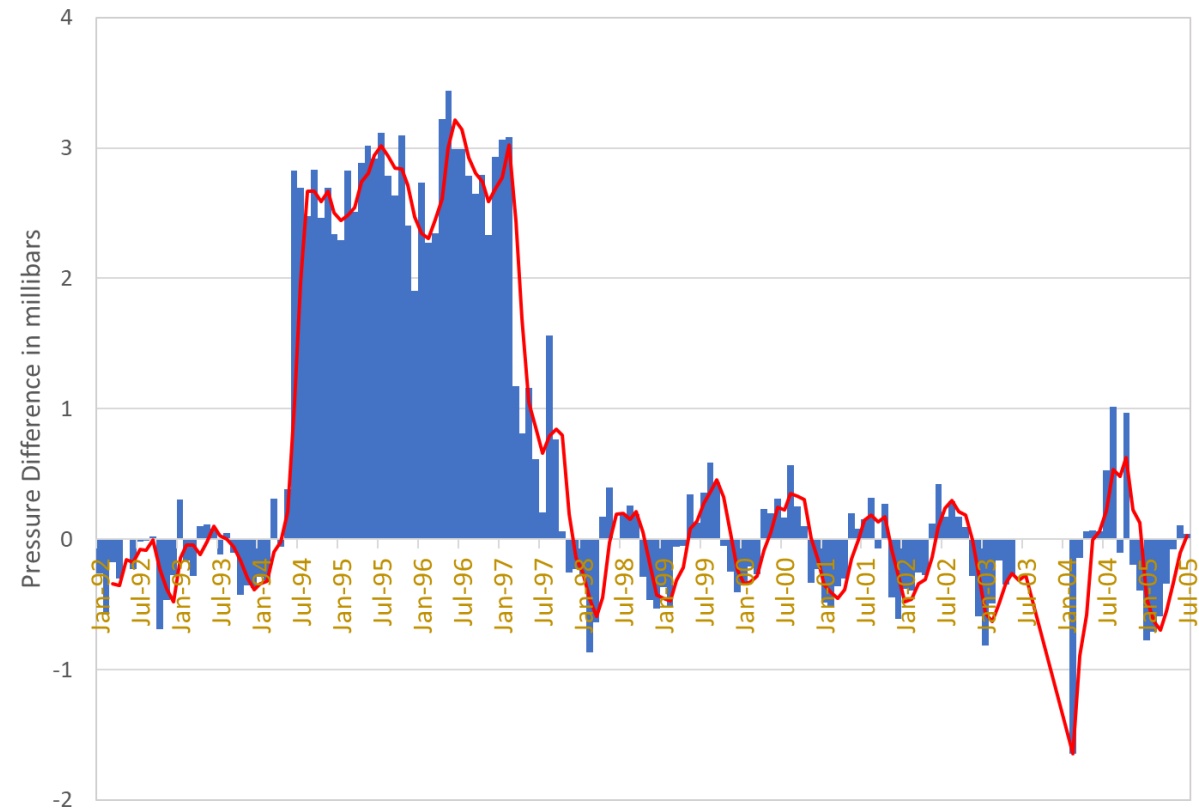
7835 GRSL Pressure Analysis



7835 GRSL Pressure Differences (Station-VMF)



7835 GRSL Monthly Pressure Differences



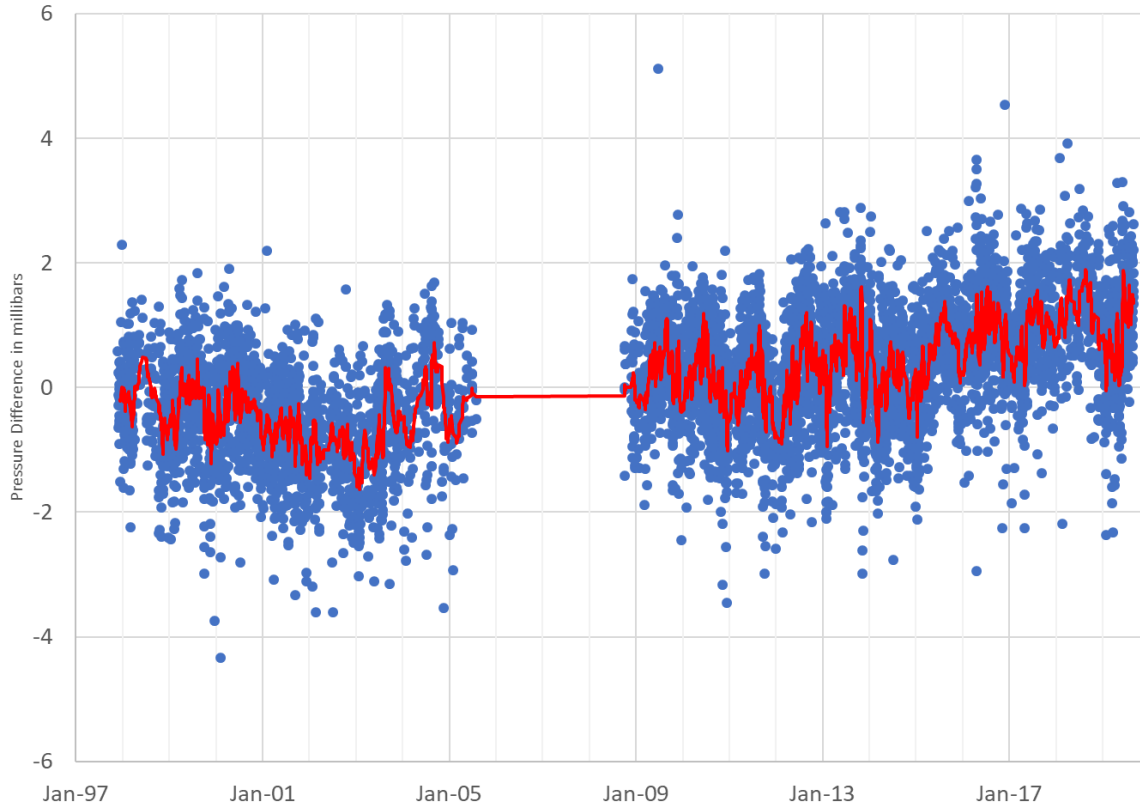
- Notice the seasonal oscillations in the differences after the Vaisala PTRB220 was installed.
- Based on the 7835 site log, there is 2.5 meter difference in height between the sensor and the system reference point. Was this height difference modelled in the data processing?



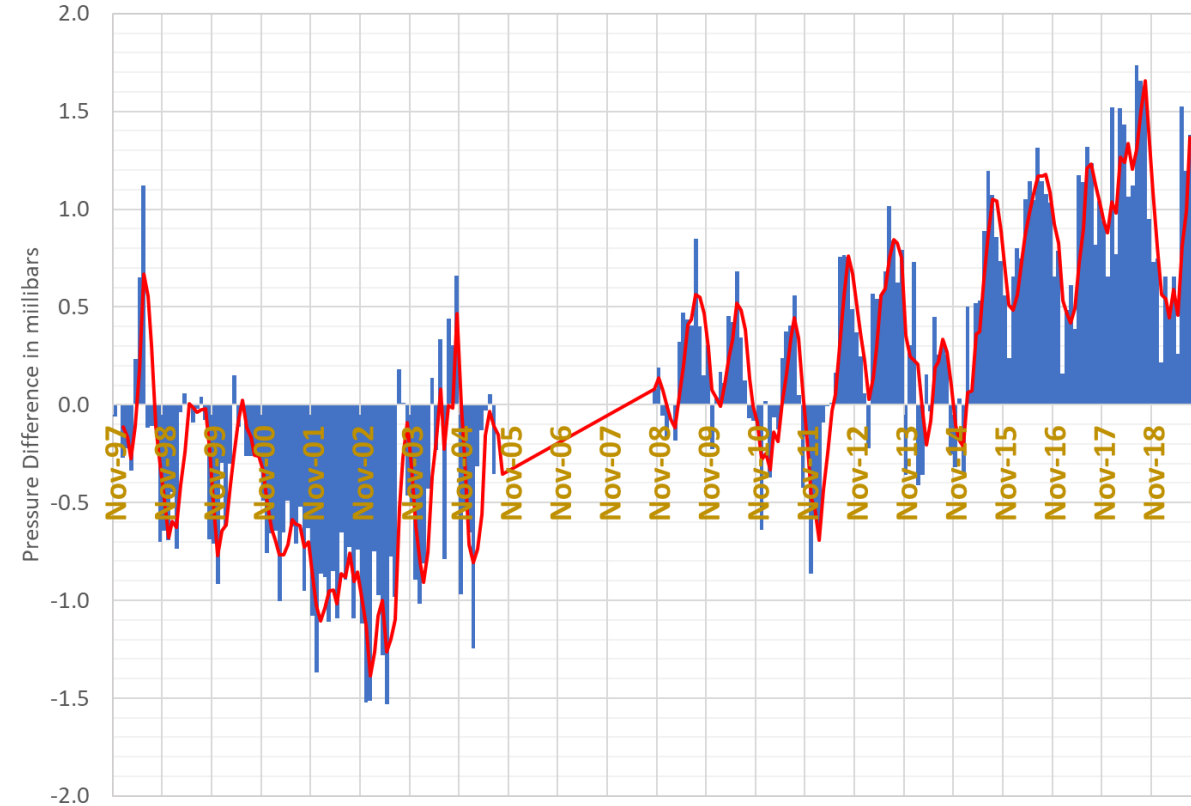
7845 GRSM Pressure Analysis



7845 GRSM Pressure Differences (Station-VMF)



7845 GRSM Monthly Pressure Differences (Station-VMF)

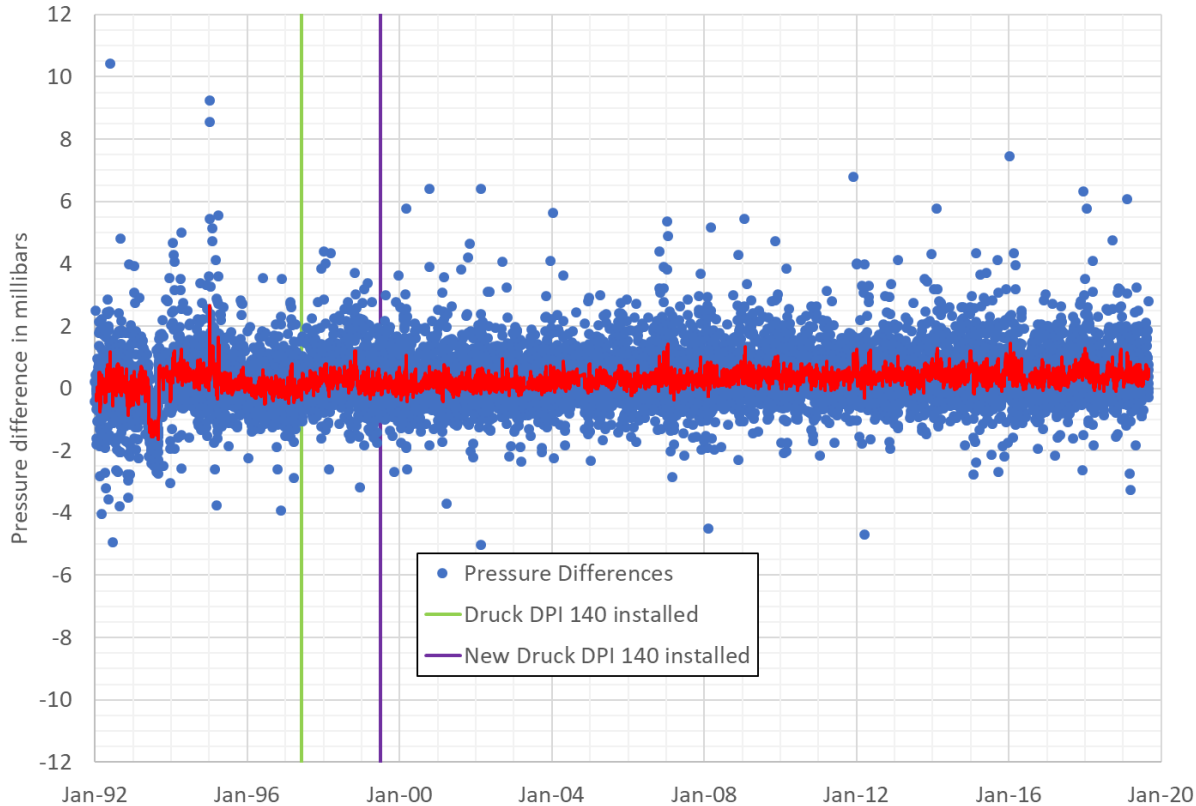




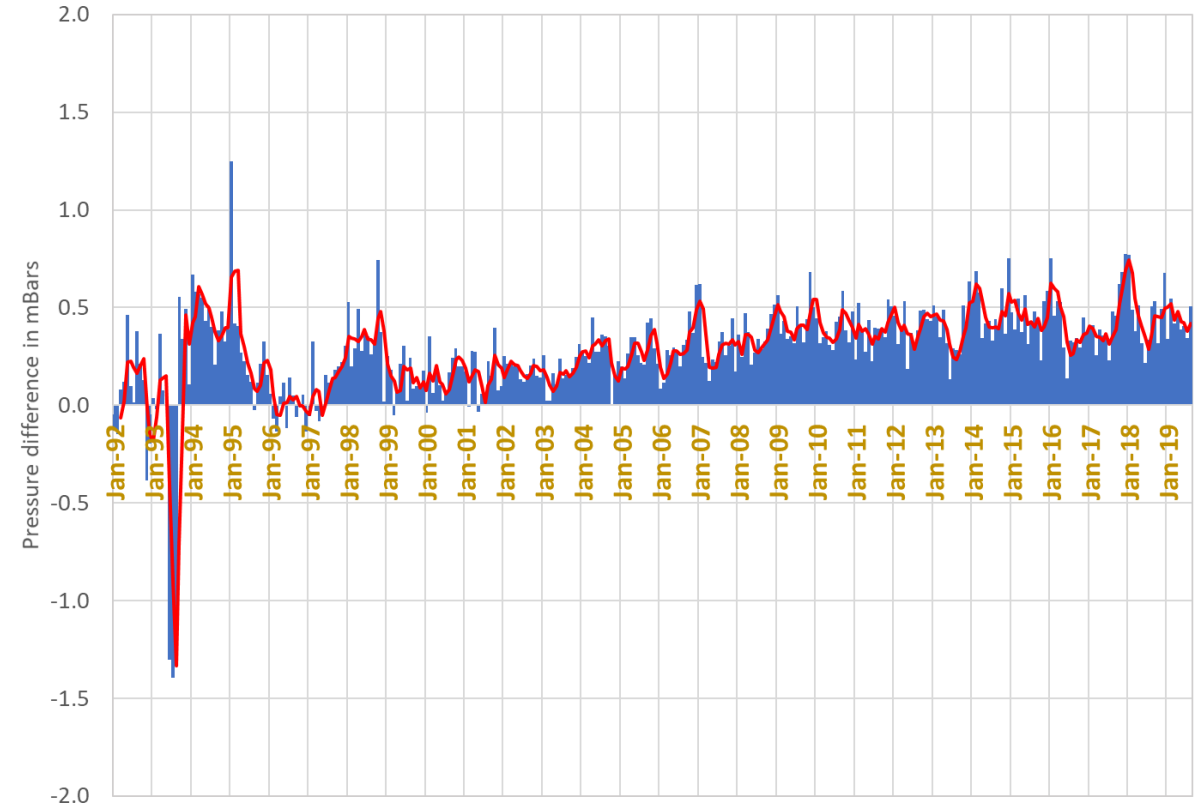
7840 HERL Pressure Analysis



7840 HERL Pressure Differences (Station-VMF)



7840 HERL Monthly Pressure Differences (Station-VMF)

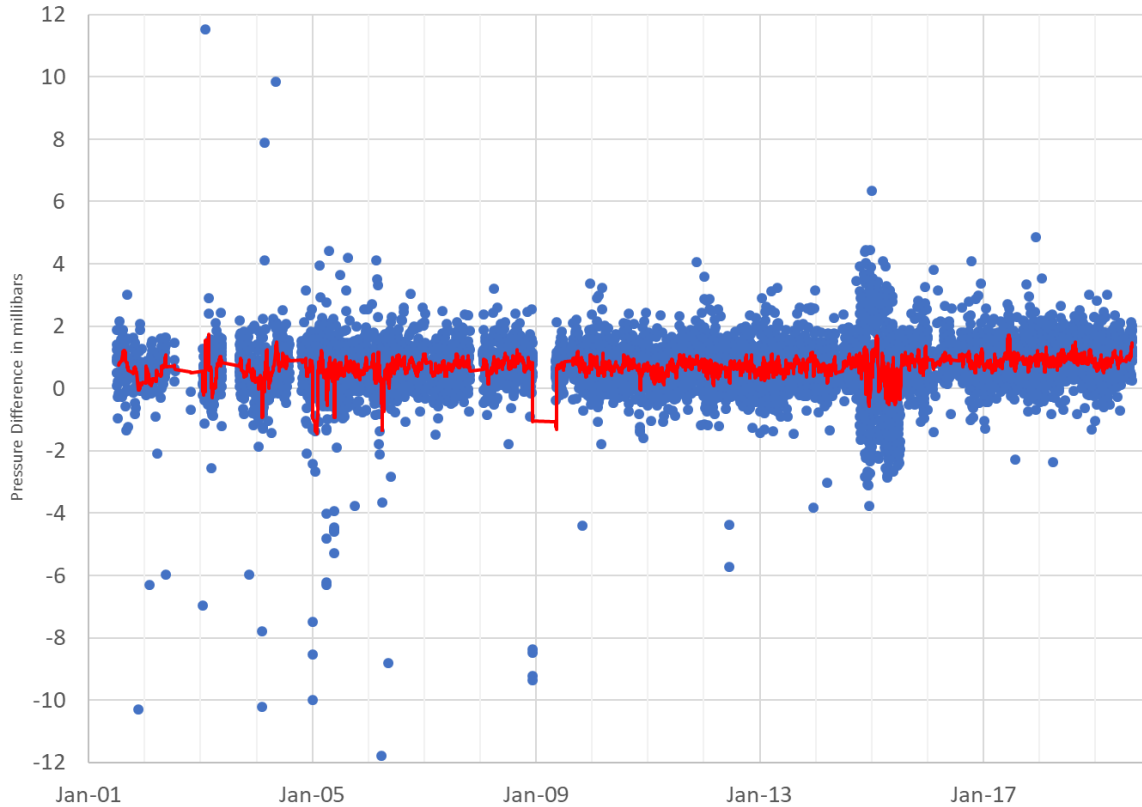




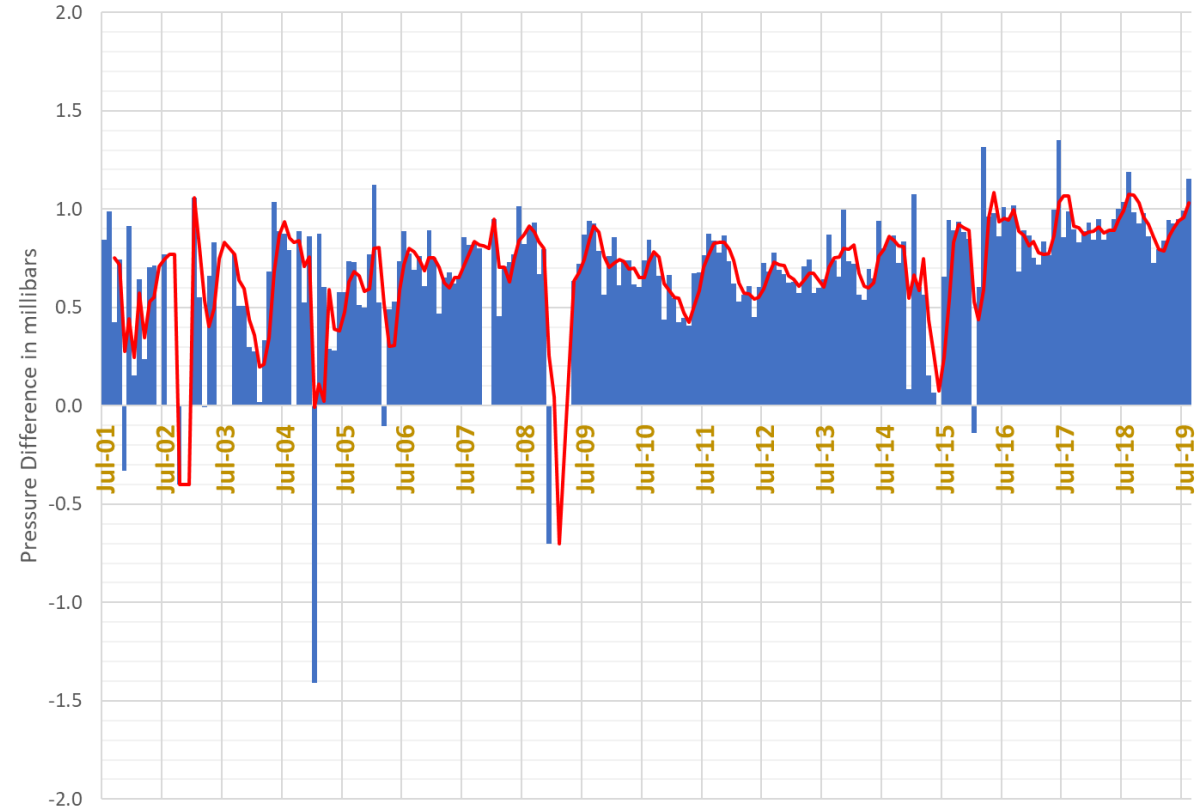
7941 MATM Pressure Analysis



7941 MATM Pressure Differences (Station-VMF)



7941 MATM Monthly Pressure Differences (Station-VMF)

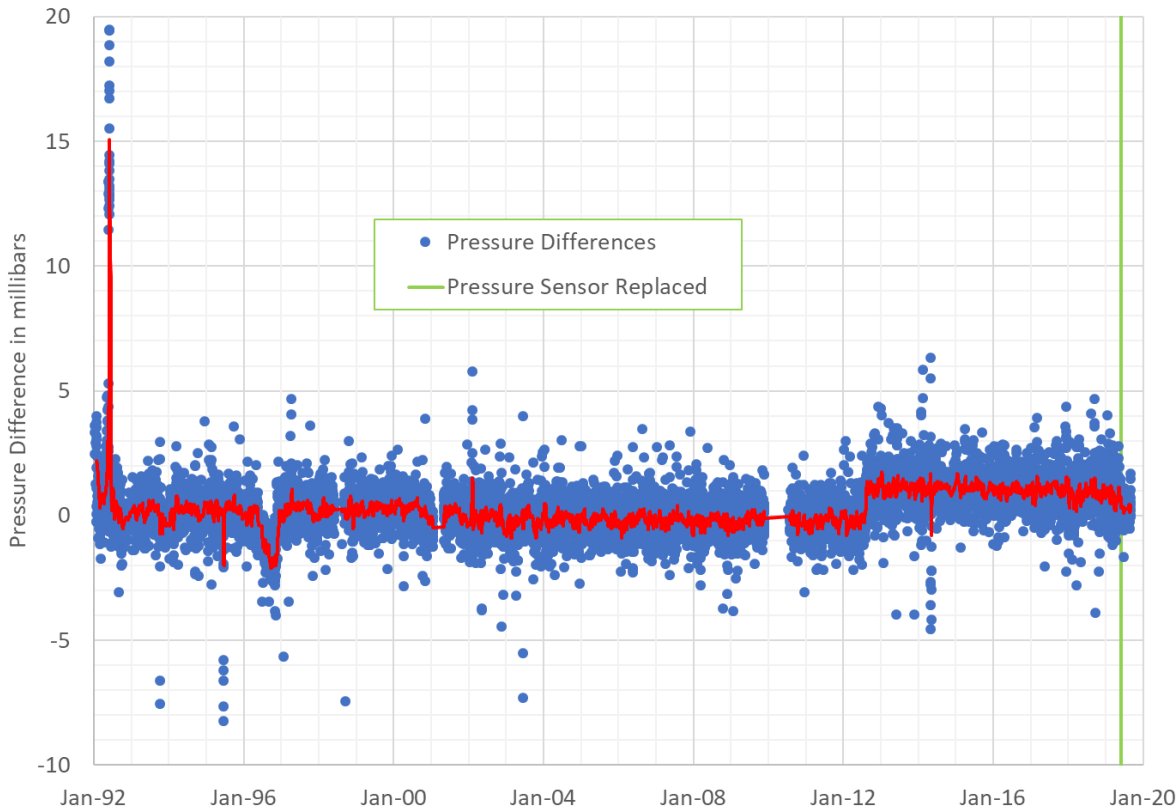




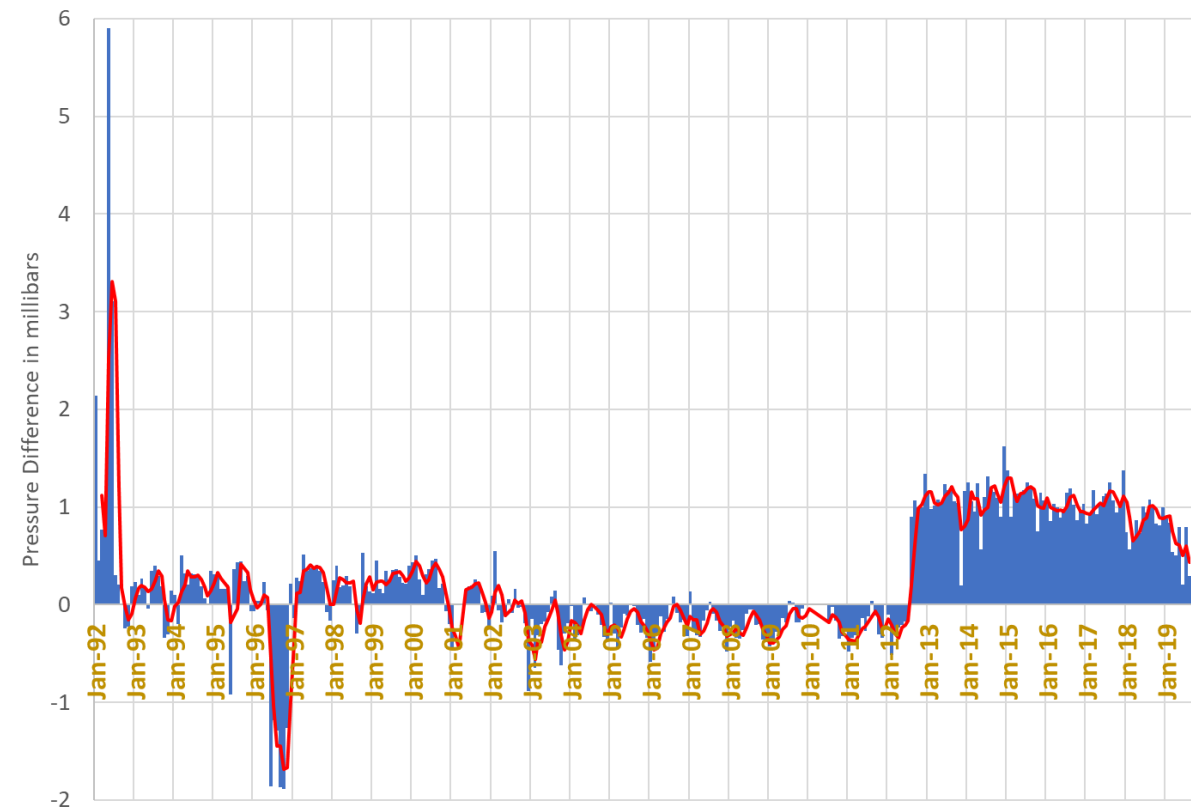
8834 WETL Pressure Analysis



8834 WETL Pressure Differences (Station-VMF)



8834 WETZL Monthly Pressure Differences (Station-VMF)



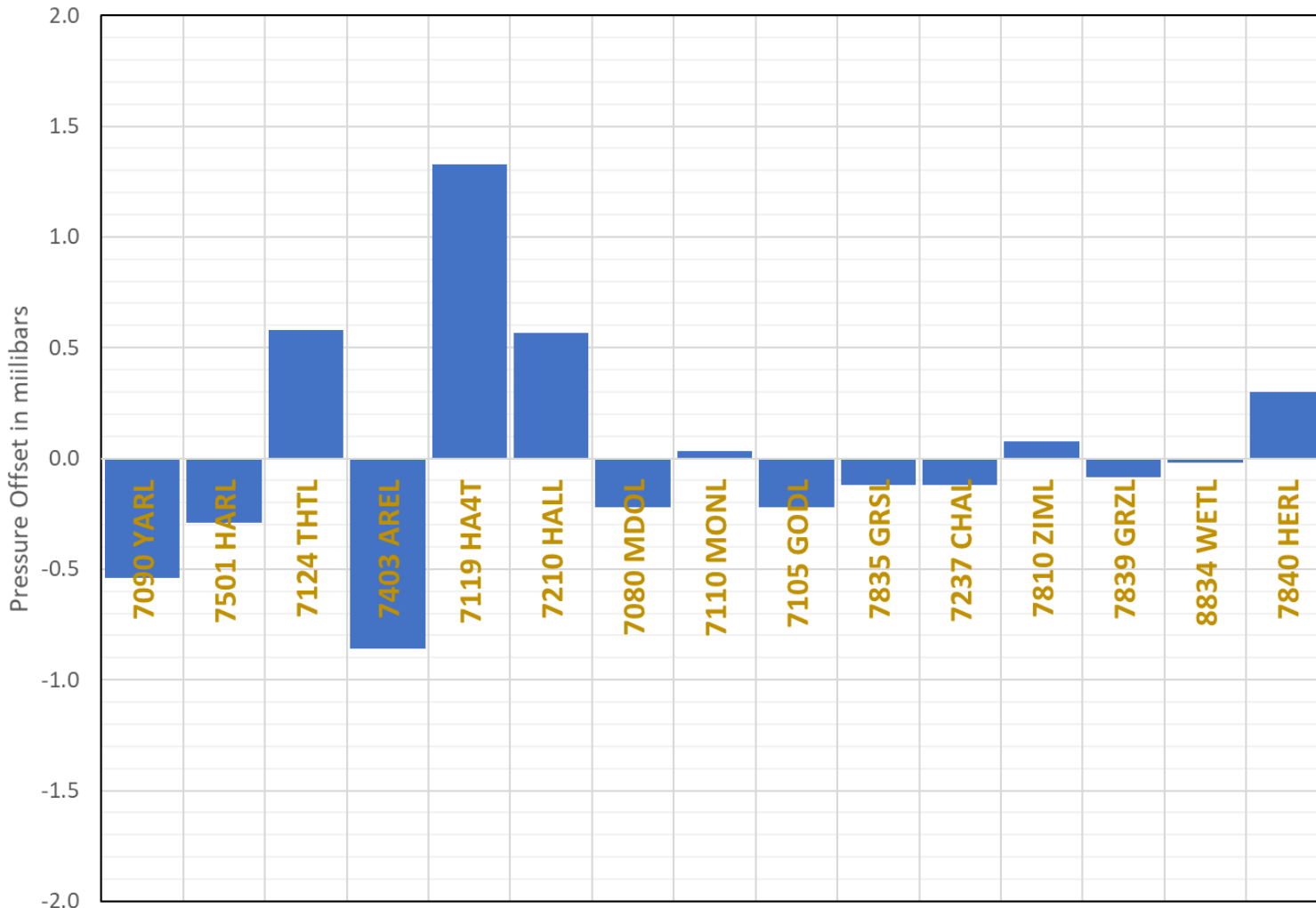
- ❑ These results are based on release 0 of the 8834 data. Release 1 fixed a height correction (9.354 meter) between the pressure sensor and the system reference point. The pressure sensor was replaced on 29-May-2019 (ref: SLRMAIL #2580).



Mean Pressure Differences (Station-VMF) Summary



Mean Pressure Differences (Station-VMF) (Sorted by Latitude)



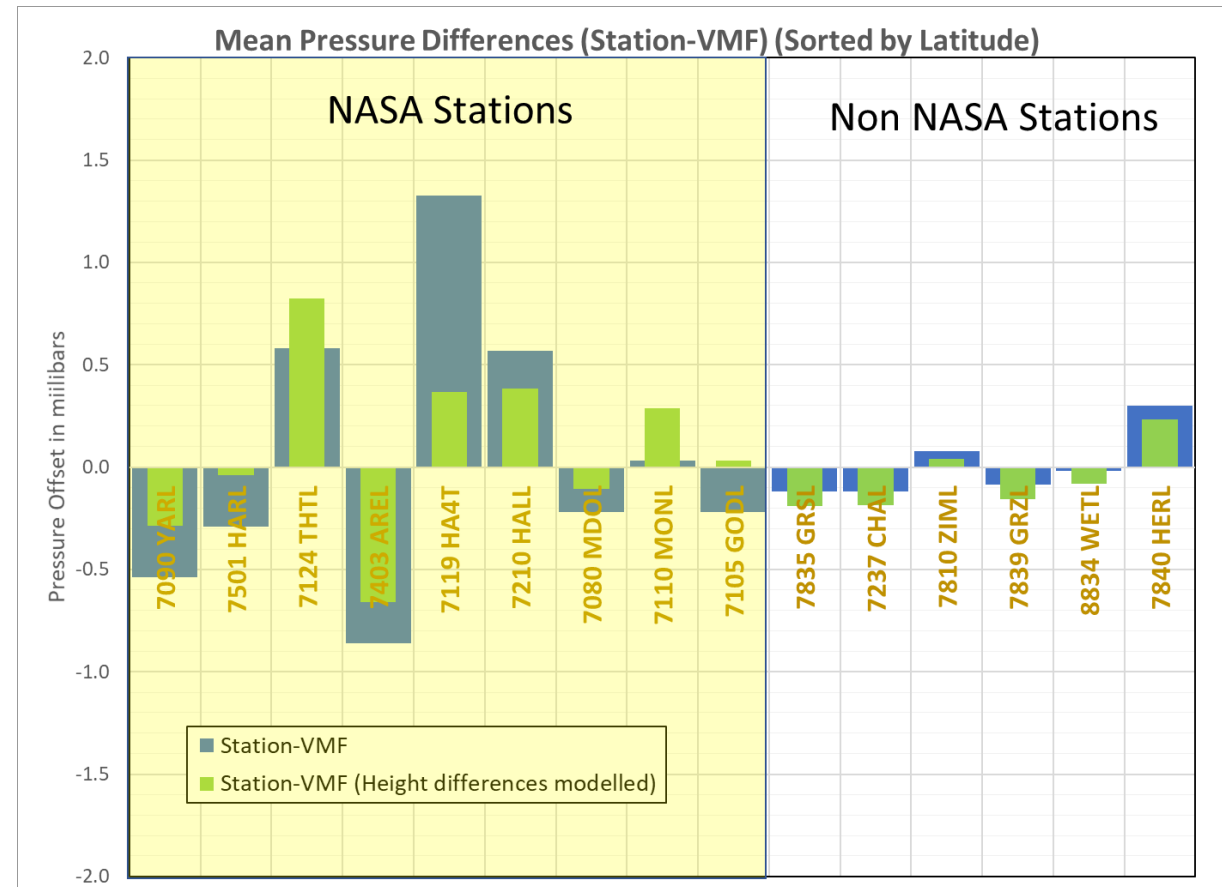
- These are the mean pressure differences when the differences appear relatively stable between the site's measurements and the VMF.
- Potential errors sources are:
 - The barometric sensor
 - Ray-Tracing
 - The station height used in the VMF
 - Unmodeled height errors between the barometric sensor and the system reference point
- Reducing barometric systematic errors to the sub-mm level requires absolute pressure accuracies of 0.10 to 0.15 millibars
- Station heights in the VMF need to be accurate to better than 1 meter to keep the uncertainty in the barometric pressure to less than 0.1 millibars



Mean Pressure Differences (Station-VMF) Summary



Station Type	Station	Latitude	VMF-Station SRP Height (m)
NASA	7090 YARL	-29.046	-2.516
NASA	7501 HARL	-25.890	-2.507
NASA	7124 THTL	-17.577	-2.429
NASA	7403 AREL	-16.466	-2.000
NASA	7119 HA4T	20.706	9.609
NASA	7210 HALL	20.707	-0.159
NASA	7080 MDOL	30.680	-1.140
NASA	7110 MONL	32.892	-2.517
NASA	7105 GODL	39.021	-2.521
Non-NASA	7835 GRSL	43.755	0.676
Non-NASA	7237 CHAL	43.791	0.669
Non-NASA	7810 ZIML	46.877	0.368
Non-NASA	7839 GRZL	47.068	0.714
Non-NASA	8834 WETL	49.144	0.621
Non-NASA	7840 HERL	50.867	0.700



- ❑ The VMF station heights are based on approximate heights from the ILRS site eccentricity file.
- ❑ For the NASA systems, the VMF heights are based on the marker/monument and NOT the SRP
- ❑ NASA system pressure differences moved more toward the positive except for the Hawaii stations (7119, 7210) while the non-NASA pressure differences moved more toward the negative.



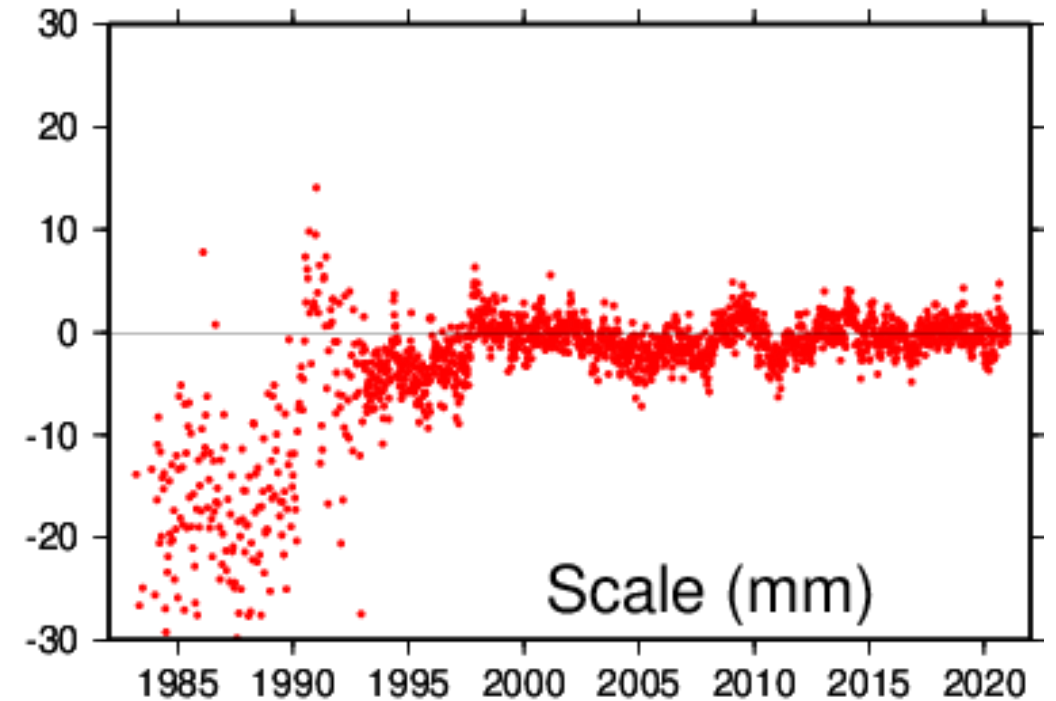
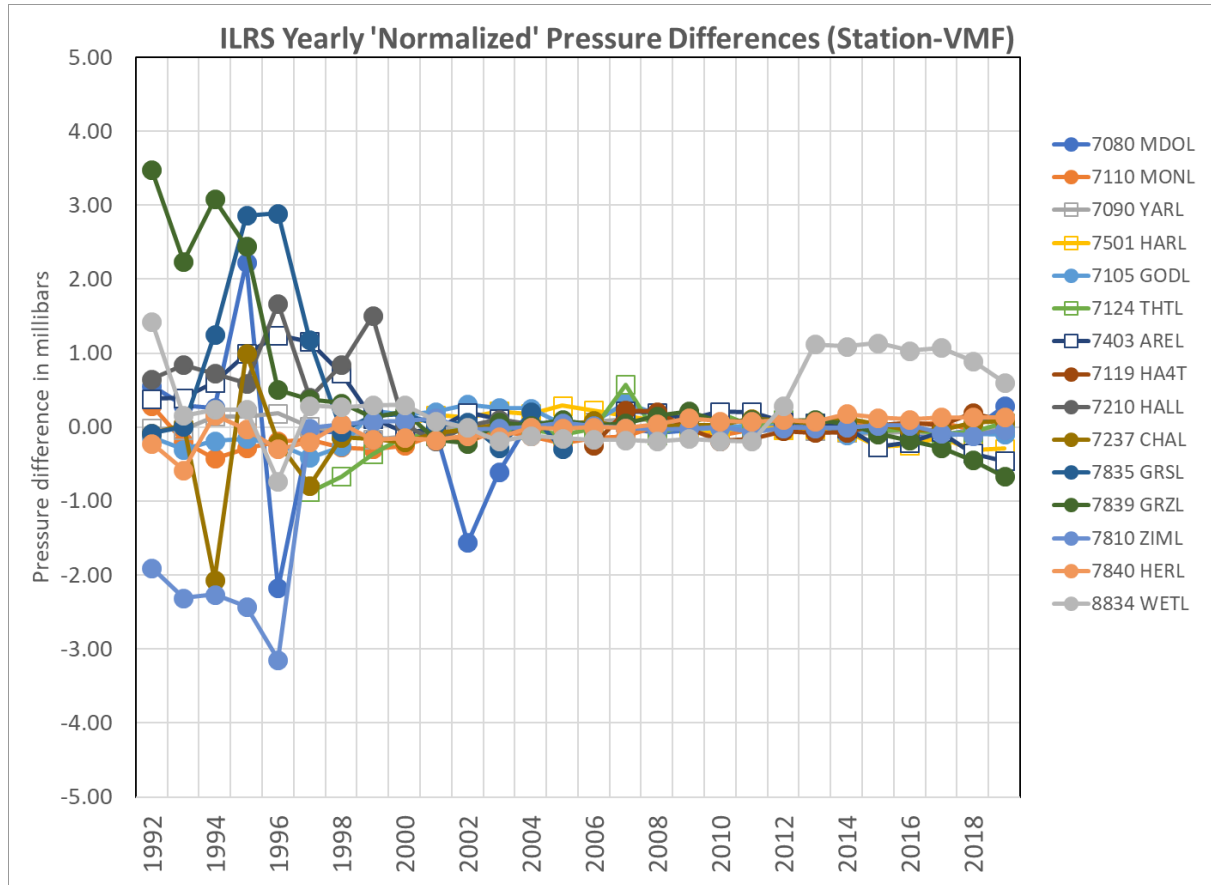
Notable Height Differences between the SRP and the Barometric Sensor



Mark	Location	Height Difference	Modelled
1824	Golosiiv, Russia	-2.5	?
1893	Katzively, Ukraine	-3.5	?
7210	Haleakala, HI, USA	2	?
7249	Beijing, China	-1.2	?
7810	Zimmerwald, Switzerland	2	?
7824	San Fernando, Spain	12	?
7821	Shanghai, China	2	?
7835	Grasse, France	2.5	?
7836	Potsdam, Germany	-2.28	?
7837	Shanghai, China	2	?
7838	Simosato, Japan	-3	Yes
7841	Potsdam, Germany	-5.2	?
7941	Matera, Italy	2.4	Yes
8834	Wetzell, Germany	9.354	Yes



ILRS Yearly Normalized Pressure Differences and ITRF SLR Scale



- ❑ As more accurate barometric sensors were installed at each site during the mid to late 1990's, the yearly barometric offsets stabilized at these sites.
- ❑ Did unmodeled barometric errors in the early 1990's, bias the SLR scale estimates prior to 1997?



Summary/Next Steps/Recommendations



❑ Summary:

- The absolute accuracy of the VMF30 is site dependent but can be modelled
- The VMF30 data can be used to model historical errors in SLR barometric pressures which should improve SLR scale estimates
- The proliferation of more accurate SLR meteorological sensors in the mid to late 1990's had a positive impact on our SLR data quality and SLR scale.

❑ Next Steps:

- Continue this analysis for other SLR stations including legacy systems

❑ Recommendations:

- For stations that have their barometer located more than 1 meter above or below their SRP, please update the additional information in Section 12.01 of your site log, to let users know what barometric offset if any is applied to your barometric measurements!